

# MICROSCOPIC THEORY OF SUPERCONDUCTIVITY

by

Helmut Eschrig

(2001, updated 08/2008)

These lecture notes are dedicated  
to Dierk Rainer  
on the occasion of his 60th birthday in 2001.  
He pioneered the systematic treatment  
of the low-energy scale in the  
electronic theory of condensed matter.

# Contents

<b>1</b>	<b>The Solid as a Quantum Many-Body System</b>	<b>4</b>
1.1	The Coulomb Hamiltonian of the Solid . . . . .	4
1.2	Reduced Density Matrices and Densities . . . . .	7
1.3	Correlation Functions . . . . .	9
<b>2</b>	<b>Green's Functions</b>	<b>13</b>
2.1	Spectral Representation . . . . .	14
2.2	Equation of Motion . . . . .	17
2.3	Complex Time . . . . .	19
2.4	The Interaction Picture . . . . .	21
2.5	Wick's Theorem . . . . .	24
2.6	Feynman Diagrams . . . . .	26
2.7	The Self-Energy . . . . .	28
2.8	Thermodynamic Quantities . . . . .	30
<b>3</b>	<b>Green's Functions in the Superconducting State</b>	<b>31</b>
3.1	The Bogoliubov-Valatin Transformation . . . . .	32
3.2	The Nambu Structure . . . . .	34
3.3	Green's Functions and Vertices for the Electron-Nucleon System . . . . .	35
<b>4</b>	<b>Split-off of High-Energy Parts</b>	<b>39</b>
4.1	Classification of Primary Diagrams . . . . .	39
4.2	Migdal's Theorem . . . . .	42
4.3	Leading Order Self-Energies . . . . .	44
<b>5</b>	<b>The Low Energy Equations</b>	<b>46</b>
5.1	The Quasi-Particle Renormalization . . . . .	47
5.2	The Electron-Phonon Self-Energy . . . . .	48
5.3	The Electron-Electron Self-Energy . . . . .	49
5.4	Bloch Function Representation on the Fermi Surface . . . . .	49
<b>6</b>	<b>Strong Coupling Theory of the Transition Temperature</b>	<b>53</b>
6.1	Linearization of Eliashberg's Equations . . . . .	53
6.2	The $T_c$ Formula . . . . .	55
6.3	The Dirty Limit . . . . .	56
6.4	The Cut-Off Frequency . . . . .	58
<b>7</b>	<b>Physical Properties of the Superconducting State</b>	<b>59</b>
7.1	Eliashberg's Non-Linear Equations . . . . .	59
7.2	The Quasiparticle Density of States . . . . .	62
7.3	The Thermodynamic Critical Field . . . . .	63

# Chapter 1

## The Solid as a Quantum Many-Body System

Physics as a unifying science tends to trace back all empirical phenomena to a small number of fundamental principles. The microscopic theory of superconductivity is an excellent example of a steady seventy years progress towards this goal which is still further going on. These lectures attempt at a concise description of what has been achieved so far in this direction for the understanding of the electron-phonon mechanism of superconductivity. We take as a starting point the non-relativistic Hamiltonian with Coulomb interactions of electrons and nuclei, although, strictly speaking, this is already a model. However, relativistic kinematics leading to mass corrections, Darwin's contact interaction, spin-orbit coupling and spin-spin dipolar interaction (including hyperfine interaction with the nuclear spin) may later on be added as correction terms, and replacement of the Coulomb interaction by the relativistic photon exchange or consideration of internal nuclear degrees of freedom would practically not change any of the considered results.

The first fully satisfactory treatment of the theory starting from this Hamiltonian was given by Dierk Rainer<sup>1</sup> in 1986, just in the year of discovery of high temperature superconductivity of the cuprates, which latter has put a completely new and up to now essentially unsolved problem for such a type of theory. The early microscopic theory of superconductivity<sup>2</sup> was led back to the use of the Fröhlich Hamiltonian of electrons and phonons, a model Hamiltonian which cannot be derived from many-body theory and which has to be used with caution by following certain model recipes. Later on, the electron-ion system was properly treated field theoretically,<sup>3</sup> but still the separation of the low energy scale was not made completely explicit.

### 1.1 The Coulomb Hamiltonian of the Solid

As mentioned above, we take as the starting point the Hamiltonian

$$\hat{H} = \hat{t} + \hat{V}_{ee} + \hat{V}_{en} + \hat{V}_{nn} + \hat{T}, \quad (1.1)$$

---

<sup>1</sup>D. Rainer, in: D. F. Brewer (ed.), *Progress in Low Temperature Physics*, vol. X, p. 371, Elsevier, Amsterdam 1986.

<sup>2</sup>G. M. Eliashberg, *Sov. Phys.-JETP* **11**, 696 (1960); **12**, 1000 (1961).

<sup>3</sup>D. Scalapino, in: R. D. Parks (ed.), *Superconductivity*, vol. 1, p. 449, Dekker, New York 1969.

where

$$\hat{t} = - \sum_{i=1}^N \frac{1}{2} \frac{\partial^2}{\partial \mathbf{r}_i^2} \quad (1.2)$$

is the operator of the kinetic energy of the  $N$  electrons,

$$\hat{V}_{ee} = \frac{1}{2} \sum_{i \neq j}^N \frac{1}{|\mathbf{r}_i - \mathbf{r}_j|} \quad (1.3)$$

is the operator of the electron-electron interaction,

$$\hat{V}_{en} = - \sum_{i=1}^N \sum_{m=1}^M \frac{Z_m}{|\mathbf{r}_i - \mathbf{R}_m|} \quad (1.4)$$

is the operator of the interaction of the electrons with the  $M$  nuclei of charges  $Z_m$ ,  $\sum_m Z_m = N$ ,

$$\hat{V}_{nn} = \frac{1}{2} \sum_{m \neq n}^M \frac{Z_m Z_n}{|\mathbf{R}_m - \mathbf{R}_n|} \quad (1.5)$$

is the operator of the nucleus-nucleus interaction, and

$$\hat{T} = - \sum_{m=1}^M \frac{1}{2M_m} \frac{\partial^2}{\partial \mathbf{R}_m^2} \quad (1.6)$$

is the operator of the kinetic energy of the nuclei.

We used natural atomic units

$$\hbar = |e| = m_e = 1 \text{ a.u.}, \quad M_m \equiv \frac{m_m}{m_e} \approx 10^3 \dots 10^5,$$

$$\frac{\langle T \rangle}{\langle t \rangle} \approx \langle M \rangle^{-1/2} \equiv \alpha, \quad \alpha \approx 10^{-2}. \quad (1.7)$$

The last estimate is the result of the well known Born-Oppenheimer perturbation theory. The presence of the small parameter  $\alpha$  will play a key role in all what follows. It allows to split the Hamiltonian according to  $\hat{H} = \hat{H}_0 + \hat{H}_1$  into a zero-order part  $\hat{H}_0$  and the rest. To this end, reference positions  $\mathbf{R}_m^0$  of nuclei with a lattice spacing  $a$  are introduced in such a way that the nuclear displacements  $\mathbf{u}_m$  remain small all the time:

$$\mathbf{R}_m = \mathbf{R}_m^0 + \mathbf{u}_m, \quad \left( \frac{\langle \mathbf{u}_m \rangle}{a} \right)^2 \sim \alpha. \quad (1.8)$$

In addition we change the Hamiltonian into a grand canonical one by adding a chemical potential term for the electrons. (Since the nuclear wavefunctions do practically not overlap, their statistics need not be taken into consideration.<sup>4</sup>) Then we have

$$\hat{H}_0 = \hat{t} + \hat{V}_{ee} + \hat{V}_{en}(\mathbf{R}_m^0) + V_{nn}(\mathbf{R}_m^0) - \mu \hat{N}, \quad (1.9)$$

where  $V_{nn}(\mathbf{R}_m^0)$  is now just a constant number,  $\hat{N}$  is the operator of the number of electrons, and  $\mu$  is the chemical potential of the electrons. The number of electrons need not be fixed any more, instead  $\sum_m Z_m = \langle N \rangle$ . The remainder part of the Hamiltonian is

$$\hat{H}_1 = \hat{T} + \delta \hat{V}_{nn} + \delta \hat{V}_{en}, \quad \delta \hat{V} = \hat{V}(\mathbf{R}_m) - \hat{V}(\mathbf{R}_m^0). \quad (1.10)$$

<sup>4</sup>Observe  $\sum_{\mathcal{P}} (\pm 1)^{|\mathcal{P}|} \prod_m \varphi_{\mathcal{P}m}(\mathbf{R}_m) = \prod_m \varphi_m(\mathbf{R}_m)$  for non-overlapping orbitals  $\varphi_m$  such that  $\varphi_m(\mathbf{R}_m) \neq 0$ .

It can further be expanded in powers of the  $\mathbf{u}_m$ .

Usually the  $\mathbf{R}_m^0$  are chosen to form a regular crystalline lattice. Then,  $\delta\hat{V}$  may also contain terms with certain  $\delta Z_m$ , chemical defects, say. In concentrated alloys those terms may not be small, and one of the subsequently made approximations may become questionable in that dirty limit. Anyhow it may then be helpful to replace  $\hat{V}_{\text{en}}(\mathbf{R}_m^0)$  in  $\hat{H}_0$  by the real part of a self-consistent coherent potential of the alloy.

Additional, possibly time-dependent terms are to be added to the Hamiltonian, if external fields, in particular electromagnetic dc, ac, or photonic fields, are applied to the solid.

The time evolution of a wavefunction state  $\Psi(t)$  is given by

$$i\frac{\partial}{\partial t}\Psi(t) = \hat{H}\Psi(t), \quad \Psi(0) = \Psi_0, \quad \text{or} \quad \Psi(t) = e^{-it\hat{H}}\Psi_0. \quad (1.11)$$

However, neither can the wavefunction of a solid be measured nor can the solid be prepared or happen to be in a wavefunction state. For instance the time  $\Delta t$  needed to prepare a system in a stationary state is  $\Delta t \sim \hbar/\Delta E$ , where  $\Delta E$  is the distance to the neighboring stationary states in energy. For a piece of a solid of one cubic centimeter, say, this time is a huge number of orders of magnitude larger than the age of our universe...

In reality, a solid is always in some statistical state

$$\hat{\rho} = \sum_{\alpha} |\Psi_{\alpha}\rangle p_{\alpha} \langle\Psi_{\alpha}|, \quad \sum_{\alpha} p_{\alpha} = 1. \quad (1.12)$$

For instance, in thermal equilibrium at temperature  $T$  and chemical potential  $\mu$  of the electrons, the statistical state is a mixture of eigenstates of the grand canonical Hamiltonian:

$$\hat{H}|\Psi_{\alpha}\rangle = |\Psi_{\alpha}\rangle(E_{\alpha} - \mu N_{\alpha}), \quad p_{\alpha} = \frac{e^{-\beta(E_{\alpha} - \mu N_{\alpha})}}{\sum_{\alpha} e^{-\beta(E_{\alpha} - \mu N_{\alpha})}}, \quad \beta = \frac{1}{k_{\text{B}}T}, \quad (1.13)$$

which may be shortly expressed as

$$\hat{\rho} = Z^{-1}e^{-\beta\hat{H}}, \quad Z = \text{tr} e^{-\beta\hat{H}}. \quad (1.14)$$

The trace in the last expression means the trace of the operator  $e^{-\beta\hat{H}}$ , that is, the scalar multiplication of the right side of its representation of type (1.12) to its left side. Generally, a function  $f(\hat{A})$  of an operator  $\hat{A}$  is understood in the spectral sense to be

$$f(\hat{A}) = \sum_a |\Psi_a\rangle f(a) \langle\Psi_a| \quad \text{where} \quad \hat{A}|\Psi_a\rangle = |\Psi_a\rangle a \quad (1.15)$$

and the  $|\Psi_a\rangle$  form a complete set.

The electrons are fermions, and their wavefunctions depend on their position vector  $\mathbf{r}_i$  and spin variable  $s_i$  which latter can only take on two values ( $\uparrow$  and  $\downarrow$ , say). We will combine them into a compound variable

$$x_i \equiv (\mathbf{r}_i, s_i), \quad \int dx_i \equiv \sum_{s_i} \int d^3r_i. \quad (1.16)$$

The nuclei may have half-integer or integer spin; however, as already mentioned, we need not consider their statistics and will suppress their spin completely. That means, the total wavefunction must be antisymmetric with respect to electron permutation, but need not to have any symmetry with respect to permutation of nuclei:

$$\Psi(\dots, x_i, \dots, x_j, \dots; \mathbf{R}_1, \dots, \mathbf{R}_M; t) = -\Psi(\dots, x_j, \dots, x_i, \dots; \mathbf{R}_1, \dots, \mathbf{R}_M; t). \quad (1.17)$$

To account for the electronic symmetry, the most convenient way is the use of the machinery of field quantization. Electron field operators  $\hat{\psi}(x)$  are introduced which obey the canonical anticommutation relations

$$[\hat{\psi}(x), \hat{\psi}(x')] = [\hat{\psi}^\dagger(x), \hat{\psi}^\dagger(x')] = 0, \quad [\hat{\psi}(x), \hat{\psi}^\dagger(x')] = \delta(x - x') \equiv \delta_{ss'} \delta(\mathbf{r} - \mathbf{r}'). \quad (1.18)$$

With their help, a position and spin eigenstate of  $N$  electrons is created out of the vacuum state  $|\rangle$  as

$$\hat{\psi}^\dagger(x_1) \cdots \hat{\psi}^\dagger(x_N) |\rangle, \quad (1.19)$$

and the value of the wavefunction of the general  $N$ -electron state  $|\Psi(t)\rangle$  is obtained by projection on that position and spin eigenstate:

$$\Psi(x_1, \dots, x_N; t) = \langle \hat{\psi}(x_N) \cdots \hat{\psi}(x_1) |\Psi(t)\rangle. \quad (1.20)$$

The electronic parts of the Hamiltonian in that field quantization representation are

$$\hat{t} - \mu \hat{N} = \int dx \hat{\psi}^\dagger(x) \left( -\frac{1}{2} \frac{\partial^2}{\partial \mathbf{r}^2} - \mu \right) \hat{\psi}(x), \quad (1.21)$$

$$\hat{V}_{\text{ee}} = \frac{1}{2} \int dx dx' \hat{\psi}^\dagger(x) \hat{\psi}^\dagger(x') \frac{1}{|\mathbf{r} - \mathbf{r}'|} \hat{\psi}(x') \hat{\psi}(x), \quad (1.22)$$

$$\hat{V}_{\text{en}} = - \sum_{m=1}^M \int dx \hat{\psi}^\dagger(x) \frac{Z_m}{|\mathbf{R}_m - \mathbf{r}|} \hat{\psi}(x). \quad (1.23)$$

The nuclear position vectors  $\mathbf{R}_m$  of the Schrödinger representation (position representation) will occasionally be replaced by general operators  $\hat{\mathbf{R}}_m$  leaving open the representation of the nuclear part of the quantum state.

## 1.2 Reduced Density Matrices and Densities

In this section we suppress the nuclear variables for the sake of brevity and consider electronic states like (1.20) with the nuclear positions fixed, at values  $\mathbf{R}_m$ , say. We already mentioned the uselessness of the  $N$ -particle wavefunction in its full glory. Indeed, practically all for real measurements relevant operators consist of terms depending on a few of the particle variables or on simple combinations of them only. Typical examples are the operators (1.2–1.4) or their field-quantized counterparts (1.21–1.23). The operators (1.4) and (1.2) are local and quasi-local, resp., examples of a general single-particle operator  $\hat{A}_1 = \sum_i A_1(x'_i; x_i)$ :

$$V_{\text{en}}(x'_i; x_i) = v(\mathbf{r}_i) \delta(x'_i - x_i), \quad v(\mathbf{r}) = - \sum_{m=1}^M \frac{Z_m}{|\mathbf{r} - \mathbf{R}_m|}, \quad (1.24)$$

$$t(x'_i; x_i) = -\frac{1}{2} \delta(x'_i - x_i) \frac{\partial^2}{\partial \mathbf{r}_i^2} = -\frac{\delta_{s'_i s_i}}{2} \frac{\partial^2 \delta(\mathbf{r}'_i - \mathbf{r}_i)}{\partial \mathbf{r}_i^2}. \quad (1.25)$$

It is easily seen that the expectation value of a single-particle operator in the wavefunction state (1.20) at time  $t$  is obtained already with the help of the single-particle density matrix of that state,

$$n_1(x|x'; t) = N \int dx_2 \cdots dx_N \Psi(x, x_2, \dots, x_N; t) \Psi^*(x', x_2, \dots, x_N; t), \quad (1.26)$$

as

$$\langle A_1 \rangle_t = \int dx dx' n_1(x|x'; t) A_1(x'; x) = \text{tr}(n_1 A_1). \quad (1.27)$$

If  $n_{1,\alpha}$  is the single particle density matrix of the state  $|\Psi_\alpha\rangle$ , then  $n_1 = \sum_\alpha p_\alpha n_{1,\alpha}$  is the single-particle density matrix of the statistical state (1.12). The expectation value of the local operator  $\hat{V}_{\text{en}}$  can even be obtained with the particle density

$$n_1(x; t) = n_1(x|x; t) \quad (1.28)$$

only.

The electron-electron interaction operator (1.3) is a local example of a general two-particle operator  $\hat{A}_2 = (1/2) \sum_{ij} A_2(x'_i, x'_j; x_i, x_j)$ :

$$V_{\text{ee}}(x'_i, x'_j; x_i, x_j) = \frac{\delta(x'_i - x_i) \delta(x'_j - x_j)}{|\mathbf{r}_i - \mathbf{r}_j|}. \quad (1.29)$$

Its expectation value,

$$\langle A_2 \rangle_t = \int dx_1 dx_2 dx'_1 dx'_2 n_2(x_1, x_2|x'_1, x'_2; t) A_2(x'_1, x'_2; x_1, x_2) = \text{tr}(n_2 A_2), \quad (1.30)$$

is obtained with the help of the two-particle density matrix  $n_2$  which in a wavefunction state is defined as

$$n_2(x_1, x_2|x'_1, x'_2; t) = \binom{N}{2} \int dx_3 \cdots dx_N \Psi(x_1, x_2, x_3, \dots, x_N; t) \Psi^*(x'_1, x'_2, x_3, \dots, x_N; t) \quad (1.31)$$

and in a statistical state analogous to  $n_1$ . Again, the expectation value of  $\hat{V}_{\text{ee}}$  can already be obtained with the help of the two-particle density  $n_2(x_1, x_2; t) = 2! n_2(x_1, x_2|x_1, x_2; t)$  which is the probability to find one particle at  $x_1$  (no matter which one) and one particle at  $x_2$ .

It is clear how these constructions can be continued up to the  $N$ -particle density matrix  $n_N = \langle x_1, \dots, x_N | \hat{\rho}(t) | x'_1, \dots, x'_N \rangle$  with  $\hat{\rho}$  from (1.12).

In field quantization one has

$$\hat{A}_1 = \int dx' dx \hat{\psi}^\dagger(x') A_1(x'; x) \hat{\psi}(x), \quad (1.32)$$

$$\hat{A}_2 = \frac{1}{2} \int dx'_1 dx'_2 dx_1 dx_2 \hat{\psi}^\dagger(x'_1) \hat{\psi}^\dagger(x'_2) A_2(x'_1, x'_2; x_1, x_2) \hat{\psi}(x_2) \hat{\psi}(x_1) \quad (1.33)$$

and

$$n_1(x|x'; t) = \langle \hat{\psi}^\dagger(x') \hat{\psi}(x) \rangle_t \equiv \text{tr}(\hat{\rho} \hat{\psi}^\dagger(x') \hat{\psi}(x)), \quad (1.34)$$

$$n_2(x_1, x_2|x'_1, x'_2; t) = \langle \hat{\psi}^\dagger(x'_1) \hat{\psi}^\dagger(x'_2) \hat{\psi}(x_2) \hat{\psi}(x_1) \rangle_t \equiv \text{tr}(\hat{\rho} \hat{\psi}^\dagger(x'_1) \hat{\psi}^\dagger(x'_2) \hat{\psi}(x_2) \hat{\psi}(x_1)). \quad (1.35)$$

It is immediately seen that (1.27) and (1.30) hold true with these expressions.

In most cases the knowledge of  $n_1$  and  $n_2$  would suffice to determine the relevant experimental quantities. These reduced density matrices depend on a few variables instead of the  $\sim 10^{23}$  variables on which the  $N$ -particle wavefunction of a solid depends. However, the time dependence of the reduced density matrices cannot be determined in any direct way. Instead of a closed set of dynamical equations one finds himself with an open system of a quantum BBGKY hierarchy structure.



### 1.3 Correlation Functions

Up to here we used the *Schrödinger* picture of quantum theory in which the quantum states  $|\Psi(t)\rangle$  are time-dependent and describe the quantum dynamics by yielding time-dependent expectation values  $\langle A \rangle_t = \langle \Psi(t) | \hat{A} | \Psi(t) \rangle$  of time-independent operators  $\hat{A}$ . By inserting (1.11) for  $\Psi(t)$ :

$$\langle A \rangle_t = \langle \Psi(t) | \hat{A} | \Psi(t) \rangle = \langle \Psi_0 | e^{it\hat{H}} \hat{A} e^{-it\hat{H}} | \Psi_0 \rangle, \quad (1.36)$$

it is immediately seen that the dynamics is likewise described by time-dependent operators

$$\hat{A}(t) = e^{it\hat{H}} \hat{A} e^{-it\hat{H}} \quad (1.37)$$

and time-independent quantum states  $|\Psi_0\rangle$ . This is the *Heisenberg picture*. (For the sake of completeness of the argument given note that it holds for any matrix element  $\langle \Phi | \hat{A} | \Psi \rangle$ , not just for the expectation value.)

The same reasoning applies to the time evolution of an expectation value with a statistical state (1.12):

$$\langle A \rangle_t = \text{tr}(\hat{\rho}(t) \hat{A}) = \text{tr}(e^{-it\hat{H}} \hat{\rho} e^{it\hat{H}} \hat{A}) = \text{tr}(\hat{\rho} e^{it\hat{H}} \hat{A} e^{-it\hat{H}}) = \text{tr}(\hat{\rho} \hat{A}(t)). \quad (1.38)$$

The time dependence of the statistical operator  $\hat{\rho}$  follows directly from (1.12, 1.11). Since this operator describes a state and not an observable, its time-dependence is reversed to (1.37) and appears in the Schrödinger picture while  $\hat{\rho}$  is time independent in the Heisenberg picture. The transition between both pictures is provided by the invariance of the trace of a product under cyclic permutations of the factors.

From (1.37) and (1.38) it is readily seen that  $A$  is conserved if its operator  $\hat{A}$  commutes with  $\hat{H}$ .

A more democratic interpretation of the relations (1.36) and (1.38) is by giving the exponentiated operators an independent physical meaning as members of a family of time-evolution operators with algebraic group property, where the operator of evolution from time  $t_1$  to time  $t_2$  is

$$\hat{U}(t_2, t_1) = e^{-i(t_2-t_1)\hat{H}}, \quad \hat{U}(t_3, t_2) \hat{U}(t_2, t_1) = \hat{U}(t_3, t_1). \quad (1.39)$$

(Since the sequence of the conventional application to the right of a product of operators is from right to left, the ‘time arrow of formulas in this context’ is also from right to left.) Then, (1.36) is cast into

$$\langle A \rangle_t = \langle \Psi(0) | \hat{U}(0, t) \hat{A} \hat{U}(t, 0) | \Psi(0) \rangle = \langle \Psi(t_0) | \hat{U}(t_0, t) \hat{A} \hat{U}(t, t_0) | \Psi(t_0) \rangle, \quad (1.40)$$

which reads: The system was prepared in the quantum state  $\Psi$  at time  $t_0$  (or 0), evolved freely to time  $t$  when a measuring device  $A$  was applied, and the average result of this application is obtained by rewinding the manipulated state back to time  $t_0$  (or 0) and projecting it onto the initial state.

The latter interpretation immediately allows for the description of more general processes as for instance

$$\begin{aligned} \langle \Psi(t_0) | \hat{U}(t_0, t_2) \hat{\psi}(x_2) \hat{U}(t_2, t_1) \hat{\psi}^\dagger(x_1) \hat{U}(t_1, t_0) | \Psi(t_0) \rangle &= \\ = \langle \Psi(t_0) | \hat{U}(t_0, t_2) \hat{\psi}(x_2) \hat{U}(t_2, t_0) \hat{U}(t_0, t_1) \hat{\psi}^\dagger(x_1) \hat{U}(t_1, t_0) | \Psi(t_0) \rangle &= \\ = \langle \Psi(t_0) | \hat{\psi}(x_2 t_2) \hat{\psi}^\dagger(x_1 t_1) | \Psi(t_0) \rangle. \end{aligned}$$

In the system prepared at time  $t_0$  an additional particle is tried to be created at position  $\mathbf{r}_1$  with  $z$ -axis spin projection  $s_1$ , at time  $t_1$ , then a particle at  $\mathbf{r}_2, s_2$  is tried to be removed

at time  $t_2$ , and the resulting state is rewound to time  $t_0$  where it is projected onto the initial state. Here, the field operators are not observables (they are not Hermitian), they provide transitions with a change in particle number, and the square of this double-time correlation function is the probability that the system is found back in the initial state after the described sequence of manipulations has been performed. There are kinematic constraints to those transitions because of the (anti-)symmetry of the wavefunction, whence the phrase ‘is tried to’. In most applications  $\Psi(t_0)$  is assumed to be a stationary state, and then the reference time  $t_0$  is irrelevant. It may also be a (stationary) statistical state, and the final definition of the corresponding *double-time correlation function* is

$$C^>(x_2t_2, x_1t_1) \equiv -i\langle\hat{\psi}(x_2t_2)\hat{\psi}^\dagger(x_1t_1)\rangle, \quad t_2 > t_1, \quad \langle\cdots\rangle = \langle\Psi|\cdots|\Psi\rangle \text{ or } \text{tr}(\hat{\rho}\cdots). \quad (1.41)$$

(The factor  $-i$  is convention for later convenience.)

A related process of interest would be, first at time  $t_1$  to try to remove a particle from  $\mathbf{r}_1, s_1$  and, at a later time  $t_2$ , to try to add a particle at  $\mathbf{r}_2, s_2$ , expecting the system to return to the (time evolved without perturbation) initial state. The probability of this process is another double-time correlation function

$$C^<(x_1t_1, x_2t_2) \equiv i\langle\hat{\psi}^\dagger(x_2t_2)\hat{\psi}(x_1t_1)\rangle, \quad t_2 > t_1. \quad (1.42)$$

(The superscripts  $>$  and  $<$  symbolize the direction of increasing time in the arguments of  $C$ .)

Note that the Heisenberg field operators

$$\hat{\psi}(xt) = e^{it\hat{H}}\hat{\psi}(x)e^{-it\hat{H}} \quad (1.43)$$

for *different* times  $t$  and  $t'$  do not any more obey simple anticommutation relations as (1.18), which still hold at *equal* times  $t = t'$ .

Comparison with (1.34, 1.28) immediately reveal

$$C^<(xt, x't) = in_1(x|x';t), \quad C^<(xt, xt) = in_1(x;t). \quad (1.44)$$

Correlation functions of field operators are generalizations of reduced density matrices.

In order to illustrate the kind of additional information contained in double-time correlation functions, we consider a model of interaction-free electrons in a box of volume  $V$  with periodic boundary conditions,

$$\hat{H} = \hat{t} - \mu\hat{N}. \quad (1.45)$$

In the ground state, plane-wave orbitals

$$\phi_{\mathbf{k}\sigma}(\mathbf{r}, s) = \frac{1}{\sqrt{V}}e^{i\mathbf{k}\cdot\mathbf{r}}\delta_{\sigma s}, \quad \sigma = \uparrow, \downarrow \quad (1.46)$$

are occupied for  $|\mathbf{k}| \leq k_F = (3\pi^2n_1)^{1/3}$ ,  $\epsilon = k^2/2 \leq \epsilon_F = \mu = k_F^2/2$ . All plane-wave orbitals with arbitrary  $\mathbf{k}$  compatible with the boundary conditions and for both values  $\sigma$  form a complete set of orbitals, hence

$$\hat{\psi}(x) = \sum_{\mathbf{k}\sigma} \phi_{\mathbf{k}\sigma}(x)\hat{c}_{\mathbf{k}\sigma}, \quad \hat{\psi}^\dagger(x) = \sum_{\mathbf{k}\sigma} \hat{c}_{\mathbf{k}\sigma}^\dagger\phi_{\mathbf{k}\sigma}^*(x), \quad (1.47)$$

where the  $\hat{c}_{\mathbf{k}\sigma}$  and  $\hat{c}_{\mathbf{k}\sigma}^\dagger$  are destruction and creation operators, resp., of orbitals  $\phi_{\mathbf{k}\sigma}$ .

Now,  $C^>$  is easily calculated from (1.41):

$$\begin{aligned}
C^>(x_2 t_2, x_1 t_1) &= -i \sum_{\mathbf{k}\sigma} \sum_{\mathbf{k}'\sigma'} \phi_{\mathbf{k}\sigma}(x_2) \phi_{\mathbf{k}'\sigma'}^*(x_1) \langle \hat{c}_{\mathbf{k}\sigma}(t_2) \hat{c}_{\mathbf{k}'\sigma'}^\dagger(t_1) \rangle = \\
&= \frac{-i\delta_{s_1 s_2}}{V} \sum_{\mathbf{k}}^{k > k_F} e^{i\mathbf{k}\cdot(\mathbf{r}_2 - \mathbf{r}_1)} \langle \hat{c}_{\mathbf{k}s_1}(t_2) \hat{c}_{\mathbf{k}s_1}^\dagger(t_1) \rangle = \\
&= \frac{-i\delta_{s_1 s_2}}{V} \sum_{\mathbf{k}}^{k > k_F} e^{i\mathbf{k}\cdot(\mathbf{r}_2 - \mathbf{r}_1)} \langle e^{it_2 \hat{H}} \hat{c}_{\mathbf{k}s_1} e^{-i(t_2 - t_1) \hat{H}} \hat{c}_{\mathbf{k}s_1}^\dagger e^{-it_1 \hat{H}} \rangle = \\
&= \frac{-i\delta_{s_1 s_2}}{V} \sum_{\mathbf{k}}^{k > k_F} e^{i\mathbf{k}\cdot(\mathbf{r}_2 - \mathbf{r}_1)} e^{it_2 E_0} e^{-i(t_2 - t_1)(E_0 + \epsilon_k - \mu)} e^{-it_1 E_0} = \\
&= \frac{-i\delta_{s_1 s_2}}{V} \sum_{\mathbf{k}}^{k > k_F} e^{i\mathbf{k}\cdot(\mathbf{r}_2 - \mathbf{r}_1) - i(\epsilon_k - \mu)(t_2 - t_1)} = \\
&= \frac{\delta_{s_1 s_2}}{V} \sum_{\mathbf{k}} \int_{-\infty}^{\infty} \frac{d\omega}{2\pi} C_{s_1}^>(\mathbf{k}\omega) e^{i\mathbf{k}\cdot(\mathbf{r}_2 - \mathbf{r}_1) - i\omega(t_2 - t_1)}.
\end{aligned}$$

after inserting (1.47) into (1.41), one has to realize that the  $\hat{c}$ -operators in the given case create and annihilate stationary states, hence  $\langle \dots \rangle \sim \delta_{\mathbf{k}\mathbf{k}'} \delta_{\sigma\sigma'} \theta(k - k_F)$ , where  $\theta$  is the step function. Further,  $E_0 = t_0 - \mu N_0$  is the ground state expectation value of  $\hat{H}$  from (1.45), and finally,  $C_{s_1}^>$  is introduced as the Fourier transform of  $C^>(x_2 t_2, x_1 t_1)$  with respect to  $\mathbf{r}_2 - \mathbf{r}_1$  and  $t_2 - t_1$ . From comparing the last two lines (after renaming  $s_1$  into  $\sigma$ ),

$$C_\sigma^>(\mathbf{k}\omega) = -2\pi i \theta(k - k_F) \delta(\omega - \epsilon_k + \mu), \quad (1.48)$$

$$\sum_{\mathbf{k}\sigma} C_\sigma^>(\mathbf{k}\omega) = -2\pi i \theta(\omega) D(\omega), \quad (1.49)$$

which is  $-2\pi i$  times the *density of unoccupied states* with excitation energy  $\omega$ . Analogously one finds from the complex conjugate of (1.42)

$$C_\sigma^<(\mathbf{k}\omega) = 2\pi i \theta(k_F - k) \delta(\omega - \epsilon_k + \mu), \quad (1.50)$$

$$\sum_{\mathbf{k}\sigma} C_\sigma^<(\mathbf{k}\omega) = 2\pi i \theta(-\omega) D(\omega), \quad (1.51)$$

which latter is  $2\pi i$  times the *density of occupied states* with binding energy  $\omega$ .

Double-time correlation functions contain in addition to the full information on the reduced density matrix *spectroscopic information* which makes them particularly useful in thermodynamics and quantum kinetics.

The results (1.48–1.51) are easily generalized to non-zero temperature. In this case we start from

$$\begin{aligned}
e^{it\hat{H}} \hat{c}_{\mathbf{k}\sigma} e^{-it\hat{H}} &= \hat{c}_{\mathbf{k}\sigma} e^{-it(\epsilon_k - \mu)}, \\
e^{it\hat{H}} \hat{c}_{\mathbf{k}\sigma}^\dagger e^{-it\hat{H}} &= \hat{c}_{\mathbf{k}\sigma}^\dagger e^{it(\epsilon_k - \mu)},
\end{aligned} \quad (1.52)$$

which is obviously valid in application to any occupation number eigenstate and hence in general. Then,

$$\begin{aligned}
\langle \hat{c}_{\mathbf{k}\sigma}(t_2) \hat{c}_{\mathbf{k}\sigma}^\dagger(t_1) \rangle &= \text{tr}(e^{-\beta \hat{H}} e^{it_2 \hat{H}} \hat{c}_{\mathbf{k}\sigma} e^{-i(t_2 - t_1) \hat{H}} \hat{c}_{\mathbf{k}\sigma}^\dagger e^{-it_1 \hat{H}}) / \text{tr} e^{-\beta \hat{H}} = \\
&= e^{-i(\epsilon_k - \mu)(t_2 - t_1)} \text{tr}(e^{-\beta \hat{H}} \hat{c}_{\mathbf{k}\sigma} \hat{c}_{\mathbf{k}\sigma}^\dagger) / \text{tr} e^{-\beta \hat{H}} = \\
&= e^{-i(\epsilon_k - \mu)(t_2 - t_1)} \langle \hat{c}_{\mathbf{k}\sigma} \hat{c}_{\mathbf{k}\sigma}^\dagger \rangle = e^{-i(\epsilon_k - \mu)(t_2 - t_1)} (1 - \langle \hat{c}_{\mathbf{k}\sigma}^\dagger \hat{c}_{\mathbf{k}\sigma} \rangle), \\
\langle \hat{c}_{\mathbf{k}\sigma}^\dagger(t_2) \hat{c}_{\mathbf{k}\sigma}(t_1) \rangle &= e^{i(\epsilon_k - \mu)(t_2 - t_1)} \langle \hat{c}_{\mathbf{k}\sigma}^\dagger \hat{c}_{\mathbf{k}\sigma} \rangle.
\end{aligned}$$

With the well known result from statistical physics,

$$\langle \hat{c}_{\mathbf{k}\sigma}^\dagger \hat{c}_{\mathbf{k}\sigma} \rangle = f_T(\epsilon_{\mathbf{k}} - \mu) = [e^{\beta(\epsilon_{\mathbf{k}} - \mu)} + 1]^{-1}, \quad \beta = T^{-1}, \quad (1.53)$$

the final answer is that in (1.48–1.51) the step function  $\theta$  has to be replaced by  $(1 - f_T)$  and  $f_T$ , resp. (We have put  $k_B = 1$  and measure temperatures in energy units.)

The simple structure of the above correlation functions followed directly from the stationarity of single-particle excitations in an interaction-free system. This had the consequence that for a given momentum  $\mathbf{k}$  of the particle its excitation energy or binding energy (excitation energy of the hole a removed particle leaves behind) is uniquely determined. In an interacting system like real matter this is no longer true. A single-particle (or hole) excitation at time  $t_1$  will dissipate its momentum and energy into the whole system and thus decay. However, in most cases the decay time has a maximum at a certain relation between energy and momentum of the excited particle (hole) which is large enough so that in a zero-order approximation the decay process can be neglected. Then, the interaction only will be manifested in an (often dramatically) modified dispersion relation between energy and momentum of this *quasi-particle* excitation. Even in the general case, the expectation values (1.41, 1.42) remain relevant for the response of the system to a time-dependent external perturbation or to an energy-biasing external potential. Then, the expressions (1.49) and (1.51) *define* a density of states, and it is exclusively this type of quantity which is addressed if one speaks of a density of states in condensed matter physics.

Of course, correlation functions may be considered for all kinds of field operators as well as for more general operators formed of a few field operators:

$$C^{AB}(t_2, t_1) = -i \langle \hat{A}(t_2) \hat{B}(t_1) \rangle. \quad (1.54)$$

However, their direct calculation for an interacting system is still an awful task, and we will not consider them before having studied certain combinations of correlation functions with enormously helpful properties, called Green's functions.

## Chapter 2

# Green's Functions

There figure two classes of Green's functions<sup>1</sup> in Quantum Statistics with complementary properties but with equal importance. The *ordinary*, sometimes called causal Green's functions are defined as

$$G(x, x'; t) = -i \langle \mathbf{T} [\hat{\psi}(xt) \hat{\psi}^\dagger(x'0)] \rangle, \quad \langle \cdots \rangle = \text{tr}(e^{-\beta \hat{H}} \cdots) / \text{tr} e^{-\beta \hat{H}} \text{ or } \langle \Psi_0 | \cdots | \Psi_0 \rangle, \quad (2.1)$$

where  $\mathbf{T}$  is Wick's time ordering operator which orders any product of Heisenberg operators right to its appearance in the order of descending times from left to right, independent of the order of writing in the product, and necessary permutations of fermionic operators thereby providing with a statistics factor  $-1$ . For non-zero temperature the average is understood with the grand-canonical statistical operator, and for  $T \rightarrow 0$  it is, in the simplest case, with the ground state  $\Psi_0$ .<sup>2</sup> It has been taken into account that those averages depend only on the time difference  $t$  between the two Heisenberg operators as mentioned before (1.41), whence the reference time has been put arbitrarily to zero in the above definition. This Green's function is (after a generalization of the time argument in the  $T > 0$  case, see Section 2.3) subject to the famous Wick theorem which is the basis of a diagrammatic expansion. It is this function which is normally calculated. It has the disadvantage that its Fourier transform is not analytic on either side of the real energy axis, in particular not for  $T > 0$ . The connection of this Green's function with the double-time correlation functions of the last chapter and hence also with reduced density matrices and mean values of observables is obvious from the definition.

The *retarded* and *advanced* Green's functions are defined as

$$G^{r/a}(x, x'; t) = \mp i \theta(\pm t) \left\langle [\hat{\psi}(xt), \hat{\psi}^\dagger(x'0)]_{\zeta} \right\rangle, \quad \zeta = \begin{cases} + & \text{fermions} \\ - & \text{bosons} \end{cases}. \quad (2.2)$$

The upper sign in front and in the time argument of the step function  $\theta$  is for the retarded and the lower sign for the advanced functions. The (anti-)commutator  $[\cdots]_{\zeta}$  is to be taken in accordance with the statistics of the field operators  $\hat{\psi}$ . These Green's functions are by definition non-zero only for a definite sign of time, and hence their Fourier transforms are Herglotz: they are analytic in the whole of one half-plane of the complex energy plane. They are in particular providing densities of states and spectral properties of physical relevance. They are in a well defined way connected with the ordinary Green's functions and that is how they are obtained in practical calculations.

<sup>1</sup>A. A. Abrikosov, L. P. Gorkov and I. E. Dzyaloshinski, *Methods of Quantum Field Theory in Statistical Physics*, Dover, New York, 1975.

L. D. Landau and E. M. Lifshits, *Statistical Physics*, Part II, Pergamon, London, 1980.

<sup>2</sup>See, however, W. Kohn and J. M. Luttinger, *Phys. Rev.* **118**, 41 (1960).

Like in the case of correlation functions, one may consider more general Green's functions  $G_{AB}(t)$  for pairs of operators  $\hat{A}$  and  $\hat{B}$  (cf. (1.54)).

## 2.1 Spectral Representation

Let us start with the retarded and advanced Green's functions. Introduce a complete set of stationary states of the grand canonical Hamiltonian:

$$\hat{1} = \sum_m |\Psi_m\rangle\langle\Psi_m|, \quad \hat{H}|\Psi_m\rangle = |\Psi_m\rangle\epsilon_m = |\Psi_m\rangle(E_m - \mu N_m), \quad \epsilon_{mn} = \epsilon_m - \epsilon_n, \quad (2.3)$$

where  $\hat{1}$  is the unit operator, and

$$e^{-\beta\hat{H}} = \sum_n |\Psi_n\rangle e^{-\beta\epsilon_n} \langle\Psi_n|, \quad p_n = e^{-\beta\epsilon_n} / \text{tr} e^{-\beta\hat{H}}. \quad (2.4)$$

Then,

$$\begin{aligned} G^{r/a}(x, x'; t) &= \frac{\mp i\theta(\pm t)}{\text{tr} e^{-\beta\hat{H}}} \left\{ \text{tr} (e^{-\beta\hat{H}} e^{it\hat{H}} \hat{\psi}(x) e^{-it\hat{H}} \hat{\psi}^\dagger(x')) + \zeta \text{tr} (e^{-\beta\hat{H}} \hat{\psi}^\dagger(x') e^{it\hat{H}} \hat{\psi}(x) e^{-it\hat{H}}) \right\} \\ &= \mp i\theta(\pm t) \sum_{mn} e^{-i\epsilon_{mn}t} \langle\Psi_n|\hat{\psi}(x)|\Psi_m\rangle \langle\Psi_m|\hat{\psi}^\dagger(x')|\Psi_n\rangle \frac{\{e^{-\beta\epsilon_n} + \zeta e^{-\beta\epsilon_m}\}}{\text{tr} e^{-\beta\hat{H}}} = \\ &= \mp i\theta(\pm t) \sum_{mn} e^{-i\epsilon_{mn}t} A_{mn}(x, x') p_n (1 + \zeta e^{-\beta\epsilon_{mn}}). \end{aligned} \quad (2.5)$$

In the second trace, the summations over  $m$  and  $n$  were interchanged as compared to the first in order to get the same matrix elements. Then, the abbreviation  $A_{mn}(x, x') = \langle\Psi_n|\hat{\psi}(x)|\Psi_m\rangle \langle\Psi_m|\hat{\psi}^\dagger(x')|\Psi_n\rangle = A_{mn}^*(x', x)$  was introduced.

Fourier transformation of the retarded function yields (for the sake of brevity we omit the arguments  $x, x'$ ; to ensure convergence of the Fourier integral, an infinitesimal imaginary part is added to the energy variable  $\epsilon$ .)

$$\begin{aligned} G^r(\epsilon + i0) &= -i \int_0^\infty dt e^{i(\epsilon+i0)t} \sum_{mn} e^{-i\epsilon_{mn}t} A_{mn} p_n (1 + \zeta e^{-\beta\epsilon_{mn}}) = \\ &= \sum_{mn} \frac{A_{mn} p_n}{\epsilon - \epsilon_{mn} + i0} (1 + \zeta e^{-\beta\epsilon_{mn}}), \end{aligned} \quad (2.6)$$

and for the advanced function,

$$G^a(x, x'; \epsilon - i0) = i \int_{-\infty}^0 dt e^{i(\epsilon-i0)t} \sum_{mn} \dots = i \int_0^\infty du e^{-i(\epsilon-i0)u} \sum_{mn} \dots = \left[ G^r(x', x; \epsilon + i0) \right]^*,$$

or, more generally,

$$G^a(x, x'; \epsilon^*) = \left[ G^r(x', x; \epsilon) \right]^*. \quad (2.7)$$

Hence,  $G^r(\epsilon)$  has poles below the real  $\epsilon$ -axis for  $\epsilon = \epsilon_{mn} - i0$ , and is analytic in the upper complex  $\epsilon$ -half-plane.  $G^a(\epsilon)$  has poles above the real  $\epsilon$ -axis and is analytic in the lower complex  $\epsilon$ -half-plane. In the thermodynamic limit, the pole positions  $\epsilon_{mn} \mp i0$  become dense and coalesce into branch lines of the complex functions  $G^{r/a}(\epsilon)$ .

By definition, the Green's function is given by *finite* expectation values for any  $t$ . Hence, the double sum of (2.6) is absolutely converging in the domain of analyticity. If we consider the limes  $|\epsilon| \rightarrow \infty$  in this domain, it may be interchanged with the summations, resulting in

$$\lim_{|\epsilon| \rightarrow \infty} G^{r/a}(\epsilon) = \frac{1}{\epsilon} \sum_{mn} A_{mn} p_n (1 + \zeta e^{-\beta \epsilon_{mn}}) \quad \text{for} \quad \text{Im} \epsilon \begin{cases} > 0 & \text{retarded} \\ < 0 & \text{advanced.} \end{cases}$$

The remaining double sum may be calculated by a derivation reversed to the above:

$$\begin{aligned} \sum_{mn} A_{mn} p_n (1 + \zeta e^{-\beta \epsilon_{mn}}) &= \sum_{mn} \langle \Psi_n | \hat{\psi}(x) | \Psi_m \rangle \langle \Psi_m | \hat{\psi}^\dagger(x') | \Psi_n \rangle (e^{-\beta \epsilon_n} + \zeta e^{-\beta \epsilon_m}) / \text{tr} e^{-\beta \hat{H}} \\ &= \text{tr} \left( e^{-\beta \hat{H}} [\hat{\psi}(x), \hat{\psi}^\dagger(x')] \right) / \text{tr} e^{-\beta \hat{H}} = \delta(x - x'), \end{aligned}$$

hence, finally,

$$\lim_{|\epsilon| \rightarrow \infty} G^{r/a}(x, x'; \epsilon) = \frac{\delta(x - x')}{\epsilon} \quad \text{for} \quad \text{Im} \epsilon \begin{cases} > 0 & \text{retarded} \\ < 0 & \text{advanced.} \end{cases} \quad (2.8)$$

This result will become essential for calculating the retarded (advanced) Green's function from the normal one.

The most important consequence of the analytic properties is that for real  $\epsilon$  the real and imaginary parts of  $G^{r/a}(\epsilon)$  are connected. Use the theorem of residues to obtain (P denotes the principal value of the integral)

$$\int_{-\infty}^{\infty} d\epsilon' \frac{1}{\epsilon' - \epsilon \pm i0} = \int_{-\infty}^{\infty} d\epsilon' \left( \text{P} \frac{1}{\epsilon' - \epsilon} \mp i\pi \delta(\epsilon' - \epsilon) \right),$$

which in the meaning of distributions is *Dyson's formula*

$$\frac{1}{\epsilon' - \epsilon \pm i0} = \text{P} \frac{1}{\epsilon' - \epsilon} \mp i\pi \delta(\epsilon' - \epsilon) \quad (2.9)$$

(saying that the above integral relation remains valid, if the integrands on both sides are multiplied by a sufficiently smooth function of  $\epsilon'$ ). Multiply both sides with  $G^{r/a}(\epsilon')$  and integrate again. On the left hand side of the resulting integral relation, the path of integration may be closed in the upper half-plane for  $G^r$  and in the lower half-plane for  $G^a$  yielding zero in both cases for the closed integral. Now, the asymptotics (2.8) also yields zero separately for the integral on the infinite half-circle, and thus also for the integral along the real axis. The immediate result is

$$G^{r/a}(\epsilon) = \mp \frac{i}{\pi} \text{P} \int_{-\infty}^{\infty} d\epsilon' \frac{G^{r/a}}{\epsilon' - \epsilon}.$$

Separating in this result the real and imaginary parts yields the *Kramers-Kronig relations*:

$$\text{Re} G^{r/a}(\epsilon) = \pm \frac{1}{\pi} \text{P} \int_{-\infty}^{\infty} d\epsilon' \frac{\text{Im} G^{r/a}(\epsilon')}{\epsilon' - \epsilon}, \quad \text{Im} G^{r/a}(\epsilon) = \mp \frac{1}{\pi} \text{P} \int_{-\infty}^{\infty} d\epsilon' \frac{\text{Re} G^{r/a}(\epsilon')}{\epsilon' - \epsilon}. \quad (2.10)$$

These relations allow to complete the Green's function from the knowledge of its real or imaginary part alone.

We now provide the spectral representation for the normal Green's function:

$$\begin{aligned}
G(x, x'; t) &= \frac{-i}{\text{tr} e^{-\beta \hat{H}}} \left\{ \theta(t) \text{tr} (e^{-\beta \hat{H}} e^{it \hat{H}} \hat{\psi}(x) e^{-it \hat{H}} \hat{\psi}^\dagger(x')) - \right. \\
&\quad \left. - \zeta \theta(-t) \text{tr} (e^{-\beta \hat{H}} \hat{\psi}^\dagger(x') e^{it \hat{H}} \hat{\psi}(x) e^{-it \hat{H}}) \right\} = \\
&= -i \sum_{mn} e^{-i\epsilon_{mn} t} \langle \Psi_n | \hat{\psi}(x) | \Psi_m \rangle \langle \Psi_m | \hat{\psi}^\dagger(x') | \Psi_n \rangle \frac{\theta(t) e^{-\beta \epsilon_n} - \zeta \theta(-t) e^{-\beta \epsilon_m}}{\text{tr} e^{-\beta \hat{H}}} = \\
&= -i \sum_{mn} A_{mn} p_n e^{-i\epsilon_{mn} t} (\theta(t) - \zeta \theta(-t) e^{-\beta \epsilon_{mn}}).
\end{aligned} \tag{2.11}$$

Fourier transformation results in

$$\begin{aligned}
G(\epsilon) &= -i \sum_{mn} A_{mn} p_n \left\{ \int_0^\infty dt e^{i\epsilon t} e^{-i\epsilon_{mn} t} - \zeta \int_{-\infty}^0 dt e^{i\epsilon t} e^{-i\epsilon_{mn} t} e^{-\beta \epsilon_{mn}} \right\} = \\
&= \sum_{mn} A_{mn} p_n \left\{ \frac{1}{\epsilon - \epsilon_{mn} + i0} + \zeta \frac{e^{-\beta \epsilon_{mn}}}{\epsilon - \epsilon_{mn} - i0} \right\} = \\
&= \sum_{mn} A_{mn} p_n \left\{ \text{P} \frac{1 + \zeta e^{-\beta \epsilon_{mn}}}{\epsilon - \epsilon_{mn}} - i\pi \delta(\epsilon - \epsilon_{mn}) (1 - \zeta e^{-\beta \epsilon_{mn}}) \right\}.
\end{aligned} \tag{2.12}$$

Both time integrals do not converge any more simultaneously, so that  $G(\epsilon)$  is not an ordinary function: it is a distribution for real  $\epsilon$  and is not defined at all for complex  $\epsilon$ . In the last line, Dyson's formula (2.9) was used to separate the real and imaginary parts of  $G(\epsilon)$ .

In the bosonic case ( $\zeta = -1$ ), the imaginary part is negative. In the fermionic case ( $\zeta = 1$ ) its sign depends on the sign of  $\epsilon_{mn}$  and hence of  $\epsilon$ :

$$\begin{aligned}
\text{sign Im } G(\epsilon) &= -\text{sign } \epsilon && \text{fermions} \\
\text{Im } G(\epsilon) &< 0 && \text{bosons.}
\end{aligned} \tag{2.13}$$

Comparison with (2.6, 2.7) yields

$$G^{\text{r/a}}(\epsilon) = \text{Re } G(\epsilon) \pm i \coth^\zeta \frac{\beta \epsilon}{2} \text{Im } G(\epsilon), \tag{2.14}$$

which directly connects the Fourier transforms of the various Green's functions.

For the model (1.45) of interaction-free electrons in a box of volume  $V$  we find readily

$$\sum_{mn} A_{mn} p_n = \frac{\delta_{ss'}}{V} \sum_{\mathbf{k}} e^{i\mathbf{k} \cdot (\mathbf{r} - \mathbf{r}')} \langle \hat{c}_{\mathbf{k}s} \hat{c}_{\mathbf{k}s}^\dagger \rangle = \frac{\delta_{ss'}}{V} \sum_{\mathbf{k}} e^{i\mathbf{k} \cdot (\mathbf{r} - \mathbf{r}')} (1 - f_T(\epsilon_{\mathbf{k}} - \mu))$$

with  $f_T$  from (1.53). With  $\epsilon_{mn} = \epsilon_{\mathbf{k}} - \mu$  and  $(1 - f_T(\epsilon_{\mathbf{k}} - \mu))(1 + e^{-\beta(\epsilon_{\mathbf{k}} - \mu)}) = 1$ , (2.6) reduces to

$$G^{\text{r}}(x, x'; \epsilon + i0) = \frac{-i}{V} \sum_{\mathbf{k}} \frac{\delta_{ss'} e^{i\mathbf{k} \cdot (\mathbf{r} - \mathbf{r}')}}{\epsilon - \epsilon_{\mathbf{k}} + \mu + i0} = \frac{-i}{V} \sum_{\mathbf{k}} G_s^{\text{r}}(\mathbf{k}; \epsilon + i0) \delta_{ss'} e^{i\mathbf{k} \cdot (\mathbf{r} - \mathbf{r}')} \tag{2.15}$$

or

$$G_\sigma^{\text{r}}(\mathbf{k}; \epsilon + i0) = \frac{1}{\epsilon - \epsilon_{\mathbf{k}} + \mu + i0}, \tag{2.16}$$



$$D(\epsilon) = -\frac{1}{\pi} \text{Im} \sum_{\mathbf{k}\sigma} G_{\sigma}^r(\mathbf{k}; \epsilon) = -\frac{1}{\pi} \text{Im} \text{tr} G^r(\epsilon). \quad (2.17)$$

The free-particle retarded Green's function does not depend on temperature, and its pole for given  $\mathbf{k}$  yields the excitation energy  $\epsilon_k - \mu$  of particles and the negative of the excitation energies of holes. The imaginary part of the trace (sum of diagonal elements of the diagonal Green's function  $G_{\sigma\sigma'}^r(\mathbf{k}, \mathbf{k}') = \delta_{\sigma\sigma'} \delta_{\mathbf{k}\mathbf{k}'} G_{\sigma}^r(\mathbf{k})$ ) yields the single-particle density of states (for particles at positive  $\epsilon$  and for holes at negative  $\epsilon$ ). Observe, that  $\text{tr}_{\mathbf{k}} G = \sum_{\mathbf{k}} G(\mathbf{k}, \mathbf{k}) = \sum_{\mathbf{k}} \int d^3r d^3r' e^{-i\mathbf{k}\cdot\mathbf{r}} G(\mathbf{r}, \mathbf{r}') e^{i\mathbf{k}\cdot\mathbf{r}'} = \int d^3r d^3r' G(\mathbf{r}, \mathbf{r}') \sum_{\mathbf{k}} e^{i\mathbf{k}(\mathbf{r}'-\mathbf{r})} = \int d^3r G(\mathbf{r}, \mathbf{r}) = \text{tr}_{\mathbf{r}} G$ . For the advanced Green's function obtained from (2.7) corresponding statements hold true.

For an interacting system, (2.16) is no longer true. However, if the general retarded Green's function (2.6) which is analytical in the upper  $\epsilon$ -half-plane, for a given  $\mathbf{k}, \sigma$  is analytically continued into the lower half-plane of a corresponding Riemann surface (the lower half-plane under consideration belonging to the so called unphysical sheet of that surface), it might be that one hits a pole closest to the real  $\epsilon$ -axis, at position  $\eta_k = \text{Re} \eta_k - i |\text{Im} \eta_k|$ , so that in its vicinity the Green's function behaves as

$$G_{\sigma}^r(\mathbf{k}; \epsilon) = \frac{A_{\sigma}(\mathbf{k})}{\epsilon - \eta_k} + g_{\sigma}^r(\mathbf{k}; \epsilon), \quad (2.18)$$

where  $g_{\sigma}^r$  is regular in the vicinity of  $\epsilon = \eta_k$ . For real  $\epsilon$ , its imaginary part is

$$-\frac{1}{\pi} \text{Im} G_{\sigma}^r(\mathbf{k}; \epsilon) = \frac{A_{\sigma}(\mathbf{k}) |\text{Im} \eta_k|}{(\epsilon - \text{Re} \eta_k)^2 + (\text{Im} \eta_k)^2} - \frac{1}{\pi} \text{Im} g_{\sigma}^r. \quad (2.19)$$

The pole results in a Lorentzian peak instead of the  $\delta$ -peak in the interaction-free case. The time dependence due to this pole is

$$e^{-i \text{Re} \eta_k t} e^{-|\text{Im} \eta_k| t} = e^{-i \text{Re} \eta_k t} e^{-t/\tau_k}, \quad \tau_k = \frac{1}{|\text{Im} \eta_k|}. \quad (2.20)$$

The absolute value of the imaginary part of this pole position is the lifetime of that quasi-particle. Eq. (2.17) now defines again a spectral distribution relevant for the response of the system.

There is no real proof that the Green's function will have a pole. It appears in various approximations, or it is implemented into model expressions for Green's functions as a working approximation.

## 2.2 Equation of Motion

Differentiation of (1.43) yields the Heisenberg equation of motion of the Heisenberg field operators:

$$i \frac{\partial}{\partial t} \hat{\psi}(x,t) = [\hat{\psi}(x,t), \hat{H}] \quad (2.21)$$

and the same equation for  $\hat{\psi}^{\dagger}$ . With a (grand-canonical) Hamiltonian of the general form

$$\hat{H} = \int dx'_1 dx_1 \hat{\psi}^{\dagger}(x'_1 t) h(x'_1, x_1) \hat{\psi}(x_1 t) + \hat{H}_{\text{int}}(t), \quad (2.22)$$

where  $\hat{H}_{\text{int}}(t)$  consists of expressions with more than two field operators (recall that  $\hat{H} = \hat{H}(t)$ , but not separately  $\hat{H}_{\text{int}} = \hat{H}_{\text{int}}(t)$ ), the Heisenberg equation takes the form

$$\begin{aligned} i \frac{\partial}{\partial t} \hat{\psi}(xt) &= \int dx'_1 dx_1 h(x'_1, x_1) [\hat{\psi}(xt), \hat{\psi}^\dagger(x'_1 t) \hat{\psi}(x_1 t)] + [\hat{\psi}(x, t), \hat{H}_{\text{int}}(t)] = \\ &= \int dx'_1 dx_1 h(x'_1, x_1) \delta(x - x'_1) \hat{\psi}(x_1 t) + [\hat{\psi}(x, t), \hat{H}_{\text{int}}(t)] = \\ &= \int dx_1 h(x, x_1) \hat{\psi}(x_1 t) + [\hat{\psi}(x, t), \hat{H}_{\text{int}}(t)]. \end{aligned} \quad (2.23)$$

Now, the derivative of (2.2) is

$$i \frac{\partial}{\partial t} G^{r/a}(x, x'; t) = \delta(t) \left\langle [\hat{\psi}(xt), \hat{\psi}^\dagger(x'0)] \right\rangle \mp i\theta(\pm t) \left\langle \left[ i \frac{\partial}{\partial t} \hat{\psi}(xt), \hat{\psi}^\dagger(x'0) \right] \right\rangle.$$

Because of the  $\delta$ -function in the first term on the right hand side we may replace  $\hat{\psi}(xt)$  by  $\hat{\psi}(x0)$ , where after the equal-time (anti-)commutator is  $\delta(x - x')$ . In the second term we insert (2.23). The result is the equation of motion for the retarded and advanced Green's functions:

$$\begin{aligned} \int dx_1 \left( i\delta(x - x_1) \frac{\partial}{\partial t} - h(x, x_1) \right) G^{r/a}(x_1, x'; t) &= \delta(t) \delta(x - x') \mp \\ &\mp i\theta(\pm t) \left\langle \left[ [\hat{\psi}(x, t), \hat{H}_{\text{int}}(t)], \hat{\psi}^\dagger(x0) \right] \right\rangle. \end{aligned} \quad (2.24)$$

Depending on the actual content of  $\hat{H}_{\text{int}}(t)$ , most various terms may appear from the expansion of the last line of (2.24), they all will have the general structure of Green's functions with more than two field operators entering. Those Green's functions obviously will obey equations of motion of a similar structure, with even more complex Green's functions appearing on their right sides. Thus, we again end up with an open hierarchy of equations of motion for the Green's functions, and this is not the general way to calculate them. In rare cases it makes sense to close this hierarchy by approximating the higher Green's functions on their right hand sides with expressions in terms of the Green's functions figuring on the left hand sides and then to solve for the latter. One standard frame of this termination of the hierarchy by factorization is the Hartree-Fock approximation. We will not consider such an approach here because it is not leading to our goals.

In the interaction-free case,  $\hat{H}_{\text{int}} = 0$ , the second line of (2.24) is missing, and, after a Fourier transformation of the time dependence,  $G^{r/a}$  is just the kernel of the resolvent operator  $\hat{G} = (\epsilon - \hat{h})^{-1}$  for retarded and advanced boundary conditions:

$$\int dx_1 ((\epsilon \pm i0)\delta(x - x_1) - h(x, x_1)) G^{r/a}(x_1, x'; \epsilon) = \delta(x - x'). \quad (2.25)$$

This is a Green's function in the meaning of classical analysis, and that is where field theoretical Green's functions have got their name from. The even more specific case

$$\hat{h}\phi_{\mathbf{k}\sigma}(x) = \phi_{\mathbf{k}\sigma}(x)(\epsilon_{\mathbf{k}} - \mu) \quad (2.26)$$

via the orthonormality and completeness of the orbitals,

$$\langle \phi_{\mathbf{k}\sigma} | \phi_{\mathbf{k}'\sigma'} \rangle = \delta_{\mathbf{k}\mathbf{k}'} \delta_{\sigma\sigma'}, \quad \sum_{\mathbf{k}\sigma} \phi_{\mathbf{k}\sigma}(x) \phi_{\mathbf{k}\sigma}^*(x') = \delta(x - x'), \quad (2.27)$$

immediately reproduces (2.16) for

$$G_{\sigma}^{r/a}(\mathbf{k}; \epsilon) = \langle \phi_{\mathbf{k}\sigma} | (\epsilon \pm 0 - \hat{h})^{-1} | \phi_{\mathbf{k}\sigma} \rangle \quad (2.28)$$

with (2.17) as a direct consequence.

## 2.3 Complex Time

We now return to the ordinary Green's function (2.1) for the case of non-zero temperature and start with positive time,  $t > 0$ , that is,

$$t > 0: \quad G(x, x'; t) = -i \operatorname{tr} (e^{-\beta \hat{H}} e^{it \hat{H}} \hat{\psi}(x) e^{-it \hat{H}} \hat{\psi}^{\dagger}(x')) / \operatorname{tr} e^{-\beta \hat{H}}.$$

For algebraic manipulations of such expressions it would be desirable to include the statistical operator  $e^{-\beta \hat{H}}$  into the group of time evolution operators. To this end, we continue the time evolution group to include complex times,  $t \rightarrow t - i\tau$ . Since  $\hat{H}$  is bounded below, the operator  $e^{\alpha \hat{H}}$  has a well defined meaning for  $\operatorname{Re} \alpha \leq 0$  and the Taylor expansion of the exponential function converges absolutely for  $\operatorname{Re} \alpha < 0$  to an analytic function of  $\alpha$  (in the operator norm topology). This determines the domain of complex time, for which the above Green's function is well defined and in the interior of which it is analytic:

$$\text{domain I:} \quad -\infty < \operatorname{Re} t < \infty, \quad -\beta \leq \operatorname{Im} t \leq 0. \quad (2.29)$$

Considering

$$\begin{aligned} t < 0: \quad G(x, x'; t) &= \zeta i \operatorname{tr} (e^{-\beta \hat{H}} \hat{\psi}^{\dagger}(x') e^{it \hat{H}} \hat{\psi}(x) e^{-it \hat{H}}) / \operatorname{tr} e^{-\beta \hat{H}} = \\ &= \zeta i \operatorname{tr} (e^{-it \hat{H}} e^{-\beta \hat{H}} \hat{\psi}^{\dagger}(x') e^{it \hat{H}} \hat{\psi}(x)) / \operatorname{tr} e^{-\beta \hat{H}}, \end{aligned}$$

we see that this expression is analytic in the interior of the complex time domain

$$\text{domain II:} \quad -\infty < \operatorname{Re} t < \infty, \quad 0 \leq \operatorname{Im} t \leq \beta. \quad (2.30)$$

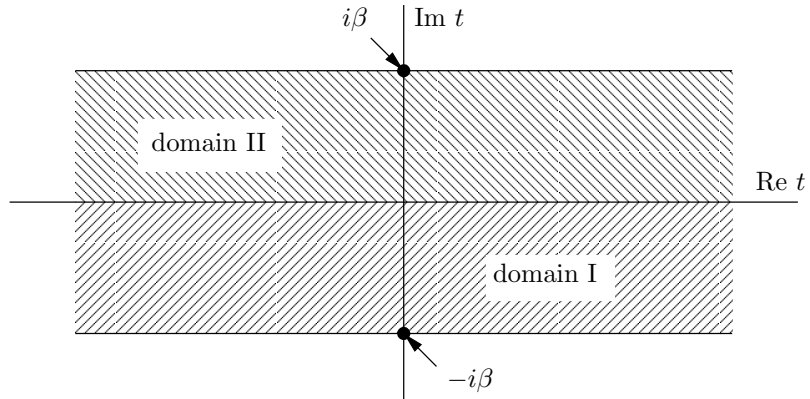


Figure 2.1: Domains of complex time.

Hence, there is a function defined on domain I and analytic in its interior which continues from the Green's function for positive real time, and there is *another* function on domain

II and analytic on its interior which continues from the Green's function for negative real time. Both functions are defined on the whole real axis of time, but are *different* there (see Fig. 2.1.). The Green's function of complex time, defined on both domains, is discontinuous on the whole real axis of time.<sup>3</sup>

There is a most important relation between the function values of the continued Green's function on both domains. Consider a  $t$ -value on domain I, the value  $t+i\beta$  is then in domain II, and the Green's function is

$$\begin{aligned} G(x, x'; t+i\beta) &= \zeta i \operatorname{tr} (e^{-\beta \hat{H}} \hat{\psi}^\dagger(x') e^{i(t+i\beta)\hat{H}} \hat{\psi}(x) e^{-i(t+i\beta)\hat{H}}) / \operatorname{tr} e^{-\beta \hat{H}} = \\ &= \zeta i \operatorname{tr} (e^{-\beta \hat{H}} e^{it\hat{H}} \hat{\psi}(x) e^{-it\hat{H}} \hat{\psi}^\dagger(x')) / \operatorname{tr} e^{-\beta \hat{H}} = \\ &= -\zeta G(x, x'; t). \end{aligned} \quad (2.31)$$

Only the definition (2.1) of the Green's function for positive and negative real time, corresponding to that on domain I and domain II, resp., and the invariance of a trace of a product under cyclic permutation of the factors was used. This relation was first considered by R. Kubo and independently by P. C. Martin and J. Schwinger, and is since called the *KMS condition*. As a condition on the Green's function it is decisive for the statistical state for which the Green's function is considered, to be thermal equilibrium.

For imaginary time,  $t = -i\tau$ , the Green's function is defined in the interval  $-\beta \leq \tau \leq \beta$ , and may be expanded into a Fourier series<sup>4</sup> (we again omit the arguments  $x, x'$ ):

$$G(-i\tau) = \frac{i}{\beta} \sum_{s=-\infty}^{\infty} e^{-i(i\epsilon_s)(-i\tau)} G(i\epsilon_s) = \frac{i}{\beta} \sum_{s=-\infty}^{\infty} e^{-i\epsilon_s \tau} G(i\epsilon_s). \quad (2.32)$$

Since the KMS condition demands  $G(-i(\tau+\beta)) = -\zeta G(-i\tau)$ ,  $e^{-i\epsilon_s(\tau+\beta)} = -\zeta e^{-i\epsilon_s \tau}$  must hold, hence

$$\epsilon_s = \begin{cases} (2s+1)\pi/\beta & \text{fermions} \\ 2s\pi/\beta & \text{bosons.} \end{cases} \quad (2.33)$$

Therefore,

$$iG(i\epsilon_s) = \frac{1}{2} \int_{-\beta}^{\beta} d\tau e^{i(i\epsilon_s)(-i\tau)} G(-i\tau) = \int_0^{\beta} d\tau e^{i\epsilon_s \tau} G(-i\tau). \quad (2.34)$$

This *Matsubara Green's function* is just the ordinary Green's function analytically continued to imaginary time, for  $\tau > 0$  from  $t > 0$  (domain I) and for  $\tau < 0$  from  $t < 0$  (domain II). Hence, its spectral representation for  $\tau > 0$  equals the analytical continuation of the spectral representation (2.11) for  $t > 0$ , and

$$\begin{aligned} G(i\epsilon_s) &= -\sum_{mn} A_{mn} p_n \int_0^{\beta} d\tau e^{i\epsilon_s \tau} e^{-i\epsilon_{mn}(-i\tau)} = \\ &= \sum_{mn} \frac{A_{mn} p_n}{i\epsilon_s - \epsilon_{mn}} (1 - e^{i\epsilon_s \beta} e^{-\epsilon_{mn} \beta}) = \\ &= \sum_{mn} \frac{A_{mn} p_n}{i\epsilon_s - \epsilon_{mn}} (1 + \zeta e^{-\epsilon_{mn} \beta}). \end{aligned}$$

<sup>3</sup>In order not to be confused the reader is reminded that we consider here the analytic properties of the Green's function as a function of complex time for the first time in this context, while in the previous sections we exclusively discussed the analytic properties of the Fourier transform of the Green's function as a function of complex energy  $\epsilon$ .

<sup>4</sup>This representation was first introduced by A. A. Abrikosov, L. P. Gorkov and I. E. Dzyaloshinski, 1959, and by E. S. Fradkin, 1959.

In the last equation,  $e^{i\epsilon_s\beta} = -\zeta$  was used which was the cause for (2.33). Comparison with (2.6) immediately reveals

$$G(i\epsilon_s) = \begin{cases} G^r(i\epsilon_s) & \text{for } \epsilon_s > 0 \\ G^a(i\epsilon_s) & \text{for } \epsilon_s < 0. \end{cases} \quad (2.35)$$

This explains our introduction of factors  $i$  in the Fourier expansion (2.32). The Fourier components of the Matsubara Green's functions are just the function values of the Fourier transforms of the retarded and advanced Green's functions for imaginary frequencies, where in (2.35) it was taken into account that the spectral representation (2.6) of the retarded Green's function continues into the upper  $\epsilon$  half-plane, and that of the advanced Green's function continues into the lower half-plane.

Knowledge of the function values on the infinite series of imaginary energies  $\epsilon_s$  together with the definite asymptotics (2.8) determines the analytic functions  $G^{r/a}(\epsilon)$  uniquely. Hence, what is left is the calculation of the Matsubara Green's function.

Since on the complex time plane the order of  $\tau$ -values corresponds to the order of real  $t$ -values, this function may be defined as

$$G(x, x'; -i\tau) = -i \langle \mathbf{T}_\tau [\hat{\psi}(x, -i\tau) \hat{\psi}^\dagger(x'0)] \rangle, \quad (2.36)$$

with

$$\hat{\psi}(x, -i\tau) = e^{i(-i\tau)\hat{H}} \hat{\psi}(x) e^{-i(-i\tau)\hat{H}} = e^{\tau\hat{H}} \hat{\psi}(x) e^{-\tau\hat{H}}. \quad (2.37)$$

$\mathbf{T}_\tau$  orders the factors in descending sequence of  $\tau$ -values from left to right, again with statistics sign factors accompanying permutations.<sup>5</sup>

## 2.4 The Interaction Picture

Up to here we used the Heisenberg picture for the time evolution, which was most effective in deriving the spectral representation and all analytic properties of the Green's functions as well as the interrelations between them. However, for all non-trivial applications with particle interaction the Heisenberg field operators  $\hat{\psi}(xt)$  are not explicitly known; the expansion of the exponentials of (1.43) and the subsequent application of the canonical (anti)-commutation relations creates an infinite number of terms which would have to be inserted into the Green's function expression.

There is a more elegant approach dealing with explicitly known field operators at the price of a non-commutative group for the time evolution between explicit actions of field operators. It starts with splitting the Hamiltonian,

$$\begin{aligned} \hat{H} &= \hat{H}_0 + \hat{W}, \\ \hat{H}_0 &= \int dx'_1 dx_1 \hat{\psi}^\dagger(x'_1) h(x'_1, x_1) \hat{\psi}(x_1) = \sum_{\mathbf{k}_1 \sigma_1} \hat{c}_{\mathbf{k}_1 \sigma_1}^\dagger (\epsilon_{\mathbf{k}_1 \sigma_1} - \mu) \hat{c}_{\mathbf{k}_1 \sigma_1} \end{aligned} \quad (2.38)$$

as in (2.22) into a part  $\hat{H}_0$  which is bilinear in the field operators, and the rest  $\hat{W}$ .<sup>6</sup>

<sup>5</sup>In non-equilibrium statistics where manifestly time-dependent Hamiltonians figure (external time-dependent fields), more path ordered Green's functions play a role besides the real time path and the imaginary time path (Matsubara path). Of particular importance there is the Keldysh path and the Keldysh Green's function (cf. J. Rammer and H. Smith, Rev. Mod. Phys. **58**, 323 (1986)). In our context we do not need it.

<sup>6</sup>As will be discussed later,  $\hat{W}$  may, besides  $\hat{H}_{\text{int}}$ , also contain part of the bilinear terms.

The interaction picture is introduced by defining new field operators,

$$\begin{aligned}\hat{\psi}_{H_0}(xt) &= e^{it\hat{H}_0}\hat{\psi}(x)e^{-it\hat{H}_0} = \sum_{\mathbf{k}\sigma} \phi_{\mathbf{k}\sigma}(x)\hat{c}_{H_0\mathbf{k}\sigma}(t), \\ \hat{\psi}_{H_0}^\dagger(xt) &= e^{it\hat{H}_0}\hat{\psi}^\dagger(x)e^{-it\hat{H}_0} = \sum_{\mathbf{k}\sigma} \hat{c}_{H_0\mathbf{k}\sigma}^\dagger(t)\phi_{\mathbf{k}\sigma}^*(x).\end{aligned}\tag{2.39}$$

Since of course  $\hat{H}_0$  commutes with itself, it follows that  $\hat{H}_0 = e^{it\hat{H}_0}\hat{H}_0e^{-it\hat{H}_0} = \hat{H}_{0H_0}(t) = \int dx'dx \hat{\psi}_{H_0}^\dagger(x't)h(x',x)\hat{\psi}_{H_0}(xt) = \sum_{\mathbf{k}\sigma} \hat{c}_{H_0\mathbf{k}\sigma}^\dagger(\epsilon_{\mathbf{k}\sigma} - \mu)\hat{c}_{H_0\mathbf{k}\sigma}$ , that is,  $\hat{H}_0$  may likewise be expressed through the  $\hat{\psi}(x)$  or the  $\hat{\psi}_{H_0}(xt)$ . Hence,

$$i\frac{\partial}{\partial t}\hat{c}_{H_0\mathbf{k}\sigma}(t) = \left[ \hat{c}_{H_0\mathbf{k}\sigma}(t), \hat{H}_{0H_0}(t) \right] = \hat{c}_{H_0\mathbf{k}\sigma}(t)(\epsilon_{\mathbf{k}\sigma} - \mu),$$

which integrates to

$$\hat{c}_{H_0\mathbf{k}\sigma}(t) = \hat{c}_{\mathbf{k}\sigma}e^{-i(\epsilon_{\mathbf{k}\sigma}-\mu)t}, \quad \hat{c}_{H_0\mathbf{k}\sigma}^\dagger(t) = e^{i(\epsilon_{\mathbf{k}\sigma}-\mu)t}\hat{c}_{\mathbf{k}\sigma}^\dagger.\tag{2.40}$$

The time evolution operator is accordingly written as

$$\hat{U}(t_2, t_1) = e^{-i(t_2-t_1)\hat{H}} = e^{-it_2\hat{H}_0}\hat{S}(t_2, t_1)e^{it_1\hat{H}_0},\tag{2.41}$$

or

$$\hat{S}(t_2, t_1) = e^{it_2\hat{H}_0}e^{-i(t_2-t_1)\hat{H}}e^{-it_1\hat{H}_0} = \hat{U}_{H_0}(t_2 - t_1).\tag{2.42}$$

It still contains the whole many-body problem. Obviously,

$$\hat{S}(t_3, t_2)\hat{S}(t_2, t_1) = \hat{S}(t_3, t_1).\tag{2.43}$$

These *scattering operators* form again a group which, however, is not commutative any more.

From the group property,

$$\hat{S}(t_2, t_1) = \prod_{n=1}^N \hat{S}(t_2 - (n-1)\delta t, t_2 - n\delta t), \quad \delta t = \frac{t_2 - t_1}{N},$$

where the order of factors with ascending  $n$  from left to right is essential, and for  $\delta t \rightarrow 0$ ,

$$\hat{S}(t + \delta t, t) = e^{it\hat{H}_0}(1 + i\delta t\hat{H}_0 - i\delta t\hat{H})e^{-it\hat{H}_0} = 1 - i\delta t\hat{W}_{H_0}(t).$$

Hence,

$$\hat{S}(t_2, t_1) = \lim_{N \rightarrow \infty} \prod_{n=1}^N (1 - i\hat{W}_{H_0}(t_1 + n\delta t)) = \mathbf{T} \exp \left\{ -i \int_{t_1}^{t_2} dt \hat{W}_{H_0}(t) \right\}.\tag{2.44}$$

The last expression is only an elegant way of writing for the previous one, with the help of Wick's time ordering operator which here acts on the expansion of the exponential into a series.

The ordinary Green's function (2.1) can now be written as

$$\begin{aligned}G(x, x'; t) &= -i\langle \hat{S}(-\infty, \infty) \mathbf{T} [\hat{S}(\infty, t)\hat{\psi}_{H_0}(xt)\hat{S}(t, 0)\hat{\psi}_{H_0}^\dagger(x'0)\hat{S}(0, -\infty)] \rangle = \\ &= -i\langle \hat{S}(-\infty, \infty) \mathbf{T} [\hat{\psi}_{H_0}(xt)\hat{\psi}_{H_0}^\dagger(x'0)\hat{S}(\infty, -\infty)] \rangle.\end{aligned}$$

In order to be surely correct with time order, the reference point of the quantum state was put to  $t = -\infty$ , and the left reference point for the  $\mathbf{T}$ -operator was put to  $t = +\infty$ . Under the  $\mathbf{T}$ -operator, the factors may be written in an arbitrary order, and the  $\hat{S}$ -operators were combined into one by observing the group property.

If the averaging is over the ground state, and if the interaction in the system is adiabatically switched on and off for  $|t| \rightarrow \infty$ , then the adiabatic theorem by M. Gell-Mann and F. Low says, that  $\hat{S}(-\infty, \infty)|\Psi_0\rangle = \hat{S}^{-1}(\infty, -\infty)|\Psi_0\rangle \sim |\Psi_0\rangle$ , which finally results in

$$G(x, x'; t) = -i \frac{\langle \mathbf{T} [\hat{\psi}_{H_0}(xt) \hat{\psi}_{H_0}^\dagger(x'0) \hat{S}(\infty, -\infty)] \rangle}{\langle \hat{S}(\infty, -\infty) \rangle}, \quad \langle \dots \rangle = \langle \Psi_0 | \dots | \Psi_0 \rangle. \quad (2.45)$$

If, however, the averaging is over the grand-canonical statistical state,  $\hat{\rho} = e^{-\beta \hat{H}} / \text{tr} e^{-\beta \hat{H}}$ , the approach does not directly lead to practical expressions for real time, and the Matsubara path has to be used.

The interaction picture for the Matsubara Green's function is introduced in a completely analogous manner:

$$\hat{\psi}_{H_0}(x, -i\tau) = e^{\tau \hat{H}_0} \hat{\psi}(x) e^{-\tau \hat{H}_0}, \quad \hat{\psi}_{H_0}^\dagger(x, -i\tau) = e^{\tau \hat{H}_0} \hat{\psi}^\dagger(x) e^{-\tau \hat{H}_0}, \quad (2.46)$$

$$\hat{S}(\tau_2, \tau_1) = \hat{U}_{H_0}(-i\tau_2, -i\tau_1) = \mathbf{T}_\tau \exp \left\{ - \int_{\tau_1}^{\tau_2} d\tau \hat{W}_{H_0}(-i\tau) \right\}, \quad (2.47)$$

$$G(x, x'; -i\tau) = -i \text{tr} \left( e^{-\beta \hat{H}} \hat{S}(0, \beta) \mathbf{T}_\tau [\hat{\psi}_{H_0}(x, -i\tau) \hat{\psi}_{H_0}^\dagger(x'0) \hat{S}(\beta, 0)] \right) / \text{tr} e^{-\beta \hat{H}}.$$

Now, for  $t_2 = -i\beta$ ,  $t_1 = 0$ , (2.41) reads

$$e^{-\beta \hat{H}} = e^{-\beta \hat{H}_0} \hat{S}(\beta, 0) \Rightarrow e^{-\beta \hat{H}_0} = e^{-\beta \hat{H}} \hat{S}(0, \beta).$$

This also implies  $\text{tr} e^{-\beta \hat{H}} = \text{tr}(e^{-\beta \hat{H}_0} \hat{S}(\beta, 0))$ , which together results in the final expression

$$G(x, x'; -i\tau) = -i \frac{\langle \mathbf{T}_\tau [\hat{\psi}_{H_0}(x, -i\tau) \hat{\psi}_{H_0}^\dagger(x'0) \hat{S}(\beta, 0)] \rangle_0}{\langle \hat{S}(\beta, 0) \rangle_0}, \quad \langle \dots \rangle_0 = \text{tr}(e^{-\beta \hat{H}_0} \dots). \quad (2.48)$$

This expression has a very close resemblance of (2.45), and indeed both cases are subject to the same technique of computation introduced in the next two sections. However, one should have in mind that for imaginary time neither  $\hat{S}$  is unitary, nor is  $\hat{\psi}_{H_0}^\dagger$  the Hermitian conjugate to  $\hat{\psi}_{H_0}$ . It is called the *Matsubara conjugate*.

Consider once more the interaction-free case  $\hat{W} \equiv 0$ , with (2.47) implying  $\hat{S}(\tau_1, \tau_2) = \hat{1}$ , and, from (2.48) or (2.36),

$$\begin{aligned} G_0(x, x'; -i\tau) &= -i \langle \mathbf{T}_\tau [\hat{\psi}_{H_0}(x, -i\tau) \hat{\psi}_{H_0}^\dagger(x'0)] \rangle = \\ &= -i \sum_{\mathbf{k}\sigma} \phi_{\mathbf{k}\sigma}(x) \phi_{\mathbf{k}\sigma}^*(x') \begin{cases} \langle \hat{c}_{H_0\mathbf{k}\sigma}(-i\tau) \hat{c}_{H_0\mathbf{k}\sigma}^\dagger(0) \rangle \\ -\zeta \langle \hat{c}_{H_0\mathbf{k}\sigma}^\dagger(0) \hat{c}_{H_0\mathbf{k}\sigma}(-i\tau) \rangle \end{cases} = \\ &= -i \sum_{\mathbf{k}\sigma} \phi_{\mathbf{k}\sigma}(x) \phi_{\mathbf{k}\sigma}^*(x') e^{-(\epsilon_{\mathbf{k}\sigma} - \mu)\tau} \begin{cases} \langle \hat{c}_{\mathbf{k}\sigma} \hat{c}_{\mathbf{k}\sigma}^\dagger \rangle & \text{for } \tau > 0 \\ -\zeta \langle \hat{c}_{\mathbf{k}\sigma}^\dagger \hat{c}_{\mathbf{k}\sigma} \rangle & \text{for } \tau < 0. \end{cases} \end{aligned}$$

In the second line (2.39) was used, and in the third line (2.40). The final result is

$$G_0(x, x'; -i\tau) = -i \sum_{\mathbf{k}\sigma} \phi_{\mathbf{k}\sigma}(x) \phi_{\mathbf{k}\sigma}^*(x') e^{-(\epsilon_{\mathbf{k}\sigma} - \mu)\tau} \begin{cases} (1 - \zeta f_T(\epsilon_{\mathbf{k}\sigma} - \mu)) & \text{for } \tau > 0 \\ -\zeta f_T(\epsilon_{\mathbf{k}\sigma} - \mu) & \text{for } \tau < 0, \end{cases} \quad (2.49)$$

with

$$f_T(\epsilon - \mu) = [e^{\beta(\epsilon - \mu)} + \zeta]^{-1} \quad (2.50)$$

as the Fermi ( $\zeta = 1$ ) or Bose ( $\zeta = -1$ ) distribution function.

## 2.5 Wick's Theorem

There are versions of Wick's theorem for path-ordered Green's functions for all possible paths in the complex time plane, differing in technical details of their proof but resulting in essentially the same statement. In order not to be unnecessarily abstract we consider only the case used further on which is the Matsubara path.<sup>7</sup>

Insertion of (2.47) into (2.48) and expanding the exponentials results in

$$G(x, x'; -i\tau) = -i \frac{\left\langle \mathbf{T}_\tau \left[ \hat{\psi}_{H_0}(x, -i\tau) \hat{\psi}_{H_0}^\dagger(x'0) \sum_{n=0}^{\infty} \frac{(-1)^n}{n!} \int_0^\beta \cdots \int_0^\beta d\tau_1 \cdots d\tau_n \hat{W}_{H_0}(-i\tau_1) \cdots \hat{W}_{H_0}(-i\tau_n) \right] \right\rangle_0}{\left\langle \mathbf{T}_\tau \left[ \sum_{n=0}^{\infty} \frac{(-1)^n}{n!} \int_0^\beta \cdots \int_0^\beta d\tau_1 \cdots d\tau_n \hat{W}_{H_0}(-i\tau_1) \cdots \hat{W}_{H_0}(-i\tau_n) \right] \right\rangle_0} \quad (2.51)$$

The structure of the numerator and denominator of this expression depends on the actual structure of  $\hat{W}$ , which normally is a sum of products of more than two fermionic and/or bosonic field operators of the general form of (2.39, 2.40). Denote those operators by  $\hat{\psi}_A, \hat{\psi}_B, \dots$  (each of which stands for some  $\hat{\psi}_{H_0}$  or  $\hat{\psi}_{H_0}^\dagger$ ). The expectation values of (2.51) are series of terms

$$\text{tr}(\hat{\rho}_0 \hat{\psi}_A \hat{\psi}_B \hat{\psi}_C \cdots \hat{\psi}_Z), \quad \hat{\rho}_0 = \frac{e^{-\beta \hat{H}_0}}{\text{tr} e^{-\beta \hat{H}_0}}$$

with an *even* number  $n_Z$  of field operators, where each  $\hat{\psi}_A, \dots$  has its imaginary time  $\tau_A, \dots$ , and the factors are already put in order of descending  $\tau_A \dots$ . Since  $\hat{H}_0$  preserves the particle number, the trace with an odd number of field operators vanishes.<sup>8</sup> With (2.39), this means

$$\sum_a \sum_b \sum_c \cdots \sum_z \phi_a^A \phi_b^B \phi_c^C \cdots \phi_z^Z \text{tr}(\hat{\rho}_0 \hat{c}_A^a \hat{c}_B^b \hat{c}_C^c \cdots \hat{c}_Z^z).$$

In the following we omit the superscripts at the  $\hat{c}$ -operators. The latter trace may be transformed into

$$\begin{aligned} \text{tr}(\hat{\rho}_0 \hat{c}_A \hat{c}_B \hat{c}_C \cdots \hat{c}_Z) &= \text{tr}(\hat{\rho}_0 [\hat{c}_A, \hat{c}_B]_{\zeta} \hat{c}_C \cdots \hat{c}_Z) - \zeta \text{tr}(\hat{\rho}_0 \hat{c}_B [\hat{c}_A, \hat{c}_C]_{\zeta} \cdots \hat{c}_Z) + \\ &+ \cdots + (-\zeta) \text{tr}(\hat{\rho}_0 \hat{c}_B \cdots [\hat{c}_A, \cdots]_{\zeta} \cdots) + \cdots + \\ &+ (-\zeta)^{n_Z-2} \text{tr}(\hat{\rho}_0 \hat{c}_B \hat{c}_C \cdots [\hat{c}_A, \hat{c}_Z]_{\zeta}) + (-\zeta)^{n_Z-1} \text{tr}(\hat{\rho}_0 \hat{c}_B \hat{c}_C \cdots \hat{c}_Z \hat{c}_A). \end{aligned}$$

Using the invariance of the trace under cyclic permutations, the last term is

$$-\zeta \text{tr}(\hat{c}_A \hat{\rho}_0 \hat{c}_B \hat{c}_C \cdots \hat{c}_Z) = -\zeta e^{\pm\beta(\epsilon_A - \mu_A)} \text{tr}(\hat{\rho}_0 \hat{c}_A \hat{c}_B \hat{c}_C \cdots \hat{c}_Z).$$

<sup>7</sup>Wick himself considered the real-time case; the Matsubara case was first proved by T. Matsubara, 1955, cf. A. L. Fetter and J. D. Walecka, *Quantum Theory of Many-Particle Systems*, McGraw-Hill, New York, 1971, Chap. 7.

<sup>8</sup>This holds also true, if the thermodynamic state contains a *pair* condensate (see next chapter); in the case of a bosonic single-particle condensate as in superfluid <sup>4</sup>He, the field operator of the condensate particle needs a simple special treatment. We do not consider this case.



We finally used relations of the type (1.52), the plus sign of the exponent holds for a creation operator  $\hat{\psi}_A$  and the minus sign for an annihilation operator. Now, combine this last expression with the left hand side and obtain

$$\begin{aligned} \text{tr}(\hat{\rho}_0 \hat{c}_A \hat{c}_B \hat{c}_C \cdots \hat{c}_Z) &= \frac{[\hat{c}_A, \hat{c}_B]_\zeta}{1 + \zeta e^{\pm\beta(\epsilon_A - \mu_A)}} \text{tr}(\hat{\rho}_0 \hat{c}_C \cdots \hat{c}_Z) - \zeta \frac{[\hat{c}_A, \hat{c}_C]_\zeta}{1 + \zeta e^{\pm\beta(\epsilon_A - \mu_A)}} \text{tr}(\hat{\rho}_0 \hat{c}_B \cdots \hat{c}_Z) \\ &+ \cdots + (-\zeta)^{n_Z - 2} \frac{[\hat{c}_A, \hat{c}_Z]_\zeta}{1 + \zeta e^{\pm\beta(\epsilon_A - \mu_A)}} \text{tr}(\hat{\rho}_0 \hat{c}_B \hat{c}_C \cdots). \end{aligned}$$

Since the (anti-)commutators are  $c$ -numbers, they may be taken out of the trace. Moreover, they are zero (and hence the written down terms are harmless in the equation) unless they contain a pair of a creation and an annihilation operator with equal quantum numbers  $a, b, \dots$ , in which case either<sup>9</sup>

$$\frac{[\hat{c}_{\mathbf{k}\sigma}^\dagger, \hat{c}_{\mathbf{k}\sigma}]_\zeta}{1 + \zeta e^{\beta(\epsilon_{\mathbf{k}\sigma} - \mu)}} = \frac{\zeta}{1 + \zeta e^{\beta(\epsilon_{\mathbf{k}\sigma} - \mu)}} = \frac{1}{e^{\beta(\epsilon_{\mathbf{k}\sigma} - \mu)} + \zeta} = f_T(\epsilon_{\mathbf{k}\sigma} - \mu) = \langle \hat{c}_{\mathbf{k}\sigma}^\dagger \hat{c}_{\mathbf{k}\sigma} \rangle_0$$

or

$$\frac{[\hat{c}_{\mathbf{k}\sigma}, \hat{c}_{\mathbf{k}\sigma}^\dagger]_\zeta}{1 + \zeta e^{-\beta(\epsilon_{\mathbf{k}\sigma} - \mu)}} = \frac{1}{1 + \zeta e^{-\beta(\epsilon_{\mathbf{k}\sigma} - \mu)}} = 1 - \zeta f_T(\epsilon_{\mathbf{k}\sigma} - \mu) = \langle \hat{c}_{\mathbf{k}\sigma} \hat{c}_{\mathbf{k}\sigma}^\dagger \rangle_0.$$

This proves our first important result:

$$\begin{aligned} \langle \hat{c}_A \hat{c}_B \hat{c}_C \cdots \hat{c}_Z \rangle_0 &= \langle \mathbf{T}_\tau \hat{c}_A \hat{c}_B \rangle_0 \langle \hat{c}_C \cdots \hat{c}_Z \rangle_0 - \zeta \langle \mathbf{T}_\tau \hat{c}_A \hat{c}_C \rangle_0 \langle \hat{c}_B \cdots \hat{c}_Z \rangle_0 + \\ &+ \cdots + (-\zeta)^{n_Z - 2} \langle \mathbf{T}_\tau \hat{c}_A \hat{c}_Z \rangle_0 \langle \hat{c}_B \hat{c}_C \cdots \rangle_0. \end{aligned}$$

We have added the  $\tau$ -ordering operators in all pair terms on the right hand side (so called contractions), since we considered all the time in this analysis a  $\tau$ -ordered product of field operators so that the inserted  $\mathbf{T}_\tau$ -operators will have no effect.

The same manipulation can now be made with each second factor of the terms on the right hand side, and by induction and returning to the  $\hat{\psi}$ s,

$$\langle \hat{\psi}_A \hat{\psi}_B \hat{\psi}_C \cdots \hat{\psi}_Z \rangle_0 = \frac{1}{2^{n_Z/2}} \sum_{\mathcal{P}} (-\zeta)^{|\mathcal{P}|} \langle \mathbf{T}_\tau \hat{\psi}_{\mathcal{P}_A} \hat{\psi}_{\mathcal{P}_B} \rangle_0 \langle \mathbf{T}_\tau \hat{\psi}_{\mathcal{P}_C} \cdots \rangle_0 \cdots \langle \mathbf{T}_\tau \cdots \hat{\psi}_{\mathcal{P}_Z} \rangle_0, \quad (2.52)$$

where  $\tau_A > \tau_B > \tau_C > \cdots > \tau_Z$ . Here,  $\mathcal{P}$  is a permutation of the series  $ABC \cdots Z$ ,  $|\mathcal{P}|$  is its order, and the prefactor accounts for the fact that up to here we did not include permutations *inside* a contraction, which due to the presence of the  $\mathbf{T}_\tau$ -operators lead only to a factor of two for each of the  $n_Z/2$  contractions.

Consider now an arbitrarily ordered product, for which

$$\langle \mathbf{T}_\tau \hat{\psi}_A \hat{\psi}_B \cdots \hat{\psi}_Z \rangle_0 = (-\zeta)^{|\mathcal{P}_\tau|} \langle \hat{\psi}_{\mathcal{P}_\tau A} \hat{\psi}_{\mathcal{P}_\tau B} \hat{\psi}_{\mathcal{P}_\tau C} \cdots \hat{\psi}_{\mathcal{P}_\tau Z} \rangle_0.$$

Apply to the right hand side (2.52) and rename  $\mathcal{P}\mathcal{P}_\tau$  into  $\mathcal{P}$ , that is,  $(-\zeta)^{|\mathcal{P}_\tau|} (-\zeta)^{|\mathcal{P}|} \rightarrow (-\zeta)^{|\mathcal{P}|}$ , to obtain the final form of Wick's theorem:

$$\langle \mathbf{T}_\tau \hat{\psi}_A \hat{\psi}_B \hat{\psi}_C \cdots \hat{\psi}_Z \rangle_0 = \frac{1}{2^{n_Z/2}} \sum_{\mathcal{P}} (-\zeta)^{|\mathcal{P}|} \langle \mathbf{T}_\tau \hat{\psi}_{\mathcal{P}_A} \hat{\psi}_{\mathcal{P}_B} \rangle_0 \langle \mathbf{T}_\tau \hat{\psi}_{\mathcal{P}_C} \cdots \rangle_0 \cdots \langle \mathbf{T}_\tau \cdots \hat{\psi}_{\mathcal{P}_Z} \rangle_0. \quad (2.53)$$

<sup>9</sup>We perform the calculations of the following two lines for two  $\hat{c}$ -operators at equal time. However, in the interaction picture the time dependence of a  $\hat{c}$ -operator is a simple  $c$ -number phase factor (see (2.40)) which equally appears everywhere in the chain of equations so that the final result is unchanged.

The sum on the right hand side runs over all possible complete contractions of the operators  $\hat{\psi}_A \cdots \hat{\psi}_Z$  into pairs. Many of those contractions are zero, so that only a small number of the  $n_Z!/2^{n_Z/2}$  different complete contractions really matters.

Wick's theorem means that both the numerator and the denominator of (2.51) may be expanded into products of interaction-free single-particle Green's functions (2.49), multiplied by interaction functions of the  $x$ -variables like those in (1.22) and integrated over all  $x$ -variables coming from  $\hat{W}$ . Likewise, the orbital representation of the Green's functions may be used with matrix elements of orbitals  $\phi_{k\sigma}$  (which appear in  $\hat{W}$ , for instance by inserting (1.47) into (1.22)) and summations over all orbital quantum numbers coming from  $\hat{W}$ .

## 2.6 Feynman Diagrams

With Wick's theorem at hand, finding the expression of the contribution in any perturbation order in  $\hat{W}$  of the numerator and the denominator of (2.51) is merely a bookkeeping of integrations over internal variables  $x_i$  over free-particle Green's functions and interaction functions, of combinatorics, and of counting prefactors and minus signs. Fortunately, this has been done once forever for all possible cases and has been cast into rules for drawing diagrams and translating them into formulas.

In order to be specific, we consider the case of fermions with the interaction (cf. (1.22))

$$\hat{W} = \frac{1}{2} \int dx_1 dx'_1 \hat{\psi}^\dagger(x_1) \hat{\psi}^\dagger(x'_1) w(\mathbf{r}_1 - \mathbf{r}'_1) \hat{\psi}(x'_1) \hat{\psi}(x_1). \quad (2.54)$$

The  $n$ -th order contribution to the numerator of (2.51) is obtained in the following way:

1. Mark  $n$  pairs of points (vertices) with co-ordinates  $x_i, x'_i, i = 1, \dots, n$ .
2. Connect the pairs with interaction lines

$$-w(x_i - x'_i) \delta(\tau_i - \tau'_i) = \begin{array}{ccc} \bullet & \text{-----} & \bullet \\ x_i & & x'_i \end{array}$$

3. Connect the points in all possible ways with free-particle Green's function lines

$$iG_0(x_A, x_B; -i(\tau_A - \tau_B)) = \begin{array}{ccc} \bullet & \longleftarrow & \bullet \\ x_A & & x_B \end{array}$$

where  $A, B$  label vertices  $x_i$  or  $x'_i$ . The connection must be made so that at each vertex one Green's function line starts and one ends, and exactly one Green's function line has a free starting point corresponding to  $x'$  of the numerator of (2.51), and one has a free endpoint corresponding to  $x$ .

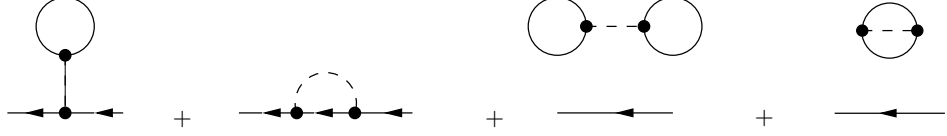
4. Interpret

$$iG_0(x_i, x_i; 0) = i \lim_{\tau \rightarrow -0} G_0(x_i, x_i; -i\tau) = -\zeta n_0(x_i) = \begin{array}{c} \circ \\ \bullet \\ x_i \end{array}$$

5. Integrate over  $\int dx_i dx'_i \int_0^\beta d\tau_i d\tau'_i$  for  $i = 1, \dots, n$ , ( $\int dx_i = \sum_{s_i} \int d^3 r_i$ ).
6. Multiply with  $(-1)^L$ , where  $L$  is the number of closed fermion loops.

7. Diagrams only differing in the labeling of the vertices are to be accounted for only once; this considers the factor  $1/n!$  of the expansion of the exponential in (2.51) and the factor  $1/2^n$  coming from  $\hat{W}$ .

For instance the first order terms for the numerator of (2.51) are<sup>10</sup>



Each connected diagram represents a multiple integral. Disconnected diagrams as the third and fourth one above represent products of separate multiple integrals. The diagrams for the denominator of (2.51) differ from those of the numerator only in the missing free-end Green's function lines. The first order terms of those *vacuum* diagrams are just:



It is easily seen that each connected diagram with two free Green's function line ends for the numerator of (2.51) will be multiplied with the sum of all possible vacuum diagrams disconnected from it. This factor, however, is precisely the complete denominator of (2.51). Hence, the full Green's function (2.51) is just given by *the sum of all connected diagrams* with two free Green's function ends. This *connected diagrams theorem* is the first big simplification deriving from Wick's theorem.

In most practical applications one uses the Fourier transformed Green's functions, by substituting (2.32), in an orbital representation (2.28) (possibly non-diagonal in  $\mathbf{k}$  and in the spin), where in many cases the orbitals are plane waves (momentum representation) or Bloch waves (quasi-momentum representation). This is achieved as previously with the help of the relations (1.47) whereafter the integrations over the  $x_i, x'_i$  produce matrix elements, and the integrations over  $\tau_i, \tau'_i$  produce Kronecker  $\delta$ s for sums of Matsubara frequencies corresponding to incoming and outgoing lines at vertices, multiplied with  $\beta$ . The topological structure of the diagrams remains exactly the same, the rules for translation into formulas are now:

1. Mark  $n$  pairs of points.
2. Connect the pairs with interaction lines<sup>11</sup>

$$-\langle \mathbf{k}_1 \sigma_1, \mathbf{k}_2 \sigma_2 | w | \mathbf{k}'_2 \sigma'_2, \mathbf{k}'_1 \sigma'_1 \rangle = \begin{array}{ccc} \mathbf{k}_1 \sigma_1 & & \mathbf{k}'_1 \sigma'_1 \\ \bullet & \text{-----} & \bullet \\ \mathbf{k}_2 \sigma_2 & & \mathbf{k}'_2 \sigma'_2 \end{array}$$

3. Connect the points as previously with Green's function lines

$$-\frac{1}{\beta} G_{0; \mathbf{k}_A \sigma_A, \mathbf{k}_B \sigma_B} (i\epsilon_s) = \begin{array}{ccc} \bullet & \text{-----} & \bullet \\ \mathbf{k}_A \sigma_A & \epsilon_s & \mathbf{k}_B \sigma_B \end{array}$$

the quantum numbers  $\mathbf{k}\sigma$  at the vertices must match since they originate from the same expansion (1.47) of which the orbital goes into the interaction matrix element

<sup>10</sup>In all cases where the directional arrow at the Green's function lines is omitted, the direction does not matter.

<sup>11</sup>We use a convention  $\langle \mathbf{k}_1 \sigma_1, \mathbf{k}_2 \sigma_2 | w | \mathbf{k}'_2 \sigma'_2, \mathbf{k}'_1 \sigma'_1 \rangle = \int dx_1 dx_2 \phi_{\mathbf{k}_1 \sigma_1}^*(x_1) \phi_{\mathbf{k}_2 \sigma_2}^*(x_2) w(x_1 - x_2) \phi_{\mathbf{k}'_2 \sigma'_2}(x_2) \phi_{\mathbf{k}'_1 \sigma'_1}(x_1)$ .

and the operator goes into the Green's function. The (sum of) incoming Matsubara frequencies must be equal to the (sum of) outgoing Matsubara frequencies at every vertex, and each vertex yields a factor  $\beta$ .<sup>12</sup>

4.

$$\frac{\zeta}{\beta} n_{0; \mathbf{k}\sigma, \mathbf{k}'\sigma'} = \frac{\zeta}{\beta} \langle \hat{c}_{\mathbf{k}\sigma}^\dagger \hat{c}_{\mathbf{k}'\sigma'} \rangle_0 = \text{Diagram: a circle with two dots on the bottom edge labeled } \mathbf{k}\sigma \text{ and } \mathbf{k}'\sigma'$$

5. Sum over all inner quantum numbers and Matsubara frequencies. Simplifications occur, if the interaction preserves quantum numbers (for instance momentum and spin).

The rules 6. and 7. are the same as in  $x$ -representation.

It is rather obvious how these rules modify for various interactions  $\hat{W}$ .

## 2.7 The Self-Energy

Besides the systematization and classification of the perturbation contributions in all orders already used in the connected diagrams theorem, further infinite summations of important partial sums of the perturbation series can be performed by solving integral equations (in  $x$ -representation) or by summing up geometrical series (in orbital representation), derived from further classification of diagrams. The most important partial sum is the self-energy.

The structure of the series of all connected diagrams with two free ends of Green's function lines representing the full single-particle Green's function (2.51) may be characterized as follows:

$$G(x, x'; -i\tau) =$$

$$\text{Diagram: a horizontal line with arrows pointing left, followed by a plus sign, then a diagram with a checkered rectangle on the line, followed by a plus sign, then a diagram with two checkered rectangles on the line, followed by a plus sign, then an ellipsis.} \quad (2.55)$$

Here, the checkered rectangle means the sum of all diagrams with two vertices (terminals) for connecting one external Green's function line to each of them, and such that they cannot be disconnected by just cutting through one internal Green's function line. For reasons discussed below it is called the (proper) self-energy.

Consider the series of diagrams right of the right terminal of the first self-energy part. It exactly repeats the whole series itself. This is precisely the algebraic structure of a geometrical series. If we introduce a thick line for the full Green's function, this structure may be expressed by the diagrammatic equation

$$\text{Diagram: a thick horizontal line with arrows pointing left} = \text{Diagram: a thin horizontal line with arrows pointing left} + \text{Diagram: a thin horizontal line with arrows pointing left, a checkered rectangle on the line, and a thick horizontal line with arrows pointing left} \quad (2.56)$$

which represents *Dyson's integral equation*

$$\begin{aligned} iG(x, x'; -i(\tau - \tau')) &= iG_0(x, x'; -i(\tau - \tau')) + \\ &+ \int dx_1 dx_2 \int_0^\beta d\tau_1 d\tau_2 iG_0(x, x_1; -i(\tau - \tau_1)) i\Sigma(x_1, x_2; -i(\tau_1 - \tau_2)) iG(x_2, x'; -i(\tau_2 - \tau')) \end{aligned} \quad (2.57)$$

<sup>12</sup>The parentheses are added for the case of a more complex  $\hat{W}$  with more operators, leading to vertices with more lines connected to them. The generalizations of the rules are rather trivial.



## 2.8 Thermodynamic Quantities

Single-particle Green's functions provide the quasi-particle excitation spectrum and quasi-particle lifetimes through the position of their poles in the unphysical sheet of the complex energy plane. They also provide information on reduced density matrices. Comparison of (2.36) with (1.34) readily yields

$$n_1(x|x') = \langle \hat{\psi}^\dagger(x') \hat{\psi}(x) \rangle = -i\zeta \lim_{\tau \rightarrow -0} G(x, x'; -i\tau). \quad (2.64)$$

Its diagonal is the particle density  $n(x) = n_1(x|x)$  (compare to the diagram rule 4. for the interaction-free density  $n_0$ ). Integration over  $x$  gives the total particle number:

$$-i\zeta \lim_{\tau \rightarrow -0} \int dx G(x, x; -i\tau) = N(V, T, \mu) = -\frac{\partial \Omega(V, T, \mu)}{\partial \mu}. \quad (2.65)$$

Integration of this relation over  $\mu$  in principle provides the thermodynamic potential  $\Omega(V, T, \mu)$ .

There is an alternative approach to the total interaction energy and the thermodynamic potential which compares to the derivation of the equations of motion in Section 2.2. From (2.37) and (2.54),

$$\left. \frac{\partial}{\partial \tau} \hat{\psi}(x, -i\tau) \right|_{\tau=0} = [\hat{H}, \hat{\psi}(x)] = - \int dx_1 h(x, x_1) \hat{\psi}(x_1) - \int dx_1 \hat{\psi}^\dagger(x_1) w(\mathbf{r} - \mathbf{r}_1) \hat{\psi}(x_1) \hat{\psi}(x).$$

Hence, again with (2.36),

$$\frac{i\zeta}{2} \lim_{\tau \rightarrow -0} \int dx dx_1 \left( \delta(x - x_1) \frac{\partial}{\partial \tau} + h(x, x_1) \right) G(x_1, x; -i\tau) = \langle \hat{W} \rangle. \quad (2.66)$$

The thermodynamic potential is defined as

$$e^{-\beta\Omega} = \text{tr} e^{-\beta\hat{H}} \quad \text{or} \quad \Omega = -\frac{1}{\beta} \ln \text{tr} e^{-\beta\hat{H}}. \quad (2.67)$$

Introduce an explicit coupling constant  $\lambda$  by writing  $\hat{H} = \hat{H}_0 + \lambda\hat{W}$ . Then,

$$\frac{\partial \Omega}{\partial \lambda} = -\frac{1}{\beta \text{tr} e^{-\beta\hat{H}}} \frac{\partial}{\partial \lambda} \left( \text{tr} e^{-\beta\hat{H}} \right) = \frac{1}{\beta \text{tr} e^{-\beta\hat{H}}} \text{tr} \left( e^{-\beta\hat{H}} \beta \hat{W} \right) = \langle \hat{W} \rangle_\lambda.$$

Integration over  $\lambda$  from 0 to 1 yields

$$\Omega = \Omega_0 + \int_0^1 d\lambda \langle \hat{W} \rangle_\lambda. \quad (2.68)$$

The thermodynamic potential of interaction-free particles,  $\Omega_0$ , is well known from the course in Statistical Physics. The rest is obtained by integrating (2.66) over the coupling constant. It might seem impractical to calculate  $\langle \hat{W} \rangle_\lambda$  for each  $\lambda$  and then to integrate. However, from a diagrammatic expansion of the Green's function in powers of  $w$ , (2.66) yields an expansion of  $\langle \hat{W} \rangle_\lambda$  in powers of  $\lambda$ . Then, integration of the  $n$ th term simply multiplies this term with  $1/(n+1)$ .

## Chapter 3

# Green's Functions in the Superconducting State

Hamiltonians in Solid State Physics preserve the electron number. (For instance the inverse  $\beta$ -decay of nuclei is not included in the Hamiltonian.) Those Hamiltonians  $\hat{H}$ , both in quantum mechanical and grand canonical form, commute with the electron number operator  $\hat{N}$ . Consequently, the eigenstates of the Hamiltonian may be chosen to be also electron number eigenstates implying that a Green's function  $\langle \mathbf{T}_\tau \hat{\psi}_A \hat{\psi}_B \cdots \hat{\psi}_Z \rangle = \sum_\alpha p_\alpha \langle \Psi_\alpha | \mathbf{T}_\tau \hat{\psi}_A \hat{\psi}_B \cdots \hat{\psi}_Z | \Psi_\alpha \rangle$  (cf. (1.12)) is only non-zero, if it contains creation and annihilation operators in equal number. If the local spectral weight  $\sum_{mn} A_{mn}(x, x') p_n$  (cf. (2.5, 2.6)) remains finite in the thermodynamic limit  $N \rightarrow \infty$ ,  $N/V = \text{const.}$ , then the above described situation preserves in this limit. Those Green's function are called *normal Green's functions*.

In the superconducting state this last condition is not true any more: There is a pair wavefunction with a definite binding energy which is macroscopically occupied, that is, its occupation number  $\langle \hat{P}^\dagger \hat{P} \rangle \sim N$  for  $N \rightarrow \infty$ ,  $N/V = \text{const.}$ , where  $\hat{P}^\dagger$  is the Cooper pair creator. Since  $\hat{P}$  expresses as a linear combination of pairs of fermionic operators,  $[\hat{P}, \hat{P}^\dagger]_- = 1$ , or, in view of  $\langle \hat{P}^\dagger \hat{P} \rangle \sim N$  equivalently,

$$\langle \hat{P} \hat{P}^\dagger \rangle = \langle \hat{P}^\dagger \hat{P} \rangle (1 + O(1/N))$$

and hence

$$\hat{P} \hat{P}^\dagger = \hat{P}^\dagger \hat{P} \quad \text{for } N \rightarrow \infty. \quad (3.1)$$

(The precise meaning of these considerations is that  $\hat{P} \hat{P}^\dagger$  is an extensive thermodynamic quantity and hence may appear in intensive quantities like for instance Green's functions only in the combination  $\hat{P} \hat{P}^\dagger / N$ ; (3.1) then holds in intensive expressions.) Likewise, if  $\hat{P}$  is expressed through fermionic operators  $\hat{c}_{\mathbf{k}\sigma}$ , all coefficients are  $\sim 1/N$ , and hence

$$[\hat{c}_{\mathbf{k}\sigma}, \hat{P}]_- = 0 = [\hat{c}_{\mathbf{k}\sigma}^\dagger, \hat{P}]_- \quad \text{for } N \rightarrow \infty \quad (3.2)$$

in the same sense.

It is well understood in Statistical Physics that in case of a macroscopic occupation of such a pair state the chemical potential of the pairs, that is twice the chemical potential of electrons, must adjust to the pair energy (again to accuracy  $\sim 1/N$ ). Hence, for any superconducting state  $\hat{P} \hat{H} \hat{P}^\dagger | \Psi \rangle = \hat{H} | \Psi \rangle + O(1/N)$  or

$$[\hat{P}, \hat{H}]_- = 0 = [\hat{P}^\dagger, \hat{H}]_- \quad \text{for } N \rightarrow \infty \quad (3.3)$$

even although this time  $[\hat{P}, \hat{H}]_-$  itself is extensive. Now, Green's functions are non-zero, if they are composed of operators  $\hat{\psi}^\dagger$  or  $\hat{\psi}\hat{P}^\dagger$  and operators  $\hat{\psi}$  or  $\hat{P}\hat{\psi}^\dagger$  in equal number out of the two groups. Because of (3.1, 3.2) the pair operators  $\hat{P}^\dagger$  and  $\hat{P}$  may be freely moved to the left or to the right in the operator products in Green's function expressions *in the Heisenberg picture* in which  $e^{it\hat{H}}$  figures, and eventually every  $\hat{P}^\dagger\hat{P}$  may be replaced by  $N$ .

The signature of the superconducting state is the appearance of non-zero *anomalous Green's functions* involving the pair operators.

### 3.1 The Bogoliubov-Valatin Transformation

In the normal Fermi liquid of interacting electrons, Wick's theorem mediates a perturbation expansion of the Green's functions in terms of interaction-free Green's functions and interaction vertices. This expansion can be summed up according to (2.55, 2.56) resulting in Dyson's equation (2.57). The most visible effect of the self-energy figuring in this equation is to modify the quasi-particle excitation energies. The basis of Wick's theorem was the interaction picture with a Hamiltonian  $\hat{H}_0$  split off the full Hamiltonian  $\hat{H}$ . Besides the condition that  $\hat{H}_0$  must be bilinear in the field operators, it can be chosen arbitrarily, defining  $\hat{W}$  as the difference between  $\hat{H}$  and  $\hat{H}_0$ . (For that reason we introduced a new name  $\hat{W}$  in (2.38) instead of  $\hat{H}_{\text{int}}$  of (2.22).) If one guesses a good approximation of the (real) quasi-particle dispersion relation in  $\hat{H}_0$ , one obtains a new expansion with a modified vertex structure due to the modification of  $\hat{W}$ , and a strongly reduced self-energy, the degree of reduction depending on the quality of the guess. As long as one does not modify the field operators, this is a very simple and transparent procedure. One has to add to the interaction vertex a 'blind' vertex without interaction lines representing the difference between the guessed energies and free-electron energies, which partially compensates the interaction part of the self-energy. The severe problem with this approach begins, if one also modifies the field operators, because then  $\hat{W}$  may become very complicated or even unknown (if the modification of the field operators is not made explicit). It must also be guessed in this case. Nevertheless, one still may obtain a useful semi-phenomenological theory (like for instance the  $t - J$  model with its  $t$  part expressed by Hubbard operators).

In the case of anomalous Green's functions of the superconducting state, Wick's theorem cannot directly be applied, because the pair operators commute with the full Hamiltonian  $\hat{H}$  due to the behavior of the chemical potential, but not with any  $\hat{H}_0$  of the normal bilinear form in the electron field operators (despite (3.2); contrary to a single  $\hat{c}_{\mathbf{k}\sigma}$ ,  $H_0 \sim N$  is extensive, and the chemical potential argument holds for  $H$  but not for  $H_0$ ). New fermionic field operators which account for the presence of the pair condensate are obtained by the well known Bogoliubov-Valatin transformation in Josephson's form which for spin-singlet pairing read:

$$\hat{\beta}_{\mathbf{k}\sigma} = u_{\mathbf{k}}\hat{c}_{\mathbf{k}\sigma} - \sigma v_{\mathbf{k}}\hat{P}\hat{c}_{-\mathbf{k}-\sigma}^\dagger, \quad \hat{\beta}_{\mathbf{k}\sigma}^\dagger = u_{\mathbf{k}}\hat{c}_{\mathbf{k}\sigma}^\dagger - \sigma v_{\mathbf{k}}\hat{c}_{-\mathbf{k}-\sigma}\hat{P}^\dagger, \quad (3.4)$$

with


$$u_{\mathbf{k}} = \cos \gamma_{\mathbf{k}}, \quad v_{\mathbf{k}} = \sin \gamma_{\mathbf{k}}, \quad (3.5)$$

that is,  $u_{\mathbf{k}}^2 + v_{\mathbf{k}}^2 = 1$ ,  $u_{\mathbf{k}}$ ,  $v_{\mathbf{k}}$  real. It is easily seen that due to (3.5) and (3.2, 3.1) the new  $\hat{\beta}$ -operators obey the same canonical fermionic anti-commutation rules as the original  $\hat{c}$ -operators. Hence, if one would split off a Hamiltonian  $\hat{H}_0$  bilinear in the  $\hat{\beta}$ -operators with the  $\gamma_{\mathbf{k}}$ s corresponding to the true condensate density, one has Wick's theorem and a diagrammatic expansion with hopefully normal Green's functions and self-energies only. (The correct  $\gamma_{\mathbf{k}}$ s would be those for which no anomalous functions appear.) Substituting back (3.4) for the  $\hat{\beta}$ -operators yields the corresponding structure of the diagrammatic expansion




with anomalous Green's functions in the representation of the original electron field operators. With the normal expansion in the  $\hat{\beta}$ -representation all manipulations made previously as for instance the summation leading to Dyson's equation remain correct. However, considering the diagrammatic expansion starting with  $\hat{H}_0$  bilinear in the  $\hat{c}$ -operators, anomalous terms cannot appear for any *finite* sum of diagrams simply by the Feynman rules. This clearly indicates the divergency of the perturbation series. It does not mean that the *formally* summed up series, Dyson's equation, is wrong. By tuning the  $\gamma_{\mathbf{k}}$  we move again contributions from  $G_0$  to  $\Sigma$  and back. Since we do not know in advance the correct  $\gamma_{\mathbf{k}}$ -values, we work with the original electron field operators and put all the anomalous parts into the self-energy. Then we have to work with skeleton diagrams, that is with closed equation systems for the skeleton parts to be solved.


The following Green's functions and Dyson equations appear in the superconducting state:<sup>1</sup>

$$G(x, x'; -i\tau) = -i\langle T_\tau[\hat{\psi}(x, -i\tau)\hat{\psi}^\dagger(x'0)] \rangle =$$


$$(3.6)$$


$$F(x, x'; -i\tau) = -i\langle T_\tau[\hat{\psi}(x, -i\tau)\hat{\psi}(x'0)]\hat{P}^\dagger \rangle =$$


$$(3.7)$$

$$\bar{F}(x, x'; -i\tau) = -i\langle T_\tau[\hat{\psi}^\dagger(x, -i\tau)\hat{\psi}^\dagger(x'0)]\hat{P} \rangle =$$


$$(3.8)$$

For the sake of symmetry we additionally consider

$$-G(x', x; +i\tau) = +i\langle T_\tau[\hat{\psi}(x', +i\tau)\hat{\psi}^\dagger(x0)] \rangle = -i\langle T_\tau[\hat{\psi}^\dagger(x, -i\tau)\hat{\psi}(x'0)] \rangle =$$


$$(3.9)$$

There are two anomalous Green functions  $F$  and  $\bar{F}$  and two anomalous self-energy parts labeled by two outward or two inward arrows. Eq. (3.9) is the 'particle-hole transposed' of (3.6). The obvious corresponding relations for the anomalous parts are

$$F(x, x'; -i\tau) = -F(x', x; +i\tau), \quad \bar{F}(x, x'; -i\tau) = -\bar{F}(x', x; +i\tau). \quad (3.10)$$

The three self-energy parts in these relations were *defined* in such a way that the direction of the arrows at their terminals must be preserved.

In these notes we will not consider spin-dependent interactions; spin-flip scattering by magnetic impurities as well as magnetic order normally strongly impairs the superconducting state.<sup>2</sup> Nevertheless, spin structures arise in quantum theory from spin-independent interactions: states are classified according to their total spin. For the following it is helpful to use a notation

$$G(x, x'; -i\tau) = G_{ss'}(\mathbf{r}, \mathbf{r}'; -i\tau), \dots \quad (3.11)$$

We will only consider cases where  $G \sim \delta_{ss'}$ , that is the spin of the quasi-particles is preserved. Recalling that the anomalous parts derive from a normal diagrammatic expansion in  $\hat{\beta}$ -representation and considering (3.4), it is clear that for spin-singlet pairing  $F \sim \begin{pmatrix} 0 & 1 \\ -1 & 0 \end{pmatrix} \sim \bar{F}$ . We introduce the Pauli matrices  $(\sigma_i)_{ss'}$ :

$$\sigma_0 = \begin{pmatrix} 1 & 0 \\ 0 & 1 \end{pmatrix}, \quad \sigma_1 = \begin{pmatrix} 0 & 1 \\ 1 & 0 \end{pmatrix}, \quad \sigma_2 = \begin{pmatrix} 0 & -i \\ i & 0 \end{pmatrix}, \quad \sigma_3 = \begin{pmatrix} 1 & 0 \\ 0 & -1 \end{pmatrix}, \quad (3.12)$$

<sup>1</sup>L. P. Gorkov, Sov. Phys.-JETP **7**, 505 (1958).

<sup>2</sup>However, exotic systems have been found where magnetic order and superconductivity coexist, and antiferromagnetic correlations need not imply spin-flip scattering.

and have

$$G \sim \sigma_0, \quad F \sim i\sigma_2 \sim \bar{F}. \quad (3.13)$$

From  $(\sigma_i)^2 = \sigma_0$  it is clear that the self-energy parts must have the same spin structure as the Green's functions.

In all what follows, the Fourier transformed Green's functions and self-energies at the Matsubara frequencies (2.34, 2.33) are used:

$$G_{\sigma\sigma'}(\mathbf{r}, \mathbf{r}'; i\epsilon_s) = - \int_0^\beta d\tau e^{i\epsilon_s\tau} \langle \mathbf{T}_\tau [\hat{\psi}_\sigma(\mathbf{r}, -i\tau) \hat{\psi}_{\sigma'}^\dagger(\mathbf{r}'0)] \rangle, \dots \quad (3.14)$$

Again making the connection to the normal Green's function in  $\hat{\beta}$ -representation for which (2.8) holds, the asymptotics of the anomalous parts derives from the behavior of the Bogoliubov-Valatin transformation (3.4) for  $|\epsilon_{\mathbf{k}\sigma}| \rightarrow \infty$ , that is from the behavior of the self-energy. One obtains

$$\lim_{|\epsilon| \rightarrow \infty} \epsilon F(\epsilon) = 0 = \lim_{|\epsilon| \rightarrow \infty} \epsilon \bar{F}(\epsilon), \quad (3.15)$$

since we know from the BCS-model that in (3.5)  $\gamma_{\mathbf{k}} \rightarrow 0$  in this limes.

## 3.2 The Nambu Structure<sup>3</sup>

The diagram structure in the superconducting state in  $\hat{\psi}$ -representation seems to be rather tangled if expressed in formulas since one has to observe the arrow rules when linking the parts of skeleton diagrams. However, Nambu observed that everything is automatically correctly arranged, if one collects the normal and anomalous parts into another  $2 \times 2$  matrix structure

$$\begin{aligned} \mathbf{G}_{\sigma\sigma'}(\mathbf{r}, \mathbf{r}'; i\epsilon_s) &= - \int_0^\beta d\tau e^{i\epsilon_s\tau} \left\langle \mathbf{T}_\tau \begin{bmatrix} \hat{\psi}_\sigma(\mathbf{r}, -i\tau) \hat{\psi}_{\sigma'}^\dagger(\mathbf{r}'0) & \hat{\psi}_\sigma(\mathbf{r}, -i\tau) \hat{\psi}_{\sigma'}(\mathbf{r}'0) \hat{P}^\dagger \\ \hat{\psi}_\sigma^\dagger(\mathbf{r}, -i\tau) \hat{\psi}_{\sigma'}^\dagger(\mathbf{r}'0) \hat{P} & \hat{\psi}_\sigma^\dagger(\mathbf{r}, -i\tau) \hat{\psi}_{\sigma'}(\mathbf{r}'0) \end{bmatrix} \right\rangle, \\ &= \begin{pmatrix} G_{\sigma\sigma'}(\mathbf{r}, \mathbf{r}'; i\epsilon_s) & F_{\sigma\sigma'}(\mathbf{r}, \mathbf{r}'; i\epsilon_s) \\ \bar{F}_{\sigma\sigma'}(\mathbf{r}, \mathbf{r}'; i\epsilon_s) & -G_{\sigma'\sigma}(\mathbf{r}', \mathbf{r}; -i\epsilon_s) \end{pmatrix} \end{aligned} \quad (3.16)$$

$$\Sigma_{\sigma\sigma'}(\mathbf{r}, \mathbf{r}'; i\epsilon_s) = \begin{pmatrix} \text{---} & \text{---} \\ \text{---} & \text{---} \end{pmatrix}. \quad (3.17)$$

Then, (3.6–3.9) simply reads

$$\mathbf{G} = \mathbf{G}_0 + \mathbf{G}_0 \Sigma \mathbf{G} \quad (3.18)$$

where  $\mathbf{G}_0$  is Nambu diagonal and has no anomalous parts. For the  $2 \times 2$  Nambu structure another basis of Pauli matrices  $\tau_i$ ,  $i = 0, 1, 2, 3$  is introduced which is identical with (3.12), but acts in the 'Nambu space' and not in the spin space. Hence, any product  $\sigma_i \tau_j$  has only a dyadic meaning as a  $4 \times 4$  matrix where the elements of the  $2 \times 2$  Nambu matrices are  $2 \times 2$  spin matrices. Our Green's functions of a superconductor are thus  $4 \times 4$  matrices in the full Nambu plus spin structure. However, as we already mentioned, *we will not consider spin-dependent interactions in the full Hamiltonian  $\hat{H}$  and will confine ourselves to spin-singlet*

<sup>3</sup>Y. Nambu, Phys. Rev. **117**, 648 (1960).

pairing. Then, every diagonal matrix element of the Nambu matrices is proportional to  $\sigma_0$  and every off-diagonal element is proportional to  $\sigma_2$  where  $(\sigma_2)^2 = \sigma_0$ . Hence, if we put

$$\begin{aligned} (G_{\sigma\sigma'}) &= \sigma_0 G, & (F_{\sigma\sigma'}) &= \sigma_2 F, & (\bar{F}_{\sigma\sigma'}) &= \sigma_2 \bar{F}, \\ (\Sigma_{\sigma\sigma'})_{ii} &= \sigma_0 \Sigma_{ii}, & (\Sigma_{\sigma\sigma'})_{i \neq j} &= \sigma_2 \Sigma_{i \neq j}, \end{aligned} \quad (3.19)$$

where the outer subscripts of  $\Sigma$  are the Nambu subscripts, then all relations like (3.18) hold for the spin-independent quantities of the right hand sides of (3.19) forming  $2 \times 2$  Nambu matrices.

In the case of spin-triplet pairing, the Nambu off-diagonal matrix elements are proportional to  $\sigma_2 \sum_{j=1}^3 \sigma_j \bar{F}_j$ . If one wants to treat spin-flip scattering or magnetic order, one has to work with the full  $4 \times 4$  structure of the Green's functions and self-energies.

### 3.3 Green's Functions and Vertices for the Electron-Nucleon System

We are now prepared to return to the Hamiltonian of Section 1.1. We expand it in powers of the lattice displacements  $\mathbf{u}_m = \mathbf{R}_m - \mathbf{R}_m^0$ :

$$\hat{H} = \hat{H}^0 + \hat{H}^1 + \hat{H}^2 + \dots, \quad (3.20)$$

$$\hat{H}^0 = \hat{t} + \hat{V}_{ee} + (\hat{V}_{en} + \hat{V}_{nn})(\mathbf{R}_m^0) - \mu \hat{N}, \quad (3.21)$$

$$\hat{H}^1 = \sum_m \frac{\partial(\hat{V}_{en} + \hat{V}_{nn})}{\partial \mathbf{R}_m^0} \cdot \mathbf{u}_m, \quad (3.22)$$

$$\hat{H}^2 = \hat{T} + \frac{1}{2} \sum_{mn} \mathbf{u}_m \cdot \frac{\partial^2(\hat{V}_{en} + \hat{V}_{nn})}{\partial \mathbf{R}_m^0 \partial \mathbf{R}_n^0} \cdot \mathbf{u}_n, \quad \hat{T} = - \sum_m \frac{1}{2M_m} \frac{\partial^2}{\partial \mathbf{u}_m^2}, \quad (3.23)$$

...

Note that  $\hat{V}_{en}$  depends on both the electron variables  $x_i$  and the nuclear positions  $\mathbf{R}_m$  or  $\mathbf{u}_m$ .  $\hat{V}_{nn}$  depends only on the nuclear positions. However, there is very strong compensation between both for the tightly bound electrons of the ionic cores, and we will further treat their sum as one potential acting on both electrons and ions and call it  $\hat{V}^0, \hat{V}^1, \hat{V}^2, \dots$  where the superscript indicates the power in  $\mathbf{u}_m$ . There is also very strong compensation between  $\hat{V}_{ee}$  and  $\hat{V}^0$  resulting in a much weaker electron self-energy compared to these potentials. In fact only the sum of all potentials is well behaving ( $\sim N$ ) in the thermodynamic limit.

We define the free-electron Green's function with the operator  $\hat{t} - \mu \hat{N}$  of (3.21) (cf. (1.25)). From the equation of motion, (2.25), we find

$$\int d^3 r_1 \left( \epsilon - \left( -\frac{1}{2} \frac{\partial^2}{\partial \mathbf{r}^2} - \mu \right) \right) \delta(\mathbf{r} - \mathbf{r}_1) G_0^{r/a}(\mathbf{r}_1, \mathbf{r}'; \epsilon) = \delta(\mathbf{r} - \mathbf{r}').$$

There is a conjugate equation of motion which is obtained if one replaces in the derivations of Section 2.2  $\hat{\psi}(xt)\hat{\psi}^\dagger(x', 0)$  with  $\hat{\psi}(x0)\hat{\psi}^\dagger(x', -t)$ . It yields

$$\int d^3 r_1 G_0^{r/a}(\mathbf{r}, \mathbf{r}_1; -\epsilon) \left( -\epsilon - \left( -\frac{1}{2} \frac{\partial^2}{\partial \mathbf{r}'^2} - \mu \right) \right) \delta(\mathbf{r}_1 - \mathbf{r}') = \delta(\mathbf{r} - \mathbf{r}').$$

By continuing both equations to the Matsubara frequencies and observing (3.9) which implies  $[G(\mathbf{r}, \mathbf{r}'; i\epsilon_s)]_{22} = -G(\mathbf{r}', \mathbf{r}; -i\epsilon_s)$ , we end up with the equation of motion for the free-electron Green's function in Nambu representation:

$$\int d^3 r_1 \left( \tau_0 i\epsilon_s - \tau_3 \left( -\frac{1}{2} \frac{\partial^2}{\partial \mathbf{r}^2} - \mu \right) \right) \delta(\mathbf{r} - \mathbf{r}_1) \mathbf{G}_0(\mathbf{r}_1, \mathbf{r}'; i\epsilon_s) = \tau_0 \delta(\mathbf{r} - \mathbf{r}') \quad (3.24)$$

with the formal solution

$$\mathbf{G}_0(\mathbf{r}, \mathbf{r}'; i\epsilon_s) = \left[ \tau_0 i\epsilon_s - \tau_3 \left( -\frac{1}{2} \frac{\partial^2}{\partial \mathbf{r}^2} - \mu \right) \right]^{-1} \delta(\mathbf{r} - \mathbf{r}'). \quad (3.25)$$

Besides (2.57) and (2.58), another useful way of writing Dyson's equation is  $(\mathbf{G}_0^{-1} - \Sigma)\mathbf{G} = \mathbf{1}$ , or

$$\int d^3 r_1 \left[ \left( \tau_0 i\epsilon_s - \tau_3 \left( -\frac{1}{2} \frac{\partial^2}{\partial \mathbf{r}^2} - \mu \right) \right) \delta(\mathbf{r} - \mathbf{r}_1) - \Sigma(\mathbf{r}, \mathbf{r}_1; i\epsilon_s) \right] \mathbf{G}(\mathbf{r}_1, \mathbf{r}'; i\epsilon_s) = \tau_0 \delta(\mathbf{r} - \mathbf{r}'). \quad (3.26)$$

Here,  $\Sigma$  has to be build from  $\hat{W} = \hat{H} - \hat{t} - \hat{T}$ , where  $\hat{T}$  does not enter  $\Sigma$  because it does not depend on the electron variables.

In a crystal lattice, the  $\mathbf{r}$  and  $\mathbf{r}'$  dependences of the Green's functions must be lattice periodic. Hence, a quasi-momentum representation may be introduced according to

$$\mathbf{G}(\mathbf{r}, \mathbf{r}'; i\epsilon_s) = \frac{(2\pi)^3}{V} \sum_{\mathbf{k}}^{\text{B.Z.}} \sum_{\mathbf{Q}, \mathbf{Q}'} e^{i(\mathbf{k} + \mathbf{Q}) \cdot \mathbf{r} - i(\mathbf{k} + \mathbf{Q}') \cdot \mathbf{r}'} \mathbf{G}(\mathbf{k}, \mathbf{Q}, \mathbf{Q}'; i\epsilon_s). \quad (3.27)$$

The sum over quasi-momenta  $\mathbf{k}$  runs over the first Brillouin zone (B.Z.) in accordance with Born-von Karman boundary conditions,  $\sum_{\mathbf{k}} = [V/(2\pi)^3] \int d^3 k$ , and  $\mathbf{Q}, \mathbf{Q}'$  are reciprocal lattice vectors. After insertion the same representation of  $\mathbf{G}_0$  into (3.24),  $-\partial^2/\partial \mathbf{r}^2$  may be replaced by  $(\mathbf{k} + \mathbf{Q})^2$  there, and then the  $\mathbf{r}_1$ -integration over the  $\delta$ -function simply replaces  $\mathbf{r}_1$  with  $\mathbf{r}$  in the Green's function. Replacing on the right hand side  $\delta(\mathbf{r} - \mathbf{r}') = (2\pi)^3/V \sum_{\mathbf{k}}^{\text{B.Z.}} \sum_{\mathbf{Q}} e^{i(\mathbf{k} + \mathbf{Q}) \cdot (\mathbf{r} - \mathbf{r}')}$  and comparing the Fourier components yields

$$\mathbf{G}_0(\mathbf{k}, \mathbf{Q}, \mathbf{Q}'; i\epsilon_s) = \delta_{\mathbf{Q}\mathbf{Q}'} \left[ \tau_0 i\epsilon_s - \tau_3 \left( \frac{(\mathbf{k} + \mathbf{Q})^2}{2} - \mu \right) \right]^{-1}. \quad (3.28)$$

This expression will be used in the estimates of the next chapter.

For the lattice motion we define a Green's function

$$D(l\lambda, l'\lambda'; i\omega_s) = - \int_0^\beta d\tau e^{i\omega_s \tau} \langle \mathbf{T}_\tau [\hat{u}_{l\lambda}(-i\tau) \hat{u}_{l'\lambda'}(0)] \rangle, \quad (3.29)$$

where  $l, l'$  count the unit cells of the crystal lattice, and  $\lambda, \lambda'$  count the degrees of freedom within a unit cell, that is  $\lambda$  runs over the Cartesian co-ordinates of all nuclei in the unit cell. The bosonic Matsubara frequencies (2.33) will be denoted by  $\omega_s$  in the following to distinguish them from the fermionic frequencies  $\epsilon_s$ . The operator  $\hat{u}_{l\lambda}(t)$  is the Heisenberg operator of the displacement of the nucleus from the regular lattice position. Likewise, a quasi-momentum (phonon) representation

$$D(l\lambda, l'\lambda'; i\omega_s) = \frac{1}{M} \sum_{\mathbf{q}}^{\text{B.Z.}} e^{i\mathbf{q} \cdot (\mathbf{R}_l^0 - \mathbf{R}_{l'}^0)} D(\mathbf{q}, \lambda, \lambda'; i\omega_s) \quad (3.30)$$

may be introduced where  $M$  is the number of unit cells in one Born-von Karman period of the crystal.

For a free-phonon Hamiltonian

$$\hat{H}_{\text{ph}} = \sum_{\mathbf{q}\lambda} \hat{b}_{\mathbf{q}\lambda}^\dagger \omega_{\mathbf{q}\lambda} \hat{b}_{\mathbf{q}\lambda}$$

where

$$\frac{1}{\sqrt{M}} \sum_l e^{i\mathbf{q}\cdot\mathbf{R}_l^0} u_{l\lambda} = \frac{1}{\sqrt{2\omega_{\mathbf{q}\lambda} M_\lambda}} (\hat{b}_{\mathbf{q}\lambda} + \hat{b}_{\mathbf{q}\lambda}^\dagger)$$

one finds (exercise)

$$\begin{aligned} D_0(\mathbf{q}, \lambda, \lambda'; i\omega_s) &= \\ &= -\frac{1}{2\omega_{\mathbf{q}\lambda} M_\lambda} \int_0^\beta d\tau e^{i\omega_s \tau} \left( \langle \mathbf{T}_\tau [\hat{b}_{\mathbf{q}\lambda}(-i\tau) \hat{b}_{\mathbf{q}\lambda'}^\dagger(0)] \rangle + \langle \mathbf{T}_\tau [\hat{b}_{\mathbf{q}\lambda}^\dagger(-i\tau) \hat{b}_{\mathbf{q}\lambda'}(0)] \rangle \right) = \\ &= \frac{\delta_{\lambda\lambda'}}{2\omega_{\mathbf{q}\lambda} M_\lambda} \left( \frac{1}{i\omega_s - \omega_{\mathbf{q}\lambda}} - \frac{1}{i\omega_s + \omega_{\mathbf{q}\lambda}} \right) = -\frac{\delta_{\lambda\lambda'}}{M_\lambda} \frac{1}{\omega_s^2 + \omega_{\mathbf{q}\lambda}^2}. \end{aligned}$$

Since in our approach the harmonic forces in  $\hat{H}_2$  (terms quadratic in  $\mathbf{u}$ ) depend also on the electronic degrees of freedom, we have to put them into  $\hat{W}$  and should define the free-phonon Green's function  $D_0$  with the operator  $\hat{T}$  alone, that is, without harmonic forces and hence with all 'bare phonon frequencies'  $\omega_{0,\mathbf{q}\lambda} = 0$ :

$$D_0(\mathbf{q}, \lambda, \lambda'; i\omega_s) = -\frac{\delta_{\lambda\lambda'}}{M_\lambda \omega_s^2} \quad (3.31)$$

or, back transformed with (3.30),

$$D_0(l\lambda, l'\lambda'; i\omega_s) = -\frac{\delta_{ll'} \delta_{\lambda\lambda'}}{M_\lambda \omega_s^2}. \quad (3.32)$$

A *phononic Dyson equation*,  $(D_0^{-1} + \Pi)D = 1$ , with a *phononic self-energy*  $\Pi$  reads in the representation (3.29, 3.32)

$$\sum_{l_1 \lambda_1} [-M_\lambda \omega_s^2 \delta_{ll_1} \delta_{\lambda\lambda_1} + \Pi(l\lambda, l_1 \lambda_1; i\omega_s)] D(l_1 \lambda_1, l' \lambda'; i\omega_s) = \delta_{ll'} \delta_{\lambda\lambda'}. \quad (3.33)$$

$\Pi$  has to be build from the same  $\hat{W}$  as  $\Sigma$ , only the two terminals of  $\Pi$  are  $D_0$ -terminals while the two terminals of  $\Sigma$  are  $\mathbf{G}_0$ -terminals.

The situation described in the previous sentence determines the primary vertices of our theory. As previously we symbolize a primary vertex by a dot. Since we will now be left with quite a number of such vertices differing by the number and kind of 'legs', that is of free-particle Green's functions to be connected to them, we symbolize them by 'dots with legs', having in mind that the legs themselves are not integral constituents of the vertex. They only indicate which types of free-particle Green's functions in which number are to be connected with that vertex when forming a complete diagram. The vertices are:

$$\begin{aligned} \hat{V}_{ee}: & \quad \text{---} \bullet \text{---} = \text{---} \times \text{---} + \text{---} \times \text{---} \\ \hat{V}^0: & \quad \text{---} \circ \text{---} \\ \hat{V}^1: & \quad \text{---} \bullet \text{---} + \text{---} \circ \text{---}, \quad \circ = \bullet + \text{---} \bullet \text{---} \\ \hat{V}^2: & \quad \text{---} \bullet \text{---} + \text{---} \circ \text{---} \\ \hat{V}^3: & \quad \text{---} \bullet \text{---} + \text{---} \circ \text{---} \\ \dots & \end{aligned} \quad (3.34)$$

We have compressed the dashed line of Section 2.6 into a four-leg vertex. A straight leg corresponds to  $G_0$  and a wiggly leg corresponds to  $D_0$ . The pure phononic vertices coming from  $\hat{V}_{nn}^i$  were combined with vertices coupling to the electron density  $n(\mathbf{r})$  and coming from  $\hat{V}_{en}^i$ . This takes into account the strong compensation of interactions mentioned at the beginning of the section. (As regards  $\hat{V}^0$ , see below.) We do not attach arrows to the lines because both the Nambu Green's functions and the phonon Green's functions are composed of parts with arrows in both directions. In momentum representation of course the total quasi-momentum on each vertex must vanish.

Typical contributions to  $\Sigma$  and  $\Pi$  are:

$$\Sigma = \text{[diagram 1]} + \text{[diagram 2]} + \text{[diagram 3]} + \text{[diagram 4]} + \text{[diagram 5]} + \text{[diagram 6]} + \dots$$

$$\Pi = \text{[diagram 7]} + \text{[diagram 8]} + \text{[diagram 9]} + \text{[diagram 10]} + \dots$$

The other strong cancellation between  $\hat{V}_{ee}$  and  $\hat{V}_{en}^0$  mentioned in the beginning of the section takes place between the first two diagrams for  $\Sigma$ . Therefore, they will be combined into the vertex  $\hat{V}^0$  of (3.34). According to our definition in the first line of (3.34), the first diagram for  $\Sigma$  consists of two parts, the direct Coulomb interaction with the electron density and the exchange interaction with the single particle density matrix (first two diagrams of the expansion of (2.51) in Section 2.6). This corresponds to the Hartree-Fock approximation.

Now recall that we have a small parameter  $\alpha$  of (1.7) in our theory, which is the ratio between the phonon and the electron energies. Before we may introduce proper full vertices and skeleton diagrams we have to classify the diagrams with respect to their order in  $\alpha$ .

## Chapter 4

# Split-off of High-Energy Parts

We are now prepared to follow the review article of D. Rainer cited in the first footnote of Section 1.1. As was stated in that section, there is a small parameter  $\alpha = \langle T \rangle / \langle t \rangle \approx \langle M \rangle^{-1/2} \approx 10^{-2}$  in the theory, where the average nuclear mass means the average over the solid which in case of a crystal is equivalent to the average over the unit cell of the crystal. The cancellations considered in the last section for the tightly bound electrons of the ionic cores make a theory with rigid ions and pseudopotentials for the valence electrons very close to the full theory, and the Born-Oppenheimer perturbation theory applies to it, too. Hence,  $\langle t \rangle$  in the above ratio is to be understood as the average kinetic energy of the valence electrons. The ratio  $\langle T \rangle / \langle t \rangle$  is in the following replaced by the equivalent ratio  $\omega_{\text{ph}} / \epsilon_{\text{F}}$ , where  $\omega_{\text{ph}}$  is some characteristic phonon energy, for instance the Debye energy. Another ratio of the same order  $\alpha$  is  $T_c / \epsilon_{\text{F}}$ , the ratio between the transition temperature into the superconducting state (in energy units) and the Fermi energy.<sup>1</sup>

The strength of Green's function theory much derives from the possibility of partial summations, that is from the possibility of deriving integral equations corresponding to equations of skeleton diagrams, which make sense even in cases when the primary perturbation series do not converge. In this chapter we will classify all primary diagrams with respect to their order in  $\alpha$ , and then perform partial summations within classes.

### 4.1 Classification of Primary Diagrams

Since the Hamiltonian (3.20) contains only Coulomb interactions, the virial theorem holds for it saying that the average kinetic and potential energies are of the same order. The kinetic energy is dominated by  $\langle t \rangle$  which is of order  $\alpha^0$ . Hence, the Coulomb interaction is also to be taken as of order  $\alpha^0$ . Now, realize that the factors  $\mathbf{u}_m$  of (3.22, 3.23) go into the phonon Green's function  $D_0$  and not into the vertex. The first statement then is:

1. All primary vertices (black dots of (3.34)) are of order  $\alpha^0$ .

Since the black dot with an electron loop attached in (3.34) represents the Coulomb potential of the electron density (cf. rule 4. of Section 2.6), the statement holds also true for the empty dots of (3.34).

With the Green's functions the situation is more involved; they consist of contributions of different orders in  $\alpha$ . The classification of those contributions can only be made in energy-momentum representation. Consider  $\mathbf{G}_0(\mathbf{k}, \mathbf{Q}, \mathbf{Q}'; i\epsilon_s)$  from (3.28). From (2.33),

---

<sup>1</sup>Normally,  $T_c$  is even much smaller than  $\omega_{\text{ph}}$ . Since, however,  $\alpha \approx 10^{-2}$ , both ratios are treated as of the same order in  $\alpha$ .

$\epsilon_s = (2s + 1)\pi T$ , which in the case  $T \sim T_c$  is of order  $\alpha^1$  for  $s \ll \alpha^{-1}$  and of order  $\alpha^0$  for  $s \geq \alpha^{-1}$ . On account of the prefactors  $\tau_0$  and  $\tau_3$  one has<sup>2</sup>

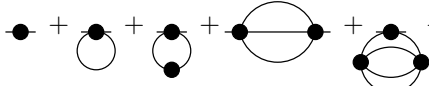
$\mathbf{G}_0$  is of order  $\alpha^{-1}$ , if both  $\epsilon_s$  and  $(\mathbf{k} + \mathbf{Q})^2/2 - \mu$  are of order  $\alpha$ ; otherwise  $\mathbf{G}_0$  is of order  $\alpha^0$ .

With  $\omega_s = 2s\pi T$  and  $M \sim \alpha^{-2}$ , (3.31) yields

2.  $D_0$  is of order  $\alpha^0$ , if  $\omega_s \sim \alpha$ , and of order  $\alpha^2$  otherwise, irrespective of  $\mathbf{q}$ .

Hence, there is a restricted range of Matsubara frequencies which in the case of electrons is further restricted to low excitation energies (while all phonon energies are to be considered low) and in which the Green's functions are of leading order. Outside of these ranges they are of lower order.

Before proceeding we observe, that any inner phononic line of a diagram increases its order in  $\alpha$  at least by one: either the phononic Green's function is  $\sim \alpha^2$  or the Matsubara frequency summation corresponding to that line is restricted  $\sim \alpha$ . Hence, the leading order electronic Green's function contributions are not affected (to leading order) by phononic contributions. This lets us introduce a purely electronic Green's function  $\mathbf{G}^0$  with use of the vertices  $\hat{V}_{ee}$  and  $\hat{V}^0$  only:

$$\mathbf{G}^0 = \mathbf{G}_0 + \mathbf{G}_0 \Sigma^0 \mathbf{G}^0, \quad \Sigma^0 = \text{diagram 1} + \text{diagram 2} + \text{diagram 3} + \text{diagram 4} + \dots \quad (4.1)$$


Like in Section 3.3, the superscript 0 in  $\mathbf{G}^0$  and in  $\Sigma^0$  means zeroth order in  $\mathbf{u}$  while  $\mathbf{G}_0$  as previously means the free-electron Green's function. Clearly, the scale of any frequency or energy dependence of  $\mathbf{G}^0$  and  $\Sigma^0$  is  $\alpha^0$  since no  $\alpha$ -dependent terms enter.

This problem of obtaining the electron Green's function in a *static arrangement of nuclei* is a problem of its own. It is nowadays solved in two steps. Before discussing the details we mention that generally Dyson's equation,  $G = G_0 + G_0 \Sigma G$ , may in an operator sense be cast into  $G^{-1} = G_0^{-1} - \Sigma$  by multiplying the first form from the left by  $G_0^{-1}$  and from the right by  $G^{-1}$  (cf. (2.58)). If now the self-energy is expanded as  $\Sigma = \Sigma_0 + \Sigma_1 + \dots$ , then we may form a sequence  $G_1^{-1} = G_0^{-1} - \Sigma_0$ ,  $G_2^{-1} = G_1^{-1} - \Sigma_1$ , ... which converges to  $G^{-1}$ , if the series for  $\Sigma$  converges. Note that stepping from one equation to the next in this series does not simply mean replacing  $\Sigma_n$  by  $\Sigma_{n+1}$ , but implies a complete diagrammatic restructuring of  $\Sigma_{n+1}$  in terms of  $G_{n+1}$  instead of  $G_n$  for the diagram lines. In terms of Dyson's integral equation the kernel  $G_n \Sigma_n$  is to be replaced by the kernel  $G_{n+1} \Sigma_{n+1}$ .

The first step towards solving our problem is now a density functional calculation. A description of density functional theory is outside of the scope of these notes.<sup>3</sup> Although it could be formulated for non-zero temperature, it is usually treated at  $T = 0$  which is completely sufficient in our context, since  $T \sim \alpha$ . It provides a Green's function  $\mathbf{G}_1^0$  which yields the correct final density of the problem as  $n(\mathbf{r}) = -i\zeta 2[G_1^0]_{11}(\mathbf{r}, \mathbf{r}; -i\tau \rightarrow +i0)$  (the factor 2 results from the sum over spins), and a self-consistent Kohn-Sham potential  $V_{\text{KS}}(\mathbf{r})$  representing the diagonal and frequency independent  $\Sigma_0^0$ :

$$\Sigma_0^0(\mathbf{r}, \mathbf{r}'; i\epsilon_s) = \tau_3 \delta(\mathbf{r} - \mathbf{r}') V_{\text{KS}}(\mathbf{r}). \quad (4.2)$$

Instead of (3.25), the unperturbed electron Green's function  $\mathbf{G}_1^0$  is now defined with the effective Kohn-Sham Hamiltonian

$$\hat{H}_{\text{KS}} = -\frac{1}{2} \frac{\partial^2}{\partial \mathbf{r}^2} + V_{\text{KS}}(\mathbf{r}) - \mu \quad (4.3)$$

<sup>2</sup> $\mathbf{G}_0$  may be even of higher order in  $\alpha$  for very large  $\epsilon_s$  or  $\mathbf{Q}$ . Since the corresponding sums over  $\epsilon_s$  and over  $\mathbf{Q}$ , however, converge, there is no need for treating this as a special case.

<sup>3</sup>See, for instance, H. Eschrig, *The Fundamentals of Density Functional Theory*, B. G. Teubner, Stuttgart, 1996.



and the remaining self-energy  $\Sigma^0 - \Sigma_0^0$  is obtained by replacing

$$\hat{V}^0 \rightarrow (\hat{V}_{\text{en}} + \hat{V}_{\text{nn}})(\mathbf{R}_m^0) + \hat{V}_{\text{ee}} * n - \hat{V}_{\text{KS}} \quad (4.4)$$

in (3.34), where the first terms on the right hand side correspond (in a symbolic way of writing) to the first two diagrams of (4.1). Therefore, the new vertex  $\hat{V}^0$  is to be expected a rather weak perturbation.  $\hat{V}_{\text{ee}}$  remains unchanged.

For a crystalline solid, instead of (3.28) the unperturbed electron Green's function is now

$$\mathbf{G}_1^0(\mathbf{k}, n, n'; i\epsilon_s) = \delta_{nn'} \left[ \tau_0 i\epsilon_s - \tau_3 (\epsilon_{\mathbf{k}n} - \mu) \right]^{-1}, \quad (4.5)$$

and, in  $x$ -representation,

$$\mathbf{G}_1^0(x, x'; i\epsilon) = \sum_{\mathbf{k}} \sum_n^{\text{B.Z.}} \phi_{\mathbf{k}n}(x) \phi_{\mathbf{k}n}^*(x') \left[ \tau_0 i\epsilon_s - \tau_3 (\epsilon_{\mathbf{k}n} - \mu) \right]^{-1}. \quad (4.6)$$

Here,  $n, n'$  are band indices of energy bands  $\epsilon_{\mathbf{k}n}$  and  $\phi_{\mathbf{k}n}(x)$  are the corresponding Bloch orbitals. (Cf. (2.25–2.28) and (2.16).) Now, the classification rule reads

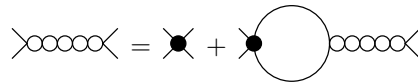
3.  $G_1^0$  is of order  $\alpha^{-1}$ , if both  $\epsilon_s$  and  $\epsilon_{\mathbf{k}n} - \mu$  are of order  $\alpha$ ; otherwise  $G_1^0$  is of order  $\alpha^0$ .

In free-electron metals like aluminum, there is not a big difference between this rule 3 and its free-electron counterpart given above. In the general case, we have to do a band structure calculation with a self-consistent potential  $V_{\text{KS}}$  as close as possible to the exact one. For that purpose, non-local Kohn-Sham potentials as LDA+ $U$  are sometimes used.

Since the new unperturbed Green's function  $G_1^0$  provides the correct density and a reasonable approximation to the quasi-particle spectrum, we have



With the latter bubble we now may introduce a screened electron-electron interaction like in (2.63):



and define

$$\Sigma_1^0 = \text{loop with one dot} + \text{chain of four circles with bubble}$$

as a variant of the so called GW approximation.<sup>4</sup> Here, according to (4.4), the first term is the difference between the Hartree-Fock potential computed with the Kohn-Sham density matrix and the Kohn-Sham potential itself. The second term dynamically screens the exchange potential.<sup>5</sup> The GW approximation is presently at the limit of computing  $\Sigma^0$ .

<sup>4</sup>U. von Barth and L. Hedin, Nuovo Cimento **B23**, 1 (1974).

<sup>5</sup>The direct Coulomb potential remains unscreened in this context, since screening this interaction only leads to contributions to the loop with the full electron Green's function and hence to correct the density which was already correctly determined by the simple loop with the unperturbed Green's function.

We now split the Green's functions into the leading order part and the rest, in quasi-momentum representation,

$$\begin{aligned} \mathbf{G}(\mathbf{k}, n, n'; i\epsilon_s) &= \mathbf{G}^{\text{low}}(\mathbf{k}, n, n'; i\epsilon_s) + \mathbf{G}^{\text{high}}(\mathbf{k}, n, n'; i\epsilon_s) = \\ &= \text{---} + \text{---} \end{aligned} \quad (4.7)$$

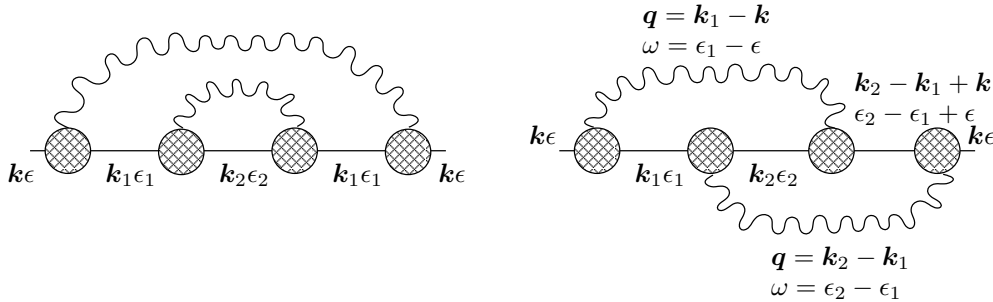
$$\begin{aligned} D(\mathbf{q}, \lambda, \lambda'; i\omega_s) &= D^{\text{low}}(\mathbf{q}, \lambda, \lambda'; i\omega_s) + D^{\text{high}}(\mathbf{q}, \lambda, \lambda'; i\omega_s) = \\ &= \text{~} + \text{~} \end{aligned} \quad (4.8)$$

This splitting is meant for both unperturbed and full Green's functions since we want to introduce skeleton parts in compatibility with our classification. The high energy parts labeled 'high' are supposed to be zero in the low frequency and energy regions and vice versa, so that the sum of both parts as the final result does not depend on fine details of the splitting.

Each diagram originally comprising  $n$  lines is now split into  $2^n$  diagrams with all possible combinations of low and high energy lines. However, any part of a diagram consisting only of high energy lines and possibly all kinds of vertices is of order  $\alpha^0$ , or of higher order, if it contains high energy phonon lines.<sup>6</sup> The sum of all such parts with given numbers of low energy terminals is uniquely defined by the latter (as a function of the variables of those low energy terminals). It will be represented by a cross-hatched blob with terminals and considered a 'high energy vertex.' It would have to be calculated by summing up all contributing high energy diagrams which comprises summation over the Matsubara frequencies and integration over the quasi-momenta as well as summation over band or branch indices. This is precisely meant in Many-Body Theory if one speaks of *integrating out the high energy degrees of freedom*.

## 4.2 Migdal's Theorem

Now we consider diagrams or skeleton diagrams consisting of low energy unperturbed or full Green's functions (thin or thick lines) and high energy vertex blobs. Examples are the following electron self-energy contributions:



Let us determine their order in  $\alpha$ . There are three low energy electron lines yielding together  $\alpha^{-3}$ , and two low energy phonon lines yielding  $\alpha^0$ . The phonon Matsubara frequencies  $\omega_s$  as well as the phonon momenta  $\mathbf{q}$  are uniquely determined by the electron Matsubara frequencies  $\epsilon_s$ ,  $\epsilon_{1s}$  and  $\epsilon_{2s}$  and by the electron momenta  $\mathbf{k}$ ,  $\mathbf{k}_1$  and  $\mathbf{k}_2$ , respectively. Frequency and momentum conservation on the vertices also makes the frequencies and momenta on the left and right halves of the left diagram equal. The independent summation over the independent two inner frequencies  $\epsilon_1$  and  $\epsilon_2$  up to order  $\alpha$  yields  $\alpha^2$ . In the left diagram,

<sup>6</sup>For the latter reason one could in all what follows completely neglect the high energy phonon contributions.

there are independent integrations over  $\mathbf{k}_1$  and  $\mathbf{k}_2$ , each over layers of thickness  $\sim \alpha$  around the sheets of the Fermi surface. (The thickness of the  $\mathbf{k}$ -layer is equal to the thickness of the  $(\epsilon_{\mathbf{k}n} - \mu)$ -layer divided by the Fermi velocity of the reference band structure which latter is on the high energy scale and hence  $\sim \alpha^0$ .) Since the low energy phonon momenta are unrestricted, there is no further restriction on the electron momenta. The two  $\mathbf{k}$ -integrations yield another factor  $\alpha^2$ . Hence, in total from the low energy lines, the frequency summations and the  $\mathbf{k}$ -integrations we find the order  $\alpha^{-3}\alpha^2\alpha^2 = \alpha$  for the left diagram.

The difference in the right diagram comes from the *additional condition* that  $\mathbf{k}_2 - \mathbf{k}_1 + \mathbf{k}$  must also lie in an  $\alpha$ -layer around a sheet of the Fermi surface. Hence,  $\mathbf{k}_2$  must now be close to the *intersection* of two sheets of the Fermi surface. One drawn from the origin and one drawn from the point  $\mathbf{k}_1 - \mathbf{k}$ . While in three and two dimensions the Fermi surface is two- and one-dimensional and that intersection is one- and zero-dimensional, respectively, in one dimension there appears no new restriction. There, if  $\mathbf{k}$ ,  $\mathbf{k}_1$  and  $\mathbf{k}_2$  are close to a Fermi point, then  $\mathbf{k}_2 - \mathbf{k}_1 + \mathbf{k}$  is either. (In particular cases which are called Fermi surface nesting this situation may also appear in higher dimensions.) In higher than one dimension and in the absence of nesting we find for the right diagram in total by an analogous count as above the order  $\alpha^{-3}\alpha^2\alpha^3 = \alpha^2$ . Only in one dimension or in case of nesting the same order as for the left diagram is obtained.

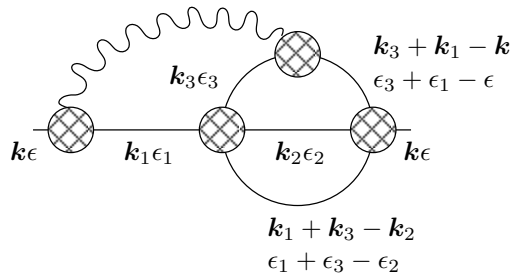
In order to calculate the full electron Green's function  $G^{\text{low}} = G_0^{\text{low}}\Sigma G^{\text{low}}$  in leading order  $\alpha^{-1}$ , one needs the self-energy  $\Sigma$  in leading order  $\alpha$ . The above considered diagrams are part of the skeleton diagrams



The inner phonon line of the previous left diagram is part of the inner full electron line of the left skeleton diagram (it contributes to the self energy of that full electron line). The checkered vertex on the right skeleton diagram means a full (high energy plus low energy) vertex, to which the right phonon line of the previous right diagram contributes. Migdal has shown<sup>7</sup> that our above findings regarding the order of such diagrams are quite general:

*In higher than one dimension and in the absence of nesting, all phononic contributions to vertices are of higher than the leading order in  $\alpha$ .*

What about low energy electronic contributions to full vertices. Consider as an example the diagram



It contributes to the right skeleton diagram above. There are four additional low energy electron lines entering the right full vertex and yielding a contribution of order  $\alpha^{-4}$ . There are two additional frequency summations over  $\epsilon_2$  and  $\epsilon_3$ , yielding  $\alpha^2$ . There are the corresponding momentum integrations over  $\mathbf{k}_2$  and  $\mathbf{k}_3$  running over Fermi surface layers. Both

<sup>7</sup>He proved it on the basis of Fröhlich's Hamiltonian, which in this context makes no difference.

momenta must, however, fulfill an additional condition which reduces both integrations to intersections of Fermi surfaces with shifted ones. These two integrations hence yield  $\alpha^4$ , and the total order of the vertex correction is  $\alpha^{-4}\alpha^2\alpha^4 = \alpha^2$ . (It is easily seen that without the phonon line the pure electron vertex would also be of order  $\alpha^2 = \alpha^{-3}\alpha^2\alpha^3$ .) By this reasoning, the factor  $\alpha^{-1}$  of each inner low energy electron line is compensated by a factor  $\alpha$  from momentum integration, and the order of the contribution is equal to the number of independent new frequency summations:

*In higher than one dimension and in the absence of nesting, all low energy electronic contributions to vertices are of higher than the leading order in  $\alpha$ .*

In all what follows we assume an effective dimension higher than one and the absence of nesting.

### 4.3 Leading Order Self-Energies

With these results, the leading order low energy electron self-energy skeleton diagrams are:

$$\Sigma = \text{[diagram 1]} + \text{[diagram 2]} + \text{[diagram 3]} + \text{[diagram 4]} \quad (4.9)$$

The first contribution is the high energy electron self-energy in the static solid ( $\Sigma^0 - \Sigma_0^0$  of Section 4.1). It is formally of order  $\alpha^0$ . This would lead to the appearance of all orders  $\alpha^{-n}$  for all  $n > 0$  in an expansion of Dyson's equation for the low energy electron Green's function (since  $\mathbf{G}_0 \sim \alpha^{-1}$  in  $\mathbf{G} = \mathbf{G}_0 + \mathbf{G}_0 \Sigma \mathbf{G}$  would not be compensated by  $\Sigma \sim \alpha$  in the second term). Hence it would completely destroy our systematics because our rule 3. of Section 4.1 would not any more carry over to the full Green's function. This is why it was so important to replace the free-electron Green's function  $\mathbf{G}_0$  by the band structure Green's function  $\mathbf{G}_1^0$  in such a way that the remaining self-energy  $\Sigma - \Sigma_0^0$ , although formally of order  $\alpha^0$ , is practically small of order  $\alpha$  *in the low energy low frequency domain*.

The second contribution was analyzed in the preceding section, and the last two contributions to  $\Sigma$  contain dressed four leg vertices which are indeed of order  $\alpha^0$ . However, both the electron and the phonon loop introduce a factor  $\alpha$ : Their frequencies and momenta are independent from those of the terminals, and hence, by way of the analysis of the last section the electron loop introduces  $\alpha^{-1}\alpha\alpha$ , and the phonon loop introduces  $\alpha^0\alpha\alpha^0$ , the latter factor since the low energy phonon momentum is unrestricted.

In view of the independence of the frequencies and momenta of the loops one could think that those last two contributions to  $\Sigma$  have a weak frequency and momentum dependence, changing only on the large energy scale like the first contribution. This is indeed the case for the last diagram, the last but one, however, will develop an anomalous part in the superconducting state since the full Green's function of the electron loop will develop such a part. Hence, *the essential low energy electronic self-energy contributions are the middle two of (4.9)*.

The leading order low energy phonon self-energy consists only of the high energy blob of order  $\alpha^0$ :

$$\Pi = \text{[diagram 1]} \quad (4.10)$$

This is consistent with our systematics, since  $D_0^{\text{low}} \sim \alpha^0$ , and hence Dyson's equation preserves this order for  $D^{\text{low}}$ . Hence, the low energy electron Green's function does not enter the phonon problem to leading order. It is completely determined by the high energy

electronic structure and hence by band structure theory. The superconducting state only weakly influences the phonon spectrum.

Since the high energy blob of (4.10) has a frequency and energy dependence of the high energy scale, to leading order this dependence can be neglected in the low energy range, hence (4.10) may be approximated by the adiabatic expression (in the representation of (3.29))

$$\Pi(l\lambda, l'\lambda'; 0) = \left. \frac{\partial^2 E_0}{\partial u_{l\lambda} \partial u_{l'\lambda'}} \right|_{\mathbf{u}=0} \quad (4.11)$$

where  $E_0$  is the total energy of the normal electronic ground state in a static assembly of nuclei at positions with coordinates  $\mathbf{R}_{l\lambda}^0 + u_{l\lambda}$ . Note that due to (3.22, 3.23) each diagram with a phononic terminal is obtained from a corresponding diagram without that terminal by differentiation with respect to the nuclear positions.

Multiplication of the force constant matrix elements on the right hand side of (4.11) with  $1/\sqrt{M_\lambda M_{\lambda'}}$  and diagonalization of the resulting matrix yields

$$\Pi(l\lambda, l'\lambda'; 0) = \frac{1}{M} \sum_{\mathbf{q}\kappa} e^{i\mathbf{q}\cdot\mathbf{R}_l^0} e_\lambda(\mathbf{q}\kappa) \omega_{\mathbf{q}\kappa}^2 e_{\lambda'}^*(\mathbf{q}\kappa) e^{-i\mathbf{q}\cdot\mathbf{R}_{l'}^0}, \quad (4.12)$$

where  $M$  is the number of unit cells as previously and the orthogonal polarization vectors  $e$  are complete and normalized in such a way that:

$$\frac{1}{M} \sum_{\mathbf{q}\kappa} e^{i\mathbf{q}\cdot\mathbf{R}_l^0} e_\lambda(\mathbf{q}\kappa) e_{\lambda'}^*(\mathbf{q}\kappa) e^{-i\mathbf{q}\cdot\mathbf{R}_{l'}^0} = \delta_{ll'} \delta_{\lambda\lambda'} M_\lambda \quad (4.13)$$

with the nuclear masses  $M_\lambda$ . Hence, from Dyson's equation in the form  $D^{-1} = D_0^{-1} - \Pi$  one finds readily

$$D(l\lambda, l'\lambda'; i\omega_s) = -\frac{1}{M} \sum_{\mathbf{q}\kappa} e^{i\mathbf{q}\cdot\mathbf{R}_l^0} e_\lambda(\mathbf{q}\kappa) \frac{1}{\omega_s^2 + \omega_{\mathbf{q}\kappa}^2} e_{\lambda'}^*(\mathbf{q}\kappa) e^{-i\mathbf{q}\cdot\mathbf{R}_{l'}^0} \quad (4.14)$$

or

$$D(\mathbf{q}, \lambda, \lambda'; i\omega_s) = -\sum_{\kappa} e_\lambda(\mathbf{q}\kappa) \frac{1}{\omega_s^2 + \omega_{\mathbf{q}\kappa}^2} e_{\lambda'}^*(\mathbf{q}\kappa). \quad (4.15)$$

If one is interested in the effect of the superconducting state on the phonon frequencies, one can of course calculate a next correction term to  $\Pi$  of a form analogous to the third diagram in (4.9).

The same type of consideration as in (4.11) immediately shows that every tadpole part of diagram with a phononic tail is exactly zero in a harmonic crystal:

$$\text{w} \text{blob} = \left. \frac{\partial E_0}{\partial u_{l\lambda}} \right|_{\mathbf{u}=0} = 0. \quad (4.16)$$

Here, the checkered blob means again a full (high plus low energy) skeleton vertex, which at variance to (4.10) is correctly to all orders in  $\alpha$  equal to the first derivative of the total energy with respect to the nuclear position. The vanishing of all those first derivatives just defines the nuclear equilibrium positions relative to which the adiabatic and harmonic phonons are defined. For that reason we did not include tadpole parts with phononic tails into our analysis of orders of  $\alpha$  (where they would not fit in, if they were non-zero). In a harmonic crystal,  $\langle \mathbf{R}_m \rangle = \mathbf{R}_m^0$  holds independent on temperature, there is no thermal expansion. Anharmonic corrections change this behavior and also correct (4.16).

## Chapter 5

# The Low Energy Equations

In the last chapter, two high energy problems have been separated from the low energy problem of superconductivity (and of low energy transport in general): the problem (4.1–4.6) of the self-consistent electronic structure of the solid without lattice displacements and the problem (4.11–4.15) of the adiabatic lattice dynamics of the solid. Both problems need a careful treatment of self-consistent screening of the Coulomb interaction and hence a careful calculation of the electronic density. *Density functional methods* provide nowadays the most powerful approach to both problems and allow effectively to solve them with the needed accuracy.

The remaining part of the electron self-energy,  $\Sigma^0 - \Sigma_0^0$ , which relates the full high energy Green's function,  $\mathbf{G}^0$ , to the unperturbed Green's function,  $\mathbf{G}_1^0$ , of non-interacting band states, may be addressed by GW methods. For the sake of brevity, this remaining part of the self-energy is denoted by  $\Sigma_1^0$  in the following. Since it is small, it may be considered to be of the low energy scale in magnitude but vary on the high energy scale as demanded. This lets us write

$$\Sigma_1^0(\mathbf{r}, \mathbf{r}'; i\epsilon_s) = \tau_3 \Sigma_1^0(\mathbf{r}, \mathbf{r}'; 0) + \tau_0 \Sigma_1^{0'}(\mathbf{r}, \mathbf{r}'; 0) i\epsilon_s. \quad (5.1)$$

as the Taylor expansion of the frequency dependence of  $\Sigma_1^0$  to linear order. From (3.16) one can see that not only the sign of the Nambu component  $G_{22}$  is reversed compared to  $G_{11}$  but also the sign of the frequency argument. This must also hold true for  $\Sigma^0$ , whence the first order Taylor term is  $\sim \tau_0$ . In a normal metal, the imaginary part of  $\Sigma^0$  is  $\sim \epsilon^2$ , hence  $\Sigma_0^0$  and  $\Sigma_1^0$  are real (and symmetric as integral operators).

As for the adiabatic lattice dynamics calculated with density functional methods, it nowadays agrees typically within five to ten percent with the experimental phonon spectra.

Given these results and the high energy vertices, the problem of superconductivity reduces to the solution of the closed non-linear equation system

$$\int d^3r_1 \left[ \tau_0 i\epsilon_s a^{-1}(\mathbf{r}, \mathbf{r}_1) - \tau_3 H^0(\mathbf{r}, \mathbf{r}_1) - \Sigma_1^{\text{ep}}(\mathbf{r}, \mathbf{r}_1; i\epsilon_s) - \Sigma_1^{\text{ee}}(\mathbf{r}, \mathbf{r}_1; i\epsilon_s) \right] \mathbf{G}^{\text{low}}(\mathbf{r}_1, \mathbf{r}'; i\epsilon_s) = \tau_0 \delta(\mathbf{r} - \mathbf{r}') \quad (5.2)$$

which is Dyson's equation for  $\mathbf{G}^{\text{low}}$  to leading order with the self-energy contributions of the first three diagrams of (4.9).  $H^0$  consists of  $H_{\text{KS}}$  and  $\Sigma_1^0$ , and  $a^{-1}$  contains  $\Sigma_1^{0'}$ . Eq. (5.2) is non-linear since  $\Sigma_1^{\text{ep}}$  and  $\Sigma_1^{\text{ee}}$  depend on  $\mathbf{G}^{\text{low}}$ .

## 5.1 The Quasi-Particle Renormalization

The first term of (5.2) contains the linear Taylor term of (5.1). Like in (2.62) it leads to a renormalization of the quasi-particle amplitude,

$$a(\mathbf{r}, \mathbf{r}') = [\delta(\mathbf{r} - \mathbf{r}') - \Sigma_1^{0'}(\mathbf{r}, \mathbf{r}'; 0)]^{-1} \approx \delta(\mathbf{r} - \mathbf{r}') + \Sigma_1^{0'}(\mathbf{r}, \mathbf{r}'; 0). \quad (5.3)$$

(The exponent  $-1$  means the kernel of the inverse integral operator.) This so called Coulomb renormalization factor barely ever has really been calculated for a real band structure.<sup>1</sup> It could be addressed by GW methods as mentioned above. In normal metals,  $|\Sigma_1^{0'}|$  is of the order of 0.1 to 0.3, and hence only  $\Sigma_1^{0'2}$  is small of order  $\alpha$ . (In (5.1), although  $\Sigma_1^0 \sim \alpha$ ,  $\Sigma_1^{0'}$  may be of order  $\alpha^0$ , since in the low frequency domain  $\epsilon_s$  is of order  $\alpha$ .)

In the standard approach the Coulomb renormalization factor is considered by renormalizing all quantities entering (5.2):

$$\mathbf{g} = \tau_3 a^{-1/2} * \mathbf{G}^{\text{low}} * a^{-1/2}, \quad (5.4)$$

$$h^0 = a^{1/2} * H^0 * a^{1/2}, \quad (5.5)$$

$$\sigma^{\text{ep}} = a^{1/2} * \Sigma_1^{\text{ep}} * a^{1/2} \tau_3, \quad (5.6)$$

$$\sigma^{\text{ee}} = a^{1/2} * \Sigma_1^{\text{ee}} * a^{1/2} \tau_3, \quad (5.7)$$

where for the sake of brevity a notation of integral operators was used,

$$a^{\pm 1/2} \approx 1 \pm \frac{1}{2} \Sigma_1^{0'}, \quad (5.8)$$

and the star means the operation

$$(a * b)(\mathbf{r}, \mathbf{r}') = \int d^3 r_1 a(\mathbf{r}, \mathbf{r}_1) b(\mathbf{r}_1, \mathbf{r}'). \quad (5.9)$$

(The factors  $\tau_3$  in (5.4–5.7) are just convention to reduce the number of factors  $\tau_3$  in the following relations.) Dyson's equation (5.2) renormalizes to

$$[\tau_3 i \epsilon_s - \tau_0 h^0 - \sigma^{\text{ee}} - \sigma^{\text{ep}}] * \mathbf{g} = \mathbf{1}. \quad (5.10)$$

The Hamiltonian  $H_0$  for the high energy quasi-particle band structure was

$$H^0(\mathbf{r}, \mathbf{r}') = H_{\text{KS}}(\mathbf{r}, \mathbf{r}') + \Sigma_1^0(\mathbf{r}, \mathbf{r}'; 0) \quad (5.11)$$

with  $H_{\text{KS}}$  from (4.3). From its renormalized form an effective quasi-particle potential

$$v^0 = h^0 - (t - \mu) = V_{\text{KS}} + \Sigma_1^0 + \frac{1}{2} [H^0, \Sigma_1^{0'}]_+ \quad (5.12)$$

may be extracted, which is meaningful for low electron energies (that is close to the Fermi surface) since (5.1) was meaningful in that domain. It is related to the quasi-particle Green's function  $\mathbf{g}$  (which in the normal state has a spectral amplitude equal to one at the quasi-particle pole and yields a quasi-particle quasi-momentum distribution which jumps from unity to zero at the Fermi surface). The quasi-particle Green's function  $\mathbf{g}$  on the other hand is related to the true electron Green's function  $\mathbf{G}$  via (5.4) in the low energy domain where we still neglect  $\text{Im } \Sigma \sim \alpha^2$ . In practical calculations  $v^0$  is often approximated by  $V_{\text{KS}}$ , while  $\Sigma_1^{0'}$  should not be neglected in (5.4, 5.6, 5.7).

<sup>1</sup>It has been calculated by many authors for the homogeneous electron liquid or for model systems.

## 5.2 The Electron-Phonon Self-Energy

The potential  $v^0$  is also intimately related to the (high energy) electron-phonon vertex entering the second diagram of (4.9). As was already explained in connection with (4.11), a diagram with a phonon leg is obtained from the corresponding diagram without that leg by differentiation with respect to the nuclear positions. In the considered case, the electron-phonon vertex denoted by  $\Gamma^{\text{ep}}(\mathbf{r}, \mathbf{r}'|l\lambda)$  is obtained by differentiating the two leg electron vertex  $\Sigma^0(\mathbf{r}, \mathbf{r}'; 0)$  of (4.1):

$$\Gamma^{\text{ep}}(\mathbf{r}, \mathbf{r}'|l\lambda) = \left. \frac{\partial \Sigma^0(\mathbf{r}, \mathbf{r}'; 0)}{\partial u_{l\lambda}} \right|_{\mathbf{u}=0}. \quad (5.13)$$

(Since we need the vertices only to zeroth order and in the low frequency range of the legs,  $\Sigma^0$  may be taken for  $\epsilon_s \rightarrow 0$  here.) In accordance with the previous section we define a renormalized electron-phonon vertex as

$$\gamma^{\text{ep}} = a^{1/2} * \Gamma^{\text{ep}} * a^{1/2}. \quad (5.14)$$

With the help of the Feynman rules of Section 2.6, the electron-phonon self-energy diagram (second diagram of (4.9)) is translated into

$$\begin{aligned} \Sigma^{\text{ep}}(\mathbf{r}, \mathbf{r}'; i\epsilon_s) = & - \int d^3 r_1 d^3 r'_1 \sum_{l\lambda, l'\lambda'} \frac{1}{\beta} \sum_{s'} \\ & \Gamma^{\text{ep}}(\mathbf{r}, \mathbf{r}_1|l\lambda) \boldsymbol{\tau}_3 \mathbf{G}^{\text{low}}(\mathbf{r}_1, \mathbf{r}'_1; i\epsilon_s - i\omega_{s'}) \boldsymbol{\tau}_3 \Gamma^{\text{ep}}(\mathbf{r}'_1, \mathbf{r}'|l'\lambda') D(l\lambda, l'\lambda'; i\omega_{s'}). \end{aligned} \quad (5.15)$$

(The two factors  $1/\beta$  attached with  $\mathbf{G}^{\text{low}}$  and  $D$  are canceled against the two factors  $\beta$  attached with the two vertices. Since a self-energy diagram has external structure like a Green's function with two vertices, it is translated into  $-\beta\Sigma$ . Additionally, like  $H^0$  in (5.2), each pair of electron legs of electron-electron and electron-phonon vertices gets a factor  $\boldsymbol{\tau}_3$ .)

Substituting (5.15) with the renormalized quantities (5.4–5.7, 5.14) yields finally

$$\begin{aligned} \boldsymbol{\sigma}^{\text{ep}}(\mathbf{r}, \mathbf{r}'; i\epsilon_s) = & - \int d^3 r_1 d^3 r'_1 \sum_{l\lambda, l'\lambda'} \frac{1}{\beta} \sum_{s'} \\ & \gamma^{\text{ep}}(\mathbf{r}, \mathbf{r}_1|l\lambda) \mathbf{g}(\mathbf{r}_1, \mathbf{r}'_1; i\epsilon_s - i\omega_{s'}) \gamma^{\text{ep}}(\mathbf{r}'_1, \mathbf{r}'|l'\lambda') D(l\lambda, l'\lambda'; i\omega_{s'}). \end{aligned} \quad (5.16)$$

The electron-phonon vertex  $\gamma^{\text{ep}}$  is obtained from (5.14) and (5.13):

$$\begin{aligned} \gamma^{\text{ep}} = & a^{1/2} * \frac{\partial \Sigma^0}{\partial \mathbf{u}} * a^{1/2} = a^{1/2} * \frac{\partial H^0}{\partial \mathbf{u}} * a^{1/2} = \\ = & a^{1/2} * \left[ \frac{\partial}{\partial \mathbf{u}} a^{-1/2} * h^0 * a^{-1/2} \right] * a^{1/2} = \frac{\partial h^0}{\partial \mathbf{u}} - \frac{1}{2} \left[ a^{-1} * \frac{\partial a}{\partial \mathbf{u}} * h^0 + h^0 * \frac{\partial a}{\partial \mathbf{u}} * a^{-1} \right]. \end{aligned} \quad (5.17)$$

Since  $h^0 \sim \alpha$  in the low energy domain while vertices are generally  $\sim \alpha^0$ , the terms in square brackets may be neglected, and the final leading order result is

$$\gamma^{\text{ep}}(\mathbf{r}, \mathbf{r}'|l\lambda) = \left. \frac{\partial v^0(\mathbf{r}, \mathbf{r}')}{\partial u_{l\lambda}} \right|_{\mathbf{u}=0}. \quad (5.18)$$

This important result says that the renormalized electron-phonon vertex is obtained as the change of the quasi-particle crystal potential for a static displacement of the nuclear position out of equilibrium. It may readily be calculated like  $v^0$  itself by means of the same density functional approach, possibly corrected with GW methods.



### 5.3 The Electron-Electron Self-Energy

The third diagram of (4.9) translates into

$$\Sigma^{\text{ee}}(\mathbf{r}, \mathbf{r}'; i\epsilon_s) = - \int d^3r_1 d^3r'_1 \frac{1}{\beta} \sum_{s'} \Gamma^{\text{ee}}(\mathbf{r}, \mathbf{r}', \mathbf{r}_1, \mathbf{r}'_1; i\epsilon_s, i\epsilon_{s'}) \tau_3 \mathbf{G}^{\text{low}}(\mathbf{r}_1, \mathbf{r}'_1; i\epsilon_{s'}) \tau_3 \quad (5.19)$$

(This relation also defines which sign and  $\beta$  factors are attached with  $\Gamma^{\text{ee}}$ .)

The Nambu structure of this diagram is

For the diagonal elements, the same holds true what was said in Section 4.3 about the fourth diagram of (4.9). They need not be considered further and we may concentrate on the off-diagonal diagrams in the sequel.

Even if the normal metallic state is not spin polarized, the exchange part of the electron-electron interaction and hence also  $\Gamma^{\text{ee}}$  depends on the spin of the electrons. For the case of singlet pairing considered throughout this text, the spin structure of  $\mathbf{G}$  and  $\Sigma$  was finally determined in (3.19). In (5.19),  $\Gamma^{\text{ee}}$  has to be taken in accordance with that spin structure. Clearly, this is different for instance for singlet and triplet pairing, respectively.

Before going into the details, we also observe that again the frequency dependence of the vertex  $\Gamma^{\text{ee}}$  may be neglected to leading order for the same reason as in all previous considerations of that point, and the vertex may be taken at zero frequencies (in the sense of analytic continuation; zero itself is not an electron Matsubara frequency). Moreover, it may be renormalized for each electron leg:

$$\begin{aligned} \gamma^{\text{ee}}(\mathbf{r}, \mathbf{r}', \mathbf{r}_1, \mathbf{r}'_1) = \\ \int d^3r_2 d^3r'_2 d^3r_3 d^3r'_3 a^{1/2}(\mathbf{r}, \mathbf{r}_2) a^{1/2}(\mathbf{r}', \mathbf{r}'_2) \Gamma^{\text{ee}}(\mathbf{r}_2, \mathbf{r}'_2, \mathbf{r}_3, \mathbf{r}'_3; 0, 0) a^{1/2}(\mathbf{r}_3, \mathbf{r}_1) a^{1/2}(\mathbf{r}'_3, \mathbf{r}'_1). \end{aligned} \quad (5.20)$$

This reduces (5.19) to

$$\sigma^{\text{ee}}(\mathbf{r}, \mathbf{r}') = - \int d^3r_1 d^3r'_1 \frac{1}{\beta} \sum_{s'} \gamma^{\text{ee}}(\mathbf{r}, \mathbf{r}', \mathbf{r}_1, \mathbf{r}'_1) \mathbf{g}(\mathbf{r}_1, \mathbf{r}'_1; i\epsilon_{s'}), \quad (5.21)$$

of which the Nambu off-diagonal matrix elements matter only. Like the vertex, the electron-electron self-energy is to leading order frequency independent.

### 5.4 Bloch Function Representation on the Fermi Surface

We now introduce a representation in terms of low energy quasi-electron Bloch states, that is, eigenstates of the (Hermitian) Hamiltonian  $\hat{h}^0$  with the kernel

$$h^0(\mathbf{r}, \mathbf{r}') = \left[ -\frac{1}{2} \frac{\partial^2}{\partial r^2} - \mu \right] \delta(\mathbf{r} - \mathbf{r}') + v^0(\mathbf{r}, \mathbf{r}') \quad (5.22)$$

defined in (5.5) and (5.12). The quasi-electron band structure is obtained from

$$\hat{h}^0 \phi_{\mathbf{k}n}(\mathbf{r}) = \phi_{\mathbf{k}n}(\mathbf{r}) \epsilon_{\mathbf{k}n}. \quad (5.23)$$

The orbitals  $\phi_{\mathbf{k}n}$  for spin up and down are assumed equal, hence the spin variables are again omitted. As usual, the orbitals are normalized within a unit cell of the crystal. The quasi-momentum varies in the first Brillouin zone, and  $n$  is the band index. The Fermi surface is given as

$$\text{FS} = \{\mathbf{k}_F : \epsilon_{\mathbf{k}_F n} = 0 \text{ for some } n\}, \quad (5.24)$$

and (5.23) is physically meaningful in a vicinity of the Fermi surface only.

Summation over Bloch states in this vicinity are done according to

$$\sum_{\mathbf{k}n} = \frac{V}{(2\pi)^3} \int_{|\epsilon_{\mathbf{k}n}| < \epsilon_c} d^3k \sum_n \cdots = MD(0) \int_{\text{FS}} d^2\kappa d(\boldsymbol{\kappa}) \int_{-\epsilon_c}^{+\epsilon_c} d\epsilon \cdots, \quad (5.25)$$

where  $\epsilon_c$  is an energy cut-off,  $\alpha\epsilon_F \ll \epsilon_c \ll \epsilon_F$ , so that  $\mathbf{G}^{\text{low}}$  is already zero on the surfaces  $\pm\epsilon_c$  in momentum space, but the local co-ordinates around the Fermi surface,  $\boldsymbol{\kappa}\epsilon$ , are still unique (cf. Fig. 5.1).  $M$  is the number of unit cells, and  $D(0)$  is the band structure density of states per unit cell at the Fermi level and  $D(0)d(\boldsymbol{\kappa})$  is the local Jacobian of the co-ordinate transformation

$$\frac{V_{\text{u.c.}}}{(2\pi)^3} d^3k = \frac{V_{\text{u.c.}}}{(2\pi)^3} \frac{d^2k_F d\epsilon}{|\partial\epsilon_{\mathbf{k}_F n}/\partial\mathbf{k}|} = D(0) d(\boldsymbol{\kappa}) d^2\kappa d\epsilon, \quad \boldsymbol{\kappa} = \boldsymbol{\kappa}(\mathbf{k}_F). \quad (5.26)$$

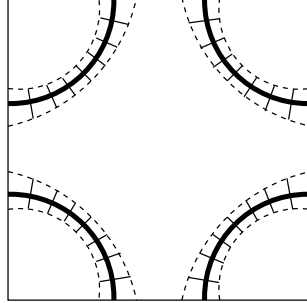


Figure 5.1: Cut through a Brillouin zone with the Fermi surface (thick lines) and surfaces of  $\epsilon = \pm\epsilon_c$  (broken lines) as well as lines of constant  $\boldsymbol{\kappa}$  (short thin lines). The thickness of the layer  $|\epsilon| < \epsilon_c$  is inversely proportional to the Fermi velocity  $v_F = \partial\epsilon_{\mathbf{k}_F n}/\partial\mathbf{k}$ .

The electron Green's function in this representation is

$$\begin{aligned} \mathbf{g}(\boldsymbol{\kappa}\epsilon; i\epsilon_s) &= \frac{1}{M} \int d^3r d^3r' \phi_{\boldsymbol{\kappa}\epsilon}^*(\mathbf{r}) \mathbf{g}(\mathbf{r}, \mathbf{r}'; i\epsilon_s) \phi_{\boldsymbol{\kappa}\epsilon}(\mathbf{r}') = \\ &= [\boldsymbol{\tau}_3 i\epsilon_s - \boldsymbol{\tau}_0 \epsilon - \boldsymbol{\sigma}^{\text{ep}}(\boldsymbol{\kappa}\epsilon; i\epsilon_s) - \boldsymbol{\sigma}^{\text{ee}}(\boldsymbol{\kappa}\epsilon)]^{-1}. \end{aligned} \quad (5.27)$$

The integration is over the total volume of the crystal, and  $M$  in the denominator appears due to the normalization of the orbitals within a unit cell. It is easily seen that the self-energies are diagonal in this representation:  $\boldsymbol{\sigma}(\boldsymbol{\kappa}\epsilon, \boldsymbol{\kappa}'\epsilon'; i\epsilon_s) = \delta_{\boldsymbol{\kappa}\epsilon, \boldsymbol{\kappa}'\epsilon'} \boldsymbol{\sigma}(\boldsymbol{\kappa}\epsilon; i\epsilon_s)$ . Hence, the Green's function is also diagonal, and Dyson's equation is trivially solved (cf. (2.59)).

Indeed, due to the conservation of the total quasi-momentum at every vertex, self-energies and Green's functions are  $\mathbf{k}$ -diagonal. However, in the considered low energy domain the band index  $n$  is uniquely determined by  $\mathbf{k}$ , and  $\mathbf{k}n$ -diagonal is the same as  $\boldsymbol{\kappa}\epsilon$ -diagonal.

Eq. (5.16) now reads

$$\begin{aligned}
\sigma^{\text{ep}}(\boldsymbol{\kappa}\epsilon; i\epsilon_s) &= - \sum_{l\lambda, l'\lambda'} \frac{1}{\beta} \sum_{s'} \frac{D(0)}{M} \int_{\text{FS}} d^2\kappa' d(\boldsymbol{\kappa}') \int d\epsilon' \\
&\quad \langle \phi_{\boldsymbol{\kappa}\epsilon} | \gamma_{l\lambda}^{\text{ep}} | \phi_{\boldsymbol{\kappa}'\epsilon'} \rangle \mathbf{g}(\boldsymbol{\kappa}'\epsilon'; i\epsilon_s - i\omega_{s'}) \langle \phi_{\boldsymbol{\kappa}'\epsilon'} | \gamma_{l'\lambda'}^{\text{ep}} | \phi_{\boldsymbol{\kappa}\epsilon} \rangle D(l\lambda, l'\lambda'; i\omega_{s'}) \approx \\
&\approx - \sum_{l\lambda, l'\lambda'} \frac{1}{\beta} \sum_{s'} \frac{D(0)}{M} \int_{\text{FS}} d^2\kappa' d(\boldsymbol{\kappa}') \\
&\quad \langle \phi_{\boldsymbol{\kappa}0} | \gamma_{l\lambda}^{\text{ep}} | \phi_{\boldsymbol{\kappa}'0} \rangle \int d\epsilon' \mathbf{g}(\boldsymbol{\kappa}'\epsilon'; i\epsilon_s - i\omega_{s'}) \langle \phi_{\boldsymbol{\kappa}'0} | \gamma_{l'\lambda'}^{\text{ep}} | \phi_{\boldsymbol{\kappa}0} \rangle D(l\lambda, l'\lambda'; i\omega_{s'}).
\end{aligned} \tag{5.28}$$

Since all  $\epsilon$  are small and the matrix element of the vertex (5.18) may depend on the energy of the orbitals on the high energy scale only, again to leading order all energy dependences in the vertex may be neglected. Then, the self-energy does not depend on  $\epsilon$  any more and only depends on the energy-integrated Green's function<sup>2</sup>

$$\mathbf{g}(\boldsymbol{\kappa}; i\epsilon_s) = \int d\epsilon \mathbf{g}(\boldsymbol{\kappa}\epsilon; i\epsilon_s), \tag{5.29}$$

which is a function on the Fermi surface only. The theory of superconductivity is then expressed in terms of functions on the Fermi surface.

With

$$I^{\text{ep}}(\boldsymbol{\kappa}, \boldsymbol{\kappa}' | l\lambda) = \langle \phi_{\boldsymbol{\kappa}0} | \frac{\partial v^0}{\partial \mathbf{u}_{l\lambda}} | \phi_{\boldsymbol{\kappa}'0} \rangle \tag{5.30}$$

and

$$\lambda(\boldsymbol{\kappa}, \boldsymbol{\kappa}'; i\omega_s) = -\frac{D(0)}{M} \sum_{l\lambda, l'\lambda'} I^{\text{ep}}(\boldsymbol{\kappa}, \boldsymbol{\kappa}' | l\lambda) D(l\lambda, l'\lambda'; i\omega_s) I^{\text{ep}}(\boldsymbol{\kappa}', \boldsymbol{\kappa} | l'\lambda') \tag{5.31}$$

the electron-phonon self-energy is

$$\sigma^{\text{ep}}(\boldsymbol{\kappa}; i\epsilon_s) = \frac{1}{\beta} \sum_{s'} \int d^2\kappa' d(\boldsymbol{\kappa}') \lambda(\boldsymbol{\kappa}, \boldsymbol{\kappa}'; i\omega_{s'}) \mathbf{g}(\boldsymbol{\kappa}'; i\epsilon_s - i\omega_{s'}). \tag{5.32}$$

This quantity is often averaged over the Fermi surface. Additionally one introduces a phonon spectral function  $B(l\lambda, l'\lambda'; \omega)$  according to

$$D(l\lambda, l'\lambda'; i\omega_s) = -2 \int_0^\infty d\omega B(l\lambda, l'\lambda'; \omega) \frac{\omega}{\omega_s^2 + \omega^2} \tag{5.33}$$

and a spectral density  $\alpha^2 F(\omega)$  of the averaged  $\lambda$ -function:

$$\lambda(i\omega_s) = \int_{\text{FS}} d^2\kappa d^2\kappa' d(\boldsymbol{\kappa}) d(\boldsymbol{\kappa}') \lambda(\boldsymbol{\kappa}, \boldsymbol{\kappa}'; i\omega_s) = 2 \int_0^\infty d\omega \alpha^2 F(\omega) \frac{\omega}{\omega_s^2 + \omega^2}, \tag{5.34}$$

<sup>2</sup>G. Eilenberger, Z. Phys. **214**, 195 (1968); A. I. Larkin and Yu. N. Ovchinnikov, Sov. Phys.-JETP **28**, 1200 (1969).

$$\alpha^2 F(\omega) = D(0) \int_{\text{FS}} d^2\kappa d^2\kappa' d(\boldsymbol{\kappa}) d(\boldsymbol{\kappa}') \quad (5.35)$$

$$\frac{1}{M} \sum_{l\lambda, l'\lambda'} I^{\text{ep}}(\boldsymbol{\kappa}, \boldsymbol{\kappa}' | l\lambda) B(l\lambda, l'\lambda'; \omega) I^{\text{ep}}(\boldsymbol{\kappa}', \boldsymbol{\kappa} | l'\lambda').$$

The electron-phonon mass enhancement is  $\lambda = \lambda(0)$ .

Finally, the matrix elements of the electron-electron vertex are

$$\mu^*(\boldsymbol{\kappa}, \boldsymbol{\kappa}') = \frac{D(0)}{M} \langle \phi_{\boldsymbol{\kappa}0} | \langle \phi_{-\boldsymbol{\kappa}0} | \gamma^{\text{ee}} | \phi_{\boldsymbol{\kappa}'0} \rangle | \phi_{-\boldsymbol{\kappa}'0} \rangle, \quad (5.36)$$

where  $\phi_{-\boldsymbol{\kappa}0}$  is the time reversal of the state  $\phi_{\boldsymbol{\kappa}0}$ , that is, the state with reversed quasi-momentum  $\mathbf{k}$  (and reversed spin). The Nambu non-diagonal electron-electron self-energy on the Fermi surface reads

$$[\sigma^{\text{ee}}(\boldsymbol{\kappa})]_{i \neq j} = - \int d^2\kappa' d(\boldsymbol{\kappa}') \mu^*(\boldsymbol{\kappa}, \boldsymbol{\kappa}') \frac{1}{\beta} \sum_{s'}^{|\epsilon_{s'}| < \epsilon_c} [g(\boldsymbol{\kappa}'; i\epsilon_{s'})]_{i \neq j}. \quad (5.37)$$

The frequency cut-off has again been put to a value where the low energy Green's function should have converged so that the final results of the theory to leading order do not depend on this cut-off. For the electron-electron pseudopotential  $\mu^*$  also a Fermi surface average

$$\mu^* = \int d^2\kappa d^2\kappa' d(\boldsymbol{\kappa}) d(\boldsymbol{\kappa}') \mu^*(\boldsymbol{\kappa}, \boldsymbol{\kappa}') \quad (5.38)$$

is introduced for later use.

With (5.32) and (5.37), the energy integrated Green's function (5.29) is now

$$\mathbf{g}(\boldsymbol{\kappa}; i\epsilon_s) = \int d\epsilon [\tau_3 i\epsilon_s - \tau_0 \epsilon - \boldsymbol{\sigma}^{\text{ep}}(\boldsymbol{\kappa}; i\epsilon_s) - \boldsymbol{\sigma}^{\text{ee}}(\boldsymbol{\kappa})]^{-1}. \quad (5.39)$$

From the integral

$$\int_{-a}^{+a} dx \frac{1}{z-x} = \text{Ln}(z-a) - \text{Ln}(z+a) = \ln \left| \frac{z-a}{z+a} \right| + i \text{Arg} \left( \frac{z-a}{z+a} \right) \approx \quad (5.40)$$

$$\approx -4 \frac{\text{Re } z}{a} - i \left( \pi - 2 \frac{\text{Im } z}{a} \right) \text{sign}(\text{Im } z) \approx -i\pi \text{sign}(\text{Im } z),$$

where  $z$  is complex and  $x$  is real, we see that for a large enough cut-off energy  $\epsilon_c$  (5.39) has to leading order a meaning independent of the cut-off.

Now the general electron-phonon theory of superconductivity for normal metals without Fermi surface nesting is reduced to *Eliashberg's equations* (5.39), (5.32) and (5.37), the low energy equations of the microscopic theory for arbitrarily strong coupling.

## Chapter 6

# Strong Coupling Theory of the Transition Temperature

In the introduction to Chapter 3 we found that the signature of the superconducting state is the appearance of non-zero anomalous Green's functions involving the pair operators, that is, the appearance of Nambu off-diagonal components of the Green's function. Above the transition temperature  $T_c$ , in the normal conducting state, those components are zero. Since in the absence of an external magnetic field the transition into the superconducting state is a second order phase transition, those components veer off continuously to non-zero values below  $T_c$ . Hence, close to  $T_c$  the off-diagonal components are small, and Eliashberg's equations (5.39), (5.32) and (5.37) may be linearized in those components. This is why the theory of the transition temperature for given quasi-particle band structure,  $\lambda(\mathbf{s}, \mathbf{s}'; i\omega_s)$  and  $\mu^*(\mathbf{s}, \mathbf{s}')$  is the simplest part of the microscopic theory of superconductivity.

In the BCS theory,<sup>1</sup> which is correct in the weak coupling limit, that is, for  $T_c \ll \omega_{\text{ph}}$  in addition to the small parameter  $\alpha$ ,  $T_c$  is obtained from the solubility condition of a simple gap equation to be

$$T_c = \frac{2\gamma}{\pi} \omega_{\text{ph}} \exp\left\{-\frac{1}{g_{\text{BCS}}D(0)}\right\} \quad (6.1)$$

with  $\gamma = e^C$  where  $C$  is Euler's constant,  $2\gamma/\pi \approx 1.13$ . Here,  $\omega_{\text{ph}}$  is the relevant phonon energy determining the cut-off for the BCS attraction with coupling constant  $g_{\text{BCS}}$ . Hence,  $T_c$  is known once one has calculated  $g_{\text{BCS}}$ ,  $\omega_{\text{ph}}$  and  $D(0)$  from a microscopic theory with the above mentioned ingredients. However, calculating  $g_{\text{BCS}}$  is not really simpler than the direct solution of the strong coupling  $T_c$ -equations as described below, and there is no reason any more to use one of the many semi-empirical derivatives of (6.1) found in the literature.

### 6.1 Linearization of Eliashberg's Equations

We continue to consider singlet pairing in the absence of magnetic fields or spin dependent direct interactions. Hence the spin structure of the Nambu Green's function and self-energy is given by (3.19). We continue to omit the factors  $\sigma_0$  and  $\sigma_2$  since they are automatically correctly replaced in Nambu matrix multiplications:

$$\begin{pmatrix} \sigma_0 & \sigma_2 \\ \sigma_2 & \sigma_0 \end{pmatrix} \begin{pmatrix} \sigma_0 & \sigma_2 \\ \sigma_2 & \sigma_0 \end{pmatrix} = 2 \begin{pmatrix} \sigma_0 & \sigma_2 \\ \sigma_2 & \sigma_0 \end{pmatrix}. \quad (6.2)$$

---

<sup>1</sup>J. Bardeen, L. Cooper and J. R. Schrieffer, Phys. Rev. **108**, 1175 (1957); G. Rickayzen, in: R. D. Parks (ed.), *Superconductivity*, vol. 1, p. 51, Dekker, New York 1969.

Apart from these Pauli spin factors, traditionally the Green's function is expressed as<sup>2</sup>

$$\mathbf{g}(\boldsymbol{\kappa}; i\epsilon_s) = \begin{pmatrix} g(\boldsymbol{\kappa}; i\epsilon_s) & if(\boldsymbol{\kappa}; i\epsilon_s) \\ if^*(-\boldsymbol{\kappa}; i\epsilon_s) & g^*(-\boldsymbol{\kappa}; i\epsilon_s) \end{pmatrix} \quad (6.3)$$

and the self-energy as

$$\boldsymbol{\sigma}^{\text{ep}}(\boldsymbol{\kappa}; i\epsilon_s) + \boldsymbol{\sigma}^{\text{ee}}(\boldsymbol{\kappa}) = \begin{pmatrix} i(\epsilon_s - \tilde{\epsilon}_s(\boldsymbol{\kappa})) & i\phi_s(\boldsymbol{\kappa}) \\ i\phi_s^*(\boldsymbol{\kappa}) & -i(\epsilon_s - \tilde{\epsilon}_s(\boldsymbol{\kappa})) \end{pmatrix}. \quad (6.4)$$

We insert (6.4) into (5.39), invert the  $2 \times 2$  matrix according to

$$\begin{pmatrix} a & b \\ c & d \end{pmatrix}^{-1} = \frac{1}{ad - bc} \begin{pmatrix} d & -b \\ -c & a \end{pmatrix}, \quad (6.5)$$

and obtain

$$g(\boldsymbol{\kappa}; i\epsilon_s) = \int d\epsilon \frac{-\epsilon - i\tilde{\epsilon}_s(\boldsymbol{\kappa})}{(-\epsilon + i\tilde{\epsilon}_s(\boldsymbol{\kappa}))(-\epsilon - i\tilde{\epsilon}_s(\boldsymbol{\kappa})) + \phi_s(\boldsymbol{\kappa})\phi_s^*(\boldsymbol{\kappa})} \quad (6.6)$$

and

$$if(\boldsymbol{\kappa}; i\epsilon_s) = \int d\epsilon \frac{i\phi_s(\boldsymbol{\kappa})}{(-\epsilon + i\tilde{\epsilon}_s(\boldsymbol{\kappa}))(-\epsilon - i\tilde{\epsilon}_s(\boldsymbol{\kappa})) + \phi_s(\boldsymbol{\kappa})\phi_s^*(\boldsymbol{\kappa})}. \quad (6.7)$$

Linearizing these relations with respect to the off-diagonal matrix elements means neglecting  $\phi\phi^*$  in the denominators. Then, the integrations are elementary with the results

$$g(\boldsymbol{\kappa}; i\epsilon_s) = -i\pi \text{sign}(\tilde{\epsilon}_s(\boldsymbol{\kappa})), \quad f(\boldsymbol{\kappa}; i\epsilon_s) = \pi \frac{\phi_s(\boldsymbol{\kappa})}{|\tilde{\epsilon}_s(\boldsymbol{\kappa})|}. \quad (6.8)$$

(The first integral is a principal value integral, cf. (5.40), the second one can for instance be done by contour integration.)

Below we will see that  $\text{sign}(\tilde{\epsilon}_s(\boldsymbol{\kappa})) = \text{sign} \epsilon_s$ , hence we can make this replacement. If we now insert these results into (5.32) and (5.37) and compare to (6.4), we obtain

$$i(\epsilon_s - \tilde{\epsilon}_s(\boldsymbol{\kappa})) = \frac{1}{\beta_c} \sum_{s'} \int d^2\kappa' d(\boldsymbol{\kappa}') \lambda(\boldsymbol{\kappa}, \boldsymbol{\kappa}'; i\omega_{s'}) (-i\pi \text{sign}(\epsilon_s - \omega_{s'})), \quad (6.9)$$

$$\begin{aligned} i\phi_s(\boldsymbol{\kappa}) &= \frac{1}{\beta_c} \sum_{s'} \int d^2\kappa' d(\boldsymbol{\kappa}') \lambda(\boldsymbol{\kappa}, \boldsymbol{\kappa}'; i(\epsilon_s - \epsilon_{s'})) i\pi \frac{\phi_{s'}(\boldsymbol{\kappa}')}{|\tilde{\epsilon}_{s'}(\boldsymbol{\kappa}')|} - \\ &- \int d^2\kappa' d(\boldsymbol{\kappa}') \mu^*(\boldsymbol{\kappa}, \boldsymbol{\kappa}') \frac{1}{\beta_c} \sum_{s'}^{|\epsilon_{s'}| < \epsilon_c} i\pi \frac{\phi_{s'}(\boldsymbol{\kappa}')}{|\tilde{\epsilon}_{s'}(\boldsymbol{\kappa}')|}. \end{aligned} \quad (6.10)$$

Here,  $\beta_c = 1/T_c$  since the linearized relations are valid close to the transition temperature,  $T_c$ , only. In the first term of the last relation we have changed the summation over  $\omega_{s'}$  into a summation over  $\epsilon_{s'}$ , where  $\epsilon_{s'} = \epsilon_s - \omega_{s'}$ . This summation may again be cut off at a large frequency  $\epsilon_c$  without specifying the (earlier) cut off of the low energy Green's function  $f(\boldsymbol{\kappa}'; i\epsilon_{s'})$  because the factor  $\lambda(i\omega_{s'}) \sim D(i\omega_{s'}) \sim \omega_{s'}^{-2}$  provides a sufficient convergency factor.

<sup>2</sup>Compare (3.16) with (2.35) and (2.7). Then, from (5.27) with  $\phi_{-\boldsymbol{\kappa}\epsilon}(\mathbf{r}, s) = \phi_{\boldsymbol{\kappa}\epsilon}^*(\mathbf{r}, -s)$ , transposition of  $x$  with  $x'$  replaces  $\boldsymbol{\kappa}$  with  $-\boldsymbol{\kappa}$  in the spin singlet Green's function, and multiplication with  $\boldsymbol{\tau}_3$  in (5.4) removes the factors  $-1$  in the lower line of the Nambu matrix. For the off-diagonal elements, (6.3) is an ansatz which fixes the phase of the superconducting order parameter to be zero.

In view of (5.32) and (5.37),  $\boldsymbol{\sigma}$  has the same structure as  $\mathbf{g}$ , only it does not depend on the sign of  $\boldsymbol{\kappa}$  due to time reversion symmetry implying  $\lambda(-\boldsymbol{\kappa}, -\boldsymbol{\kappa}') = \lambda(\boldsymbol{\kappa}, \boldsymbol{\kappa}')$ ,  $\mu^*(-\boldsymbol{\kappa}, -\boldsymbol{\kappa}') = \mu^*(\boldsymbol{\kappa}, \boldsymbol{\kappa}')$ .

Consider first (6.9) and realize that  $\lambda$ , like  $D$ , is an even function of  $\omega_{s'}$ . Hence, due to the presence of the sign factor, in the  $s'$ -summation all items for positive  $\omega_{s'} > |\epsilon_s|$  cancel all items for negative  $\omega_{s'} < -|\epsilon_s|$ . Between these limits, the sign of  $\epsilon_s - \omega_{s'}$  is equal to the sign of  $\epsilon_s$ , and the final result is

$$\tilde{\epsilon}_s(\boldsymbol{\kappa}) = \epsilon_s + \text{sign}(\epsilon_s) \frac{\pi}{\beta_c} \sum_{s'}^{|\omega_{s'}| < |\epsilon_s|} \int d^2 \boldsymbol{\kappa}' d(\boldsymbol{\kappa}') \lambda(\boldsymbol{\kappa}, \boldsymbol{\kappa}'; i\omega_{s'}). \quad (6.11)$$

Since from (2.33)  $(\pi/\beta) \sum_{s'}^{|\omega_{s'}| < |\epsilon_s|} 1 \approx |\epsilon_s|$ , we see that the normal component of the electron-phonon self-energy is proportional to  $\lambda$  and proportional to  $\epsilon_s$ . Eq. (6.11) holds also for  $\omega_{\text{ph}} > \beta^{-1} > \beta_c^{-1}$  in the normal state where  $\phi_s = 0 = f$ . This results in  $G^{-1} = i\epsilon_s(1 + \lambda) - \epsilon_{\mathbf{k}n}$  which for the quasi-particle pole means  $\tilde{\epsilon}_{\mathbf{k}n} = \epsilon_{\mathbf{k}n}/(1 + \lambda)$ , the well known result for the normal state at low temperatures. Moreover, since  $\lambda$  was defined in (5.31) to be positive at imaginary frequencies ( $D$  is negative definite at imaginary frequencies, cf. (4.14)), it follows from (6.11) that indeed  $\text{sign}(\tilde{\epsilon}_s(\boldsymbol{\kappa})) = \text{sign}(\epsilon_s)$ , consistent with the assumption in (6.9).

The determination of the normal component of the low energy electron self-energy via (6.11) reduces now to the computation of a finite number of Fermi surface integrals over  $\lambda$ .

## 6.2 The $T_c$ Formula

Having computed the normal component of the self-energy via (6.11) and (5.30, 5.31), the integral equation (6.10) for the anomalous component  $\phi_s(\boldsymbol{\kappa})$  may be considered. (The less rigorous treatment of  $\mu^*$  from (5.36) is postponed to Section 6.4.) We symmetrize (6.10) by introducing a new function

$$\psi_s(\boldsymbol{\kappa}) = \frac{\phi_s(\boldsymbol{\kappa})}{\sqrt{d(\boldsymbol{\kappa})|\tilde{\epsilon}_s(\boldsymbol{\kappa})|}} \quad (6.12)$$

and the kernel

$$K(\boldsymbol{\kappa}, s; \boldsymbol{\kappa}', s') = \sqrt{\frac{\pi d(\boldsymbol{\kappa})}{\beta_c |\tilde{\epsilon}_s(\boldsymbol{\kappa})|}} \left[ \lambda(\boldsymbol{\kappa}, \boldsymbol{\kappa}'; i(\epsilon_s - \epsilon_{s'})) - \mu^*(\boldsymbol{\kappa}, \boldsymbol{\kappa}') \right] \sqrt{\frac{\pi d(\boldsymbol{\kappa}')}{\beta_c |\tilde{\epsilon}_{s'}(\boldsymbol{\kappa}')|}}. \quad (6.13)$$

$$\epsilon_s = (2s + 1)\pi/\beta_c. \quad (6.14)$$

Then, (6.10) reads

$$\psi_s(\boldsymbol{\kappa}) = \sum_{s'}^{|\epsilon_{s'}| < \epsilon_c} \int d^2 \boldsymbol{\kappa} K(\boldsymbol{\kappa}, s; \boldsymbol{\kappa}', s') \psi_{s'}(\boldsymbol{\kappa}'). \quad (6.15)$$

This equation may have a non-zero solution, if the operator defined by the kernel  $K$  has an eigenvalue equal to unity.

The integral operator  $\hat{K}$  is defined by a *finite* sum and an integral over a *finite* surface over the Hermitian kernel  $K$  which is bounded and continuous as a function of two variables  $\boldsymbol{\kappa}$  and  $\boldsymbol{\kappa}'$  on the Fermi surface. Hence  $\hat{K}$  is compact and self-adjoint, and due to the Hilbert-Schmidt theorem it has a bounded sequence of eigenvalues  $k_i$  which cluster at  $k = 0$ .

In (6.11), the number of items in the sum is  $\sim \beta_c/\pi$ . Since  $\lambda(i\omega)$  converges to a non-zero value for  $\omega \rightarrow 0$ , those items become equal for low  $\omega_s$ , and the temperature dependence of the sum is canceled by the prefactor: The normal component of the self-energy and  $\tilde{\epsilon}$  for a given fixed  $\epsilon$  is nearly temperature independent at low temperatures. Consequently, the square roots in (6.13) and hence  $K$  itself are again nearly temperature independent, and the summation in (6.15) introduces a factor  $\beta_c/\pi$  into the norm of  $\hat{K}$ .

The operator and hence its spectrum is tuned with this prefactor  $\beta_c/\pi$ . For  $T_c \rightarrow \infty$  it is tuned down to zero. Hence, if we lower the temperature, there may be a highest value  $T_c$  at which the largest eigenvalue of  $\hat{K}$  becomes unity. This is the superconducting transition temperature, since above it the only solution for  $\psi_s(\boldsymbol{\kappa})$  and hence for  $\phi_s(\boldsymbol{\kappa})$  is zero. (Below this temperature, on the one hand we obtain a discrete sequence of temperatures for which eigenvalues of  $\hat{K}$  pass through unity and hence at which there are non-zero solutions, and on the other hand all those solutions may have an arbitrary amplitude. Both facts are artificial aftereffects of our linearization. Non-linear corrections determine the amplitude of  $\phi_s(\boldsymbol{\kappa})$  and enable nontrivial solutions of the equations (5.39), (5.32) and (5.37) for all  $T < T_c$ : As  $\phi_s(\boldsymbol{\kappa})$  is tuned up the temperature of the solution shifts downward.)

For a practical calculation in the general case, one would introduce a set of orthogonal basis functions on the Fermi surface and expand  $\psi_s(\boldsymbol{\kappa})$  and  $K$  in this basis. Appropriate basis functions are the so called Fermi surface harmonics. The kernel  $K$  has the symmetry of the Fermi surface, the point symmetry of the reciprocal lattice, and the solution  $\psi_s(\boldsymbol{\kappa})$  of this linear problem may always be chosen to have the same symmetry. Like the kernel  $K$ , the eigenfunction to the highest eigenvalue will have no nodes on the Fermi surface: Electron-phonon coupling leads normally to  $s$ -wave or extended  $s$ -wave pairing. (The latter means that, although not constant on the Fermi surface,  $\psi_s(\boldsymbol{\kappa})$  has no nodes.) It is clear that rapid basis convergence is expected, and (6.15) is transformed into a purely algebraic matrix problem with a not too high dimension which can easily be solved on a PC with standard software. In most cases the largest eigenvalue is well separated from the absolute values of all other eigenvalues of  $\hat{K}$  (which are all smaller). Then, the simple von Mises iterations are efficient to solve the eigenvalue problem for this largest eigenvalue.

The condition for this formulation of the theory in Bloch wave representation is that the energy width of a quasi-particle  $\boldsymbol{\kappa}$ -state is small compared to the energy scale of the superconducting coupling. This is the *clean limit* in which the Bloch electron mean free path is large compared to the coherence length of the pair correlation for  $T = 0$ .

### 6.3 The Dirty Limit

If there is impurity scattering, then  $\boldsymbol{\kappa}$  is not conserved any more. For strong impurity scattering the Bloch function representation loses its physical relevance. In this dirty limit we return to the Hamiltonian (5.22) and include the impurity potential into  $v^0$ . The stationary eigenstates  $\phi_\nu(\mathbf{r})$ ,

$$\hat{h}^0 \phi_\nu(\mathbf{r}) = \phi_\nu(\mathbf{r}) \epsilon_\nu, \quad (6.16)$$

are again to be considered in the low energy range only. We denote with  $\phi_{-\nu}$  the time reversal of the state  $\phi_\nu$  (that is the complex conjugated and spin reversed orbital) and have to consider the analogue of (3.4) for pairs of mutually time reversed states.

Instead of (5.30, 5.31) we now have

$$\lambda_{\nu,\nu';\nu_1,\nu'_1}(i\omega_s) = \sum_{l\lambda,l'\lambda'} \langle \nu | \frac{\partial v^0}{\partial \mathbf{u}_{l\lambda}} | \nu_1 \rangle D(l\lambda, l'\lambda'; i\omega_s) \langle \nu'_1 | \frac{\partial v^0}{\partial \mathbf{u}_{l'\lambda'}} | \nu' \rangle. \quad (6.17)$$

The functions  $\phi_\nu(\mathbf{r})$  have phases randomly changing from atom position to atom position, which in particular are not correlated to the phases contained in  $D$ . Products  $\phi_\nu^* \phi_{\nu'}$  have again random phases and the average of  $\lambda_{\nu,\nu';\nu_1,\nu'_1}(i\omega_s)$  over  $\nu'$  will essentially not depend on  $\nu'_1$  any more. The average over  $\nu'$  and  $\nu_1$ ,

$$\lambda(i\omega_s) = \overline{\lambda_{\nu,\nu';\nu_1,\nu'_1}(i\omega_s)}^{\nu'\nu_1}, \quad (6.18)$$

is a function of  $\omega_s$  only.



Instead of (5.32) we have

$$\sigma_{\nu,\nu'}^{\text{ep}}(i\epsilon_s) = \frac{1}{\beta} \sum_{s'} \sum_{\nu_1,\nu'_1} \lambda_{\nu,\nu';\nu_1,\nu'_1}(i\omega_s) \mathbf{g}_{\nu_1,\nu'_1}(i\epsilon_s - i\omega_{s'}), \quad (6.19)$$

where

$$\mathbf{g}_{\nu,\nu'}(i\epsilon_s) = \langle \nu | \mathbf{g}(\mathbf{r}, \mathbf{r}'; i\epsilon_s) | \nu' \rangle \quad (6.20)$$

averaged over  $\nu'$  keeps only a dependence on  $\epsilon_\nu$ :

$$\mathbf{g}(\epsilon_\nu; i\epsilon_s) = \overline{\mathbf{g}_{\nu,\nu'}(i\epsilon_s)}^{\nu'}, \quad \mathbf{g}(i\epsilon_s) = \int d\epsilon \mathbf{g}(\epsilon; i\epsilon_s). \quad (6.21)$$

If now (6.19) is averaged over  $\nu'$ , then the summation over  $\nu'_1$  only averages  $\mathbf{g}_{\nu_1,\nu'_1}$ , and after this the summation over  $\nu_1$  eventually averages  $\lambda$ :

$$\sigma^{\text{ep}}(i\epsilon_s) = \overline{\sigma_{\nu,\nu'}^{\text{ep}}(i\epsilon_s)}^{\nu'} = \frac{1}{\beta} \sum_{s'} \lambda(i\omega_s) \mathbf{g}(i\epsilon_s) \quad (6.22)$$

Finally, instead of (5.36, 5.37) we have

$$[\sigma^{\text{ee}}]_{i \neq j} = -\frac{\mu^*}{\beta} \sum_{s'}^{|\epsilon_{s'}| < \epsilon_c} [g(i\epsilon_{s'})]_{i \neq j} \quad (6.23)$$

where  $\mu^*$  is the average over the analogue of (5.36).

Now, (5.39) is replaced by

$$\sum_{\nu'} \left[ (\tau_3 i\epsilon_s - \tau_0 \epsilon_\nu) \delta_{\nu\nu'} - \sigma_{\nu\nu'}^{\text{ep}}(i\epsilon_s) - \sigma_{\nu\nu'}^{\text{ee}} \right] \mathbf{g}_{\nu'\nu''}(i\epsilon_s) = \tau_0 \delta_{\nu\nu''}. \quad (6.24)$$

Averaging this relation over  $\nu''$  yields

$$[\tau_3 i\epsilon_s - \tau_0 \epsilon - \sigma^{\text{ep}}(i\epsilon_s) - \sigma^{\text{ee}}] \mathbf{g}(\epsilon; i\epsilon_s) = \tau_0. \quad (6.25)$$

In the dirty limit, (6.25), (6.22) and (6.23) are the analogues to Eliashberg's equations (5.39), (5.32) and (5.37). They have precisely the same structure except that averaged quantities figure and there is no  $\kappa$ -dependence. This holds obviously also true for the solutions which read

$$\tilde{\epsilon}_s - \epsilon_s + \text{sign}(\epsilon_s) \frac{\pi}{\beta_c} \sum_{s'}^{|\omega_{s'}| < |\epsilon_s|} \lambda(i\omega_{s'}), \quad (6.26)$$

$$\phi_s = \frac{\pi}{\beta_c} \sum_{s'}^{|\epsilon_{s'}| < \epsilon_c} (\lambda(i\epsilon_s - i\epsilon_{s'}) - \mu^*) \frac{\phi_{s'}}{|\tilde{\epsilon}_{s'}|}. \quad (6.27)$$

The latter equation may be written as

$$\psi_s = \sum_{s'}^{|\epsilon_{s'}| < \epsilon_c} K_{ss'} \psi_{s'}, \quad \psi_s = \frac{\phi_s}{\sqrt{|\tilde{\epsilon}_s|}} \quad (6.28)$$

with the obvious meaning of  $K_{ss'}$ . This  $T_c$ -equation is solved in the same manner as (6.15), only it is even much simpler.

This analysis shows that non-magnetic impurities (we used spin singlet pairing conditions and did not introduce spin flip scattering) do not suppress superconductivity. It does,

however, not really provide a computational approach to the averaged coupling terms  $\lambda(i\epsilon_s)$  and  $\mu^*$ . If the electron mean free path is small compared to the coherence length (which is the condition for the dirty limit) but still large compared to interatomic distances, then Bloch functions are not a bad starting point to describe the electronic states, and the averages (5.34) and (5.38) may be used in the above relations. This is the case for which most strong coupling calculations of  $T_c$  in the literature have been done.

## 6.4 The Cut-Off Frequency

The Green's function (6.3) is the low energy low frequency Green's function according to the splitting (4.7). It should die away somewhere between the characteristic phonon energy, the Debye energy  $\omega_D$  say, and well below the Fermi energy. The solution (6.8) of the linearized Eliashberg equations does not automatically provide this behavior for the frequency dependence.

For the Nambu diagonal component  $g(i\epsilon_s)$  this is not a problem. Due to the dependence of  $\lambda$  on  $\omega_s^2$  only, first of all the  $s'$ -sum of (6.9) is cut off at  $|\epsilon_s|$  independently of the actual form of damping of  $g(i\epsilon_s)$  for large  $\epsilon_s$ . Moreover, since  $\lambda \sim \omega_s^{-2}$  for  $\omega_s \gg \omega_D$ , this sum converges towards a constant for large  $|\epsilon_s|$ , where this constant is determined by the low frequency part of  $g(i\epsilon_s)$  only.

The same decay of  $\lambda(i\omega)$  provides a decay of the  $\lambda$ -contribution to the kernel  $K$  of (6.13) or of (6.28) away from the diagonal. Together with the  $\epsilon_s^{-1}$ -decay along the diagonal this provides sufficient convergence again to render results independent of the actual high frequency damping of the Green's function. This is, however, not the case for the  $\mu^*$ -contribution since it does not decay off the diagonal of  $K$ . To get rid of an unphysical dependence of the results on the frequency cut-off,  $\epsilon_c$ , through this contribution to  $K$ , one introduces a compensating  $\epsilon_c$ -dependence of  $\mu^*$  in the following way:

Since the correction term in (6.11) converges to a constant, one has  $\tilde{\epsilon}_s/\epsilon_s \rightarrow 1$  for large  $|\epsilon_s|$  and hence, from (6.8),  $[g(i\epsilon_s)]_{12} = \pi[\sigma^{ee}]_{12}/|\epsilon_s|$  in this limit (where the contribution of  $[\sigma^{ep}]_{12}$  can already be neglected). From (5.37) one then has

$$\frac{1}{\mu^*(\epsilon'_c)} - \frac{1}{\mu^*(\epsilon_c)} = -\frac{2\pi}{\beta} \sum_{s'}^{\epsilon_c < \epsilon_{s'} < \epsilon'_c} \frac{1}{\epsilon_{s'}} \approx -\int_{\epsilon_c}^{\epsilon'_c} \frac{d\epsilon}{\epsilon} = \ln\left(\frac{\epsilon_c}{\epsilon'_c}\right). \quad (6.29)$$

It is convention to determine  $\mu^*$  for  $\epsilon_c = 5\omega_D$ , and it is good scientific practice to report the value of  $\epsilon_c$  used in publications whenever a  $\mu^*$  was determined or used. With a  $\mu^*(\epsilon_c)$  according to (6.29) the results for  $\tilde{\epsilon}_s$  and  $\phi_s$  normally well converge as functions of  $\epsilon_c$  for  $\epsilon_c = 5\omega_D$ .

## Chapter 7

# Physical Properties of the Superconducting State

The relative simplicity of the theory of the transition temperature derives from the linearization of Eliashberg's equations (5.39), (5.32) and (5.37). This linearization (with respect to the anomalous self-energy  $\phi_s(\boldsymbol{\kappa})$ ) is only justified in the vicinity of  $T_c$  where  $\phi$  is small indeed. Otherwise, the full non-linear Eliashberg equations have to be solved.

The solution of Eliashberg's equations yields the low energy Green's function and hence all the information on the superconducting state in thermal equilibrium which is contained in this Green's function. As an example for the spectral information we consider below the quasi-particle spectral density, and as an example for the information on thermodynamic potentials we consider the thermodynamic critical field.

This chapter concludes our introduction to the modern microscopic theory of superconductivity. Much more can be obtained on its basis for which we have to refer to current literature. The microscopic theory is used in both important directions: to obtain quantitative results 'from first principles' and to guide the formation of phenomenological model theories. Both fields have proved their predictive power in the history of the physics of superconductivity.

### 7.1 Eliashberg's Non-Linear Equations

We return to the Green's function (6.3), the self-energy (6.4) and the expressions (6.6, 6.7) for the solution of (5.39), which we write as

$$g(\boldsymbol{\kappa}; i\epsilon_s) = \int d\epsilon g(\boldsymbol{\kappa}\epsilon; i\epsilon_s), \quad g(\boldsymbol{\kappa}\epsilon; i\epsilon_s) = -\frac{i\tilde{\epsilon}_s(\boldsymbol{\kappa}) + \epsilon}{\tilde{\epsilon}_s(\boldsymbol{\kappa})^2 + \epsilon^2 + |\phi_s(\boldsymbol{\kappa})|^2} \quad (7.1)$$

and

$$f(\boldsymbol{\kappa}; i\epsilon_s) = \int d\epsilon f(\boldsymbol{\kappa}\epsilon; i\epsilon_s), \quad f(\boldsymbol{\kappa}\epsilon; i\epsilon_s) = \frac{\phi_s(\boldsymbol{\kappa})}{\tilde{\epsilon}_s(\boldsymbol{\kappa})^2 + \epsilon^2 + |\phi_s(\boldsymbol{\kappa})|^2}. \quad (7.2)$$

In the spirit of the high-energy cut-off, the first integral is again to be treated as a principal value integral like (5.40). Technically it can be obtained by closing the integration path half by an upper and half by a lower infinite half-circle in the complex  $\epsilon$ -plane. The result is

$$g(\boldsymbol{\kappa}; i\epsilon_s) = -i\pi \frac{\tilde{\epsilon}_s(\boldsymbol{\kappa})}{\sqrt{\tilde{\epsilon}_s(\boldsymbol{\kappa})^2 + |\phi_s(\boldsymbol{\kappa})|^2}}. \quad (7.3)$$

The second integral is again converging and is for instance obtained by closing the path in the upper half-plane with the result

$$f(\boldsymbol{\kappa}; i\epsilon_s) = \frac{\pi\phi_s(\boldsymbol{\kappa})}{\sqrt{\tilde{\epsilon}_s(\boldsymbol{\kappa})^2 + |\phi_s(\boldsymbol{\kappa})|^2}}. \quad (7.4)$$

In the limit  $|\phi_s(\boldsymbol{\kappa})|^2 \rightarrow 0$ , the linearized results (6.8) are reproduced.

Instead of (6.9, 6.10), we now have

$$\tilde{\epsilon}_s(\boldsymbol{\kappa}) = \epsilon_s + \frac{\pi}{\beta} \sum_{s'} \int d^2\kappa' d(\boldsymbol{\kappa}') \lambda(\boldsymbol{\kappa}, \boldsymbol{\kappa}'; i(\epsilon_s - \epsilon_{s'})) \frac{\tilde{\epsilon}_{s'}(\boldsymbol{\kappa}')}{\sqrt{\tilde{\epsilon}_{s'}(\boldsymbol{\kappa}')^2 + |\phi_{s'}(\boldsymbol{\kappa}')|^2}}, \quad (7.5)$$

$$\phi_s(\boldsymbol{\kappa}) = \frac{\pi}{\beta} \sum_{s'}^{|\epsilon_{s'}| < \epsilon_c} \int d^2\kappa' d(\boldsymbol{\kappa}') [\lambda(\boldsymbol{\kappa}, \boldsymbol{\kappa}'; i(\epsilon_s - \epsilon_{s'})) - \mu^*(\boldsymbol{\kappa}, \boldsymbol{\kappa}')] \frac{\phi_{s'}(\boldsymbol{\kappa}')}{\sqrt{\tilde{\epsilon}_{s'}(\boldsymbol{\kappa}')^2 + |\phi_{s'}(\boldsymbol{\kappa}')|^2}}. \quad (7.6)$$

These are Eliashberg's non-linear equations for the electron self-energy  $\sigma^{\text{ep}} + \sigma^{\text{ee}}$ . Their simplified variants in the dirty limit are readily read off from (6.27, 6.28):

$$\tilde{\epsilon}_s = \epsilon_s + \frac{\pi}{\beta} \sum_{s'} \lambda(i\epsilon_s - i\epsilon_{s'}) \frac{\tilde{\epsilon}_{s'}}{\sqrt{\tilde{\epsilon}_{s'}^2 + |\phi_{s'}|^2}}, \quad (7.7)$$

$$\phi_s = \frac{\pi}{\beta} \sum_{s'}^{|\epsilon_{s'}| < \epsilon_c} (\lambda(i\epsilon_s - i\epsilon_{s'}) - \mu^*) \frac{\phi_{s'}}{\sqrt{\tilde{\epsilon}_{s'}^2 + |\phi_{s'}|^2}}. \quad (7.8)$$

A notation  $\tilde{\epsilon}_s/\epsilon_s = Z(\epsilon_s)$  is often used in the literature.

A most important feature of these equations is again, that the expressions under the  $s'$ -sums in (7.5) and (7.7) change sign together with  $\epsilon_{s'}$  (recall  $\text{sign } \tilde{\epsilon}_s = \text{sign } \epsilon_s$ ) while those of (7.6) and (7.8) do not: the relevant solution  $\phi_s$  related to the largest eigenvalue in (6.15) or (6.28) has a unique sign since the kernel  $K$  has a definite sign.

There are several ways of rewriting these equations prior to self-consistent numerical solution. First, the  $T \rightarrow 0$  limit ( $\beta \rightarrow \infty$ ) is obtained via  $(\pi/\beta) \sum_s F(\epsilon_s) \rightarrow (1/2) \int d\epsilon F(\epsilon)$ . The summation over the Matsubara frequencies may be transformed into a contour integration by means of Poisson's formulas: Observe that

$$e^{\pm\beta z} = e^{\pm\beta x} (\cos \beta y \pm i \sin \beta y) = \begin{cases} -1 & \text{iff } x = 0 \text{ and } \beta y = (2s+1)\pi \\ +1 & \text{iff } x = 0 \text{ and } \beta y = 2s\pi \end{cases} \quad (7.9)$$

with any integer  $s$ . Hence,  $(e^{\pm\beta\epsilon} + 1)^{-1}$  has single poles at the fermionic Matsubara frequencies  $\epsilon = i\epsilon_s$ , and  $(e^{\pm\beta\omega} - 1)^{-1}$  has single poles at the bosonic Matsubara frequencies  $\omega = i\omega_s$ . With Cauchy's theorem,<sup>1</sup>

$$\sum_{s=-\infty}^{\infty} F(i\epsilon_s) = -\frac{\beta}{2\pi i} \int_C d\epsilon \frac{F(\epsilon)}{e^{\beta\epsilon} + 1} = \frac{\beta}{2\pi i} \int_C d\epsilon \frac{F(\epsilon)}{e^{-\beta\epsilon} + 1}, \quad (7.10)$$

$$\sum_{s=-\infty}^{\infty} F(i\omega_s) = \frac{\beta}{2\pi i} \int_C d\omega \frac{F(\omega)}{e^{\beta\omega} - 1} = -\frac{\beta}{2\pi i} \int_C d\omega \frac{F(\omega)}{e^{-\beta\omega} - 1}, \quad (7.11)$$

<sup>1</sup>There is of course no relation between the frequency  $\epsilon$  appearing here and on the next page and the same letter  $\epsilon$  appearing in (7.1, 7.2).

where  $C$  is a closed contour in the complex frequency plane which encircles all Matsubara frequencies counterclockwise and excludes any singularity of  $F$ . ( $F$  must not have singularities in a connected set containing all Matsubara frequencies as inner points.) If  $F$  has only poles as singularities and the contour  $C$  is folded out into the contour  $C'$  without slipping over singularities of  $F$  as shown in Fig. 7.1, then one has

$$\sum_{s=-\infty}^{\infty} F(i\epsilon_s) = \beta \sum_n \frac{F_{\text{res}}(\epsilon_n)}{e^{\beta\epsilon_n} + 1} = -\beta \sum_n \frac{F_{\text{res}}(\epsilon_n)}{e^{-\beta\epsilon_n} + 1}, \quad (7.12)$$

where  $F_{\text{res}}(\epsilon_n)$  is the residuum of  $F$  at its pole  $\epsilon_n$  and the sum is over all poles of  $F$ . It is assumed that  $F(\epsilon)/(e^{\pm\beta\epsilon} + 1) \rightarrow 0$  sufficiently fast for  $|\epsilon| \rightarrow \infty$ , so that the infinite circle of the contour  $C'$  gives no contribution. The sign of the exponent can be chosen with respect to further demands.

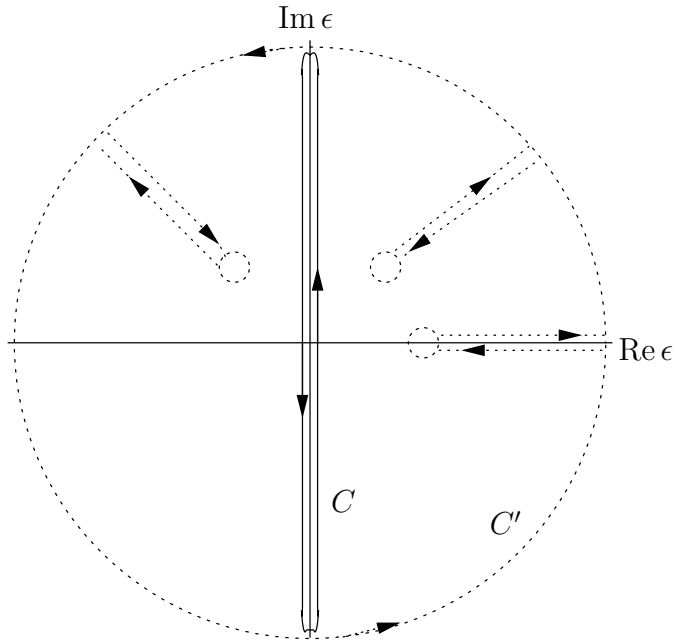


Figure 7.1: Deformation of the contour  $C$  into  $C'$  as described in the text.

The general case of Eliashberg's equations rather corresponds to an  $F(\epsilon)$  which continues to retarded Green's function expressions in the upper half-plane and to advanced ones in the lower half-plane with the real  $\epsilon$ -axis forming a branch line. In that case the contour  $C$  may be folded out into an upper and a lower infinite half-circle, each closed along the real axis, with the result

$$\begin{aligned} \sum_{s=-\infty}^{\infty} F(i\epsilon_s) &= -\frac{\beta}{2\pi i} \int_{-\infty}^{\infty} d\epsilon \frac{F(\epsilon + i0) - F(\epsilon - i0)}{e^{\beta\epsilon} - 1} = \\ &= \frac{\beta}{2\pi i} \int_{-\infty}^{\infty} d\epsilon \frac{F(\epsilon + i0) - F(\epsilon - i0)}{e^{-\beta\epsilon} - 1} \end{aligned} \quad (7.13)$$

(In case of a bosonic summation,  $F(0)$  has to be added since it is not encircled by the folded out paths.)

When applied to (7.5–7.8), one must realize that  $\lambda(\omega)$  inherits the branch line of the phonon Green's function  $D(\omega)$  as readily seen from (5.31). Hence one has to insert (5.31) and (5.33) into Eliashberg's equations before one can make these transformations. In the dirty limit, (5.34) may be inserted instead. As regards the continuation of the Green's function (7.3, 7.4) to the real frequency axis, one first uses a notation  $i\tilde{\epsilon}_s(\boldsymbol{\kappa}) = i\tilde{\epsilon}(\boldsymbol{\kappa}; i\epsilon_s) = i\epsilon_s Z(\boldsymbol{\kappa}; i\epsilon_s)$  which implies  $i\tilde{\epsilon}(\boldsymbol{\kappa}; \epsilon) = \epsilon Z(\boldsymbol{\kappa}; \epsilon)$  by replacing  $i\epsilon_s$  with  $\epsilon$ . With the same replacements one obtains

$$g(\boldsymbol{\kappa}; \epsilon) = -\pi \frac{\epsilon Z(\boldsymbol{\kappa}; \epsilon)}{\sqrt{-\epsilon^2 Z^2(\boldsymbol{\kappa}; \epsilon) + |\phi(\boldsymbol{\kappa}; \epsilon)|^2}}, \quad f(\boldsymbol{\kappa}; \epsilon) = \pi \frac{\phi(\boldsymbol{\kappa}; \epsilon)}{\sqrt{-\epsilon^2 Z^2(\boldsymbol{\kappa}; \epsilon) + |\phi(\boldsymbol{\kappa}; \epsilon)|^2}} \quad (7.14)$$

with branch lines of the square root on the real  $\epsilon$ -axis for  $|\epsilon Z(\boldsymbol{\kappa}; \epsilon)| > |\phi(\boldsymbol{\kappa}; \epsilon)|$ . This makes connection to the real frequency representations of Eliashberg's equations in the literature which are usually given in the dirty limit, that is, averaged over  $\boldsymbol{\kappa}$ .

## 7.2 The Quasiparticle Density of States

As seen from the definition (3.6), the Nambu component  $G_{11}$  of the Green's function is the normal electron propagator. Its analytic continuation from the positive imaginary Matsubara frequencies to the real frequency axis yields the retarded propagator which, if it continues to a pole on the 'unphysical sheet' of the Riemannian surface of  $G^r$  below the real axis, describes a quasi-particle excitation according to (2.18–2.20).

Strictly speaking, the analytic properties can only be taken for granted for the full Green's functions  $G = G^{\text{low}} + G^{\text{high}}$ . If this splitting were made in an analytic way, no part would be exactly zero in any frequency region because as an analytic function it then would automatically be zero for all frequencies. At best one can expect that  $G^{\text{low}}$  is a very good approximation to the full  $G$  for low values  $|\epsilon|$ , and governs the analytic continuation of the full  $G^r$  in the region of interest. (Anyhow, the analytic continuation to a pole in (2.18–2.20) was a mere vehicle to describe Lorentzian shape features of  $\text{Im } G^r$  on the real  $\epsilon$ -axis.) The same considerations with negative Matsubara frequencies apply to  $G^a$ . In this understanding we consider the analytic continuation of the right expression of (7.1) to the real frequency axis to be a good approximation to  $G_{11}^{r/a}$ . We change the energy notation in this expression to  $\epsilon_\kappa$  in order not to confuse it with the general complex frequency  $\epsilon$ , and introduce again a notation

$$i\tilde{\epsilon}(\boldsymbol{\kappa}; \epsilon) = \epsilon Z(\boldsymbol{\kappa}; \epsilon) \quad (7.15)$$

for generally complex frequencies  $\epsilon$ . Recalling that  $\lambda(\boldsymbol{\kappa}, \boldsymbol{\kappa}'; i\omega_s)$  or  $\lambda(i\omega_s)$  depends on  $\omega_s^2$  only (cf. (5.33, 5.34)), it can be inferred from (7.5) or (7.7) that  $\tilde{\epsilon}_s(\boldsymbol{\kappa}) = -\tilde{\epsilon}_{-s}(\boldsymbol{\kappa})$ . Moreover, (7.15) is purely imaginary for imaginary  $\epsilon$  in the frame of our approximations (since  $\lambda$  is real). Hence,  $Z(\boldsymbol{\kappa}; \epsilon)$  is a real and even function of imaginary  $\epsilon$ . If it is analytic around  $\epsilon = 0$ , then its Taylor expansion has only even orders with real coefficients, which means that  $Z$  is also a real and even function of real  $\epsilon$ . We introduce additionally the notation

$$|\phi(\boldsymbol{\kappa}; \epsilon)|^2 = \Delta^2(\boldsymbol{\kappa}; \epsilon) Z^2(\boldsymbol{\kappa}; \epsilon), \quad (7.16)$$

where consequently  $\Delta$  must also be real. Then, for  $\epsilon$  real and low, the right expression of (7.1) yields

$$\begin{aligned} g_{11}^r(\boldsymbol{\kappa}; \epsilon_\kappa) &= \frac{\epsilon Z(\boldsymbol{\kappa}; \epsilon) + \epsilon_\kappa}{\epsilon^2 Z^2(\boldsymbol{\kappa}; \epsilon) - \epsilon_\kappa^2 - \Delta^2(\boldsymbol{\kappa}; \epsilon) Z^2(\boldsymbol{\kappa}; \epsilon)} \approx \\ &\approx \frac{A_+(\boldsymbol{\kappa}, \epsilon_\kappa)}{\epsilon - \sqrt{\epsilon_\kappa^2/Z^2(\boldsymbol{\kappa}) + \Delta^2(\boldsymbol{\kappa})}} + \frac{A_-(\boldsymbol{\kappa}, \epsilon_\kappa)}{\epsilon + \sqrt{\epsilon_\kappa^2/Z^2(\boldsymbol{\kappa}) + \Delta^2(\boldsymbol{\kappa})}}, \end{aligned} \quad (7.17)$$

where we further approximated  $Z(\boldsymbol{\kappa}; \epsilon) \approx Z(\boldsymbol{\kappa}; 0) = Z(\boldsymbol{\kappa})$ ,  $\Delta(\boldsymbol{\kappa}; \epsilon) \approx \Delta(\boldsymbol{\kappa}; 0) = \Delta(\boldsymbol{\kappa})$ . The spectral weights are

$$A_{\pm}(\boldsymbol{\kappa}, \epsilon_{\kappa}) = \frac{1}{2Z(\boldsymbol{\kappa})} \left( 1 \mp \frac{\epsilon_{\kappa}/Z(\boldsymbol{\kappa})}{\sqrt{\epsilon_{\kappa}^2/Z^2(\boldsymbol{\kappa}) + \Delta^2(\boldsymbol{\kappa})}} \right). \quad (7.18)$$

From these expressions one reads off the quasi-particle energies

$$E(\boldsymbol{\kappa}, \epsilon_{\kappa}) \approx \sqrt{\epsilon_{\kappa}^2/Z^2(\boldsymbol{\kappa}) + \Delta^2(\boldsymbol{\kappa})} \quad (7.19)$$

with an excitation gap  $\Delta(\boldsymbol{\kappa})$ .

At each point  $\boldsymbol{\kappa}$  of the Fermi surface, the bandstructure energies  $\pm\epsilon_{\kappa}$  both contribute to both quasi-particle poles (7.17) (of electron and hole type), and their common contribution in both cases is

$$A_{\pm}(\boldsymbol{\kappa}, \epsilon_{\kappa}) + A_{\pm}(\boldsymbol{\kappa}, -\epsilon_{\kappa}) = Z^{-1}(\boldsymbol{\kappa}). \quad (7.20)$$

The total quasi-particle spectral density is obtained as

$$D(\epsilon) \approx \int d^2\boldsymbol{\kappa} d(\boldsymbol{\kappa}) \int d\epsilon_{\kappa} Z^{-1}(\boldsymbol{\kappa}) \delta(\epsilon - E(\boldsymbol{\kappa}, \epsilon_{\kappa})). \quad (7.21)$$

Note that these last considerations are only semi-quantitatively correct. A more accurate approach needs a numerical analysis of the first line of (7.17).

### 7.3 The Thermodynamic Critical Field

To calculate the Inner Energy of the system we return to (2.66) and transform it with the help of (2.32) into

$$\begin{aligned} \langle \hat{W} \rangle &= \frac{i\zeta}{2} \lim_{\tau \rightarrow -0} \int dx dx_1 \left( \delta(x - x_1) \frac{\partial}{\partial \tau} + h^0(x, x_1) \right) \frac{i}{\beta} \sum_s e^{-i\epsilon_s \tau} G(x_1, x; i\epsilon_s) = \\ &= \frac{\zeta}{2\beta} \lim_{\tau \rightarrow -0} \sum_s e^{i\epsilon_s \tau} \int dx dx_1 \left( \sum_{\mathbf{k}n} \phi_{\mathbf{k}n}(x) \phi_{\mathbf{k}n}^*(x_1) i\epsilon_s - \right. \\ &\quad \left. - \sum_{\mathbf{k}n, \mathbf{k}'n'} \int dx' dx'_1 \phi_{\mathbf{k}n}(x) \phi_{\mathbf{k}n}^*(x') h^0(x', x'_1) \phi_{\mathbf{k}'n'}(x'_1) \phi_{\mathbf{k}'n'}^*(x_1) \right) G(x_1, x; i\epsilon_s) = \\ &= \frac{\zeta}{2\beta} \lim_{\tau \rightarrow -0} \sum_s e^{i\epsilon_s \tau} \sum_{\mathbf{k}n} (i\epsilon_s - \epsilon_{\mathbf{k}n}) G(\mathbf{k}, n, n; i\epsilon_s). \end{aligned} \quad (7.22)$$

In the second equality we replaced the  $\delta$ -function by a completeness relation of Bloch eigenfunctions of  $\hat{h}^0$  and inserted in the same manner two further integrals over  $\delta$ -functions.

With (2.64), the expectation value of  $\hat{h}^0$  is

$$\begin{aligned} \langle \hat{h}^0 \rangle &= \int dx dx_1 h^0(x, x_1) n_1(x_1|x) = -i\zeta \lim_{\tau \rightarrow -0} \int dx dx_1 h^0(x, x_1) G(x_1, x; -i\tau) = \\ &= \frac{\zeta}{\beta} \lim_{\tau \rightarrow -0} \sum_s e^{i\epsilon_s \tau} \sum_{\mathbf{k}n} \epsilon_{\mathbf{k}n} G(\mathbf{k}, n, n; i\epsilon_s). \end{aligned} \quad (7.23)$$

These two results may be combined to yield the Inner Energy  $E = \langle \hat{h}^0 + \hat{W} \rangle$  as

$$E = \frac{\zeta}{2\beta} \lim_{\tau \rightarrow -0} \sum_s e^{i\epsilon_s \tau} \sum_{\mathbf{k}n} (i\epsilon_s + \epsilon_{\mathbf{k}n}) G(\mathbf{k}, n, n; i\epsilon_s). \quad (7.24)$$

The eigenvalues  $\epsilon_{\mathbf{k}n}$  of the grand canonical Hamiltonian  $\hat{h}^0$  (band structure) are again measured from the chemical potential  $\mu$ .

Although it was not considered in Section 2.8, it is clear from the derivation given there that  $\langle \hat{W} \rangle$  contains all interaction energies of electrons with other particles appearing in the Hamiltonian in interaction terms with the electrons, notably phonons. It does not contain the single-particle energies of those other particles which would have to be added in analogy to (7.23).

For the undressed phonons one has

$$\begin{aligned} D(\mathbf{q}, \lambda, \lambda; -i\tau) &= -\frac{i}{M} \sum_{l'} e^{-i\mathbf{q}\cdot(\mathbf{R}_l - \mathbf{R}_{l'})} \left\langle \mathbf{T}_\tau [\hat{u}_{l\lambda}(-i\tau) \hat{u}_{l'\lambda}(0)] \right\rangle = \\ &= -\frac{i}{2\Omega_{\mathbf{q}\lambda} M_{\mathbf{q}\lambda}} \left( \left\langle \mathbf{T}_\tau [\hat{b}_{\mathbf{q}\lambda}(-i\tau) \hat{b}_{\mathbf{q}\lambda}^\dagger(0)] \right\rangle + \left\langle \mathbf{T}_\tau [\hat{b}_{\mathbf{q}\lambda}^\dagger(-i\tau) \hat{b}_{\mathbf{q}\lambda}(0)] \right\rangle \right). \end{aligned} \quad (7.25)$$

Hence,

$$2i\Omega_{\mathbf{q}\lambda} M_{\mathbf{q}\lambda} D(\mathbf{q}, \lambda, \lambda; \tau = 0) = \langle \hat{b}_{\mathbf{q}\lambda} \hat{b}_{\mathbf{q}\lambda}^\dagger \rangle + \langle \hat{b}_{\mathbf{q}\lambda}^\dagger \hat{b}_{\mathbf{q}\lambda} \rangle = 2n_{\mathbf{q}\lambda} + 1, \quad (7.26)$$

and

$$\langle \hat{h}_{\text{ph}} \rangle = \sum_{\mathbf{q}\lambda} \Omega_{\mathbf{q}\lambda} \left( n_{\mathbf{q}\lambda} + \frac{1}{2} \right) = \frac{-1}{\beta} \sum_s \sum_{\mathbf{q}\lambda} M_{\mathbf{q}\lambda} \Omega_{\mathbf{q}\lambda}^2 D(\mathbf{q}, \lambda, \lambda; i\omega_s), \quad (7.27)$$

which has a structure analogous to (7.23). We used a notation of ‘mode masses’ in the spirit of (4.13), that is  $M_{\mathbf{q}\lambda} = \sum_{\kappa} e_{\lambda}(\mathbf{q}\kappa) e_{\lambda}^*(\mathbf{q}\kappa)$  with properly normalized polarization vectors as in (4.13). The  $\Omega_{\mathbf{q}\lambda}$  are the frequencies of the bare ionic lattice without electrons (but of course with a neutralizing charged homogeneous background).

The thermodynamic critical field  $B_c$  of the superconducting state is defined as

$$\frac{VB_c^2}{2\mu_0} = E_N - E_S = \Delta E, \quad (7.28)$$

where  $E_S$  is the Inner Energy of the superconducting state and  $E_N$  is the normal state reference energy of a thermodynamic state in which the anomalous self-energy  $\phi_s(\mathbf{\kappa})$  is forced to be zero. (It can likewise be defined with the Free Energy difference, since small changes are the same in all thermodynamic potentials.) If we use the same indexing for the Green’s functions, we have

$$\begin{aligned} \frac{VB_c^2}{2\mu_0} &= \frac{1}{2\beta} \sum_s \left( \sum_{\mathbf{k}n} (i\epsilon_s + \epsilon_{\mathbf{k}n}) (G_N(\mathbf{k}, n, n; i\epsilon_s) - G_S(\mathbf{k}, n, n; i\epsilon_s)) - \right. \\ &\quad \left. - 2 \sum_{\mathbf{q}\lambda} M_{\mathbf{q}\lambda} \Omega_{\mathbf{q}\lambda}^2 (D_N(\mathbf{q}, \lambda, \lambda; i\omega_s) - D_S(\mathbf{q}, \lambda, \lambda; i\omega_s)) \right). \end{aligned} \quad (7.29)$$

Since the difference between the normal and superconducting Green’s functions vanishes rapidly with increasing frequencies, we need not bother any more about the  $\tau$ -limes. Of course,  $G_S$  is again the Nambu 11-component of the Green’s function.

The electronic quasi-particle renormalization of Section 5.1 is not specific for the superconducting state. The electronic Green’s functions in (7.29) may be replaced by the renormalized ones,  $g_N$  and  $g_S$ . The band structure  $\epsilon_{\mathbf{k}n}$  is then of course also to be taken renormalized, that is, with the potential (5.12).

Although the modification of the phonon Green’s function  $D$  from the normal to superconducting state does to leading order not influence the electron self-energy, it can not be neglected in (7.29). Nevertheless, the phonons in both states may be considered in harmonic approximation, whence (7.27) is just twice the kinetic energy  $T$  of the nuclei.



The kinetic energy  $T$  is homogeneous linear in the inverse average of the nuclear masses,  $\bar{\mu} = \langle 1/M_\lambda \rangle$ :  $\bar{\mu}(\partial/\partial\bar{\mu})T = T$ . If the superconductor condensation energy (7.28) has an isotopic dependence  $\bar{\mu}^{2\alpha}$  (that is,  $H_c \sim \bar{\mu}^\alpha$ ), then, by a Hellmann-Feynman argument,  $2\alpha\Delta E = \bar{\mu}(\partial/\partial\bar{\mu})\Delta E = \bar{\mu}\Delta\langle(\partial/\partial\bar{\mu})\hat{H}\rangle = \Delta T$ . Hence, the second line of (7.29), which is  $2\Delta T$ , is  $4\alpha$  times the left hand side. If we additionally insert (7.17) and its normal state counterpart (with  $\Delta(\boldsymbol{\kappa}, \epsilon) = 0$ ) into the first line, we obtain a semi-phenomenological expression (depending on the phenomenological isotope exponent  $\alpha$ ) for the condensation energy and hence for the thermodynamic critical field:

$$\frac{VB_c^2}{2\mu_0} = \frac{1}{4\alpha - 1} \frac{1}{2\beta} \sum_s \sum_{\mathbf{k}n} (i\epsilon_s + \epsilon_{\mathbf{k}n}) \cdot \left( \frac{i\epsilon_s Z_S(\boldsymbol{\kappa}, i\epsilon_s) + \epsilon_{\mathbf{k}n}}{\epsilon_s^2 Z_S^2(\boldsymbol{\kappa}, i\epsilon_s) + \epsilon_{\mathbf{k}n}^2 + \Delta^2(\boldsymbol{\kappa}, i\epsilon_s) Z_S^2(\boldsymbol{\kappa}, i\epsilon_s)} + \frac{1}{i\epsilon_s Z_N(\boldsymbol{\kappa}, i\epsilon_s) - \epsilon_{\mathbf{k}n}} \right). \quad (7.30)$$

Again, by means of the summation technique described in Section 7.1, there are different ways of writing these results possible which are met in the literature. By moving between the real and imaginary frequency axis for the various parts of the expressions to be calculated one may optimize the numerical effort and stabilize the numerical convergence of the routines used. These are, however, technical problems, although of practical importance.